AD625886

THE CLASSICAL STRUCTURE
OF BLOOD BIOCHEMISTRY–
A MATHEMATICAL MODEL

E. C. DeLand

D D C

AUG 2 1966

C

The RAND Corporation
SANTA MONICA • CALIFORNIA

THE CLASSICAL STRUCTURE
OF BLOOD BIOCHEMISTRY–
A MATHEMATICAL MODEL

E. C. DeLand

The RAND *Corporation*

PREFACE

This is the third in a continuing series of Memoranda
on the development of a mathematical simulation of human
blood biochemistry. The first--Dantzig, et al. [1]--was
a feasibility study of the methods for mathematical anal-
ysis and computer simulation; the second--DeHaven and
DeLand [2]--added some details of hemoglobin chemistry
and carefully described the behavior of that system under
various conditions.

The subsequent body of critical comment and addi-
tional laboratory data enabled further elaboration and
definition of the model. Professor F.J.W. Roughton, F.R.S.,
Cambridge University, particularly improved the hemoglobin
chemistry. In addition, the quantitative aspects of the
plasma proteins have been reviewed and their buffering
properties incorporated.

The present model therefore approaches more closely
the complexity of the real blood system. Properties of
the mathematical model such as gas exchange, buffering,
and response to chemical stress in the steady state are
practically indistinguishable from those properties of
real blood within the limits of our current validation
program.

The program consists of two parts: detailed chemical analysis of human blood under a variety of chemical stresses; and further elaboration of the model, e.g., by including the phosphate system, double-valent ion binding by proteins, and red cell organic constituents other than hemoglobin. Laboratory experiments validating the model will be published in the doctoral thesis of Eugene Magnier, M.D., Temple University Medical School.

SUMMARY

This Memorandum, one of a series on the modeling of blood biochemistry, describes, and examines the consequences of, the classical analysis of human blood. Classically, the macroscopic features of healthy blood--the principal fluid and electrolyte distributions--can be said to be in a hemostatic steady state under the influence of several interacting constraints, e.g., the osmotic effects of the fixed proteins, the (fixed) charge of the proteins and the neutral electrostatic charge condition, and the active cation pumps. Chapter I examines these constraints from the vantage of a theoretical model, and shows them to be sufficient explanation for the steady state; whether they are also necessary has not been demonstrated.

Chapter II considers the incorporation of the microscopic properties of the proteins in the model, particularly their buffering behavior. This work is ot complete, owing principally to the lack of firm data on hemoglobin.

Chapter III discusses the validation of the mathematical model and the consequences of the previous biochemical structural detail, testing the model under various conditions-- changes in gas pressure and pH, and additions of a few

chemical stresses. It compares several validation experiments with the literature. The Memorandum shows that, except for certain interesting discrepancies, the model satisfactorily agrees with the literature.

CONTENTS

FIGURES

TABLES

Chapter I

A PRELIMINARY MODEL OF BLOOD BIOCHEMISTRY

1. INTRODUCTION

This is the third in a continuing series of Memoranda detailing the development of a mathematical simulation of human blood biochemistry. The first--Dantzig, et al. [1]-- was a feasibility study of a method for mathematical formulation and computer solution of a biochemical simulation problem. An example of a "simple" problem is, given the basic molecular components (reactant species) of a chemical milieu in a single phase, compute the concentration of all species in the equilibrium mixture for which the chemical reaction coefficients and mass action constants are also given.

Such a system may, however, become complex if many reactions are interrelated, if some of the molecules in the milieu (such as proteins) are themselves complex, or if the system is multiphasic, multicompartmented, or alive. These complexities complicate the computation; in particular, for viable systems, one speaks of the computations for a supposed "steady state" of the living organism, rather than the "equilibrium state."

The Dantzig Memorandum introduced the computer method for minimizing the Gibbs free energy function to compute the (unique) steady state of a multicompartmented blood system. The procedures are described in Ref. 1, and developed further in Shapiro and Shapley [3], Shapiro [4], and Clasen [5]. DeHaven and DeLand [2] (the second Memorandum on blood simulation) explore the computer method for determining a steady state in the three-compartment model (lung gas, plasma, and red cell), emphasizing the properties of the chemical systems themselves. Even that rudimentary model had many important characteristics of a blood system, e.g., the proper distribution of water and electrolytes, and a reasonable representation of normal physiologic functions.

This Memorandum extends the previous results, documenting them in more detail, and initiates the validation of an improved model of the blood chemistry. Chapter I analyzes the biochemical structure of the two-compartment blood system. The purpose of this chapter is to elucidate, with a rudimentary blood model such as that used in Dantzig [1], the conventional roles of the fixed proteins, the neutral electrostatic charge constraints, and the active cation pumps in determining the major physical

characteristics of hemostatic blood. While these conventional roles, as is well known, yield a sufficient general explanation for the fluid and electrolyte distribution of normal blood, a mathematical model, which permits experiments impossible in the laboratory, shows their detailed interplay.

Chapter II describes a special mathematical procedure for representing large chemical systems and discusses the representation of the essential proteins. Finally, Chap. III discusses a model of the respiratory biochemistry of the blood, using the previously developed details, and shows some of the model's initial validation procedures.

2. ISOLATING AND DEFINING THE PHYSIOLOGICAL SYSTEM

The blood, contained in the vascular system, may be regarded as a uniform and continuous subsystem of the body. Of course, it changes chemically in the circuit around the body, visibly changing color. However, conceptually isolating the blood as a subsystem and considering only the biochemistry of the respiratory function, this subsystem exhibits the following properties:

a) The subsystem has natural boundaries; its extent is well-defined. It is, for practical purposes, contained within the vascular system. Important and interesting exceptions to this sometimes occur--e.g., protein may pass through the capillary walls to be returned to the vascular system by lymph flow.

b) The function of the bounding membranes can be defined and the substances crossing these membranes analyzed--i.e., the inputs to and losses from the subsystem are measurable. The actual mechanisms and biochemical processes within the membranes themselves are, for the most part, still hypothetical, but only the net results of their functions are necessary to simulations of the steady-state. Transport of substances across these bounding membranes occurs principally--and perhaps only--in capillary beds either at the lung or other body tissues.

c) Biochemical analyses of the blood can be made easily and quickly and, with care, thoroughness and accuracy is possible. Furthermore, samples from this subsystem are available. Thus, for example, conservation of mass equations, fundamental to the simulation, can be substantiated.

d) The subdivisions of the subsystem on the gross
level are clear, e.g., the red cells taken to-
gether as a compartment constitute a subdivision
of whole blood. However, the exterior environ-
ment of the vascular system must also be examined
for a model, since this environment largely de-
termines the transfer of substances across the
bounding membranes. Except in the interior of
certain organs, the environment of the vascular
system is interstitial fluid. However, in the
lung (and perhaps the brain) the layer of inter-
stitial fluid is negligibly thin. In the lung
we may consider the environment of the capillary
bed to be alveolar sac gas.

e) The physiological function of respiration for
the subsystem "blood" is well-defined; its
purpose is clear. The biochemistry involved in
accomplishing this purpose is, on the gross
level, relatively well-understood. However, on
the level of chemical detail, many unsolved
problems still exist. For example, the explana-
tions of the "chloride shift" phenomenon, or
the "Bohr shift" phenomenon, or the "sodium pump"
phenomena are, among many other such problems,
still subjects of research.

The chemical composition of blood varies, of course,

according to the point in the body, the age and sex of

the individual, his response to disease, etc. An average,

resting, young, adult male human is the standard for this

exposition. The relevant data come from many sources, but

particularly Dittmer (Ref. 6, Blood and Other Body Fluids)

and Spector (P f. 7, Handbook of Biological Data).

Table I summarizes these data for three standard
types of blood for the average, young, adult male. Table
II shows the distribution of the substance from Table I
for standard or average arterial blood between plasma and
red cell compartments. These composition tables are
generally concerned with electrolytes, water, and gases.
This chapter does not detail the amino acids, lipids,
carbohydrates, organic phosphates, or other secondary
constituents. It mentions only the constituents which
play a direct role in respiration.

The plasma proteins and impermeable macromolecules,
principally albumin and the various globulins, amount
to about 8.7×10^{-4} moles per liter of blood. At pH 7.4,
the average charge per molecule for the proteins is from
-10 to -20, as can be determined by examining the titra-
tion curves for albumin and globulin [8]. For this first
model where the proteins are not yet buffering, the value
of negative equivalents per mole will be fixed at -10.
Thus, the number of negative equivalents of plasma pro-
teins, used to determine that the solution is electrically
neutral, is 8.7×10^{-3}.

The red cell proteins present a much more complicated
situation. Of course, hemoglobin activity is crucial to

Table I

STANDARD BLOOD COMPOSITION FOR RESTING YOUNG ADULT MALE[a]

Item	Venous Blood, Large Vein	Mixed-Venous, Pulmonary Artery	Arterial, Pulmonary Vein
pH	7.37	7.3ε	7.39
pO_2	65.0 mm	40.0 mm	100.0 mm
pCO_2	46.0 mm	46.0 mm	40.0 mm
pN_2	573.0 mm	573.0 mm	573.0 mm
HCO_3^-	22.3 meq/L	22.0 meq/I.	21.0 meq/L
% Sat.	91.0	73.0	97.0
H_2O	46.50 moles/L	(b)	(b)
Cl^-	80.05 meq/L		
Na^+	84.82 "		
K^+	45.05 "		
Ca^{++}	3.210 "		
Mg^{++}	3.225 "		
$SO_4^=$	1.050 "		
$HPO_4^=$	2.860 "		
$Lactic^-$	2.033 "		
NH_4^+	0.869 "		
Urea	3.142 mmoles/L		
Glucose	3.666 "		
PL PR^{-10}	0.870 "		
PC PR^{-x}	10.57 "		
Hb_4	2.2725 "		

[a]See notes in text.

[b]All the following items in this column do not change with the type of blood, or their change has not been measured, or the change is not significant at this stage of the simulation

Table II

DISTRIBUTION OF SPECIES IN LITER OF STANDARD ARTERIAL
BLOOD (Adult Male) AND ALVEOLAR SAC GAS

Item	Alveolar Sac (%)	Plasma	Red Cell
pH		7.39	7.19
O_2	13.15	6.33×10^{-5} moles	6.43×10^{-5} moles
CO_2	5.26	7.01×10^{-4} "	4.76×10^{-4} "
N_2	75.4	2.20×10^{-4} "	2.20×10^{-4} "
H_2O	6.11	28.50 "	18.0 "
Cl^-		56.65 meq	23.40 meq
Na^+		76.45 "	8.37 "
K^+		2.310 "	42.75 "
Ca^{++}		2.86 "	0.344 "
Mg^{++}		0.935 "	2.295 "
$SO_4^=$		0.680 "	-----[a]
$HPO_4^=$		1.88 "	-----
$Lactic^-$		1.30 "	-----
NH_4^+		0.054 "	-----
HCO_3^-		13.836 "	6.025 "
Glucose		2.00 mmoles	-----
Urea		1.73 "	1.40 mmoles
Misc PR		0.87 "	10.568 "
Hb_4		-----	2.2725 "

[a] "-----" indicates the value is either not reported or is reported in a form not pertinent to this representation.

respiration, carrying CO_2 as well as oxygen in combination. In more complex models (Chap. III), the buffering activity of hemoglobin also pertains. This preliminary, illustrative model treats hemoglobin simply as a protein combining with oxygen and contributing to the osmolarity and, hence, hematocrit of the blood.

However, the red cells also contain miscellaneous proteins, complex phosphates, and other anionic species (excluding hemoglobin) generally represented in the literature [7] by X^-. This symbol indicates an undetermined anion residue necessary to make the red cell milieu neutrally charged and to make the osmolarity of the red cell milieu equal to that of plasma. Chapter III examines this assumption of equal osmolarity, but the preliminary model uses the undetermined anion residue to obtain the proper hematocrit and a neutral electrical charge.

Neither the distributions of glucose and urea nor of the various sulphates and phosphates between plasma and red cell have been carefully detailed for this preliminary model. The diffusion of glucose through the red cell membrane is presumably an intricate process, while urea is thought to pass freely through the membrane. Table II reflects neither of these facts. The species represented

n.

by $SO_4^=$ and $HPO_4^=$ are the acid-soluble sulphates and phosphates reported in the literature. Table II does not indicate that these substances may also be intricately bound to the proteins of red cell and plasma. Similarly, Ca^{++} and Mg^{++} may be bound by protein. Chapter III will discuss these conditions.

Most of the Na^+ and a large part of the Cl^- are in plasma, while most of the K^+ is in the red cell compartment, a consequence of the "sodium pump" and the Gibbs-Donnan phenomenon. The distribution of the species H_2O in Table II requires some exp   nation. When large proteins and other aggregated molecules are dissolved in water, the volume of the solution is usually larger than the volume of solvent. This "volume factor" has been found to be 94 percent for normal plasma; that is, in Table II, the 28.50 moles of H_2O, which is 516 cc at 38^oC, represent 516/ 0.94 = 549 cc of plasma per liter of blood. The red cell volume is, thus, 451 cc per liter of blood and the hematocrit is 45.1 percent. Since, in the red cells, there are only 18.0 moles or 326 cc of H_2O, the volume factor is 72.3 percent, which includes the volume occupied by the stroma.

3. DEVELOPMENT OF THE BLOOD MODEL

GENERAL CONSIDERATIONS

The data of the previous section enable the simulation of the average arterial blood of Table II, which represents a liter of blood in the steady, resting state.

We assume that metabolism continues at a steady rate and, because metabolism in the red cells is principally anaerobic, gives a net production of H^+ ions and lactate ion along with other minor products. We also assume a complex but undefined activity (referred to as the "sodium pump") for the red cell membrane. One result is that all mobile ions, particularly Na^+ and K^+, acquire across this membrane steady concentration gradients different from those without the active membrane. Also, the system has a steady "membrane potential"--roughly, that electrical potential which is measured by suitable electrodes suitably placed (Chap. III analyzes this definition). A steady pH exists in the plasma and, because of the activity of the cell, a different, lower pH holds in the "interior" of the red cell.

The structure of the red cell is simpler than other body cells since the red cell is not nucleated and contains

but one principal protein. In the model, the interiors
of all red cells in the liter of blood are taken together
as a single "compartment," uniformly mixed and separated
from the plasma by an ideal semi-permeable, though active,
membrane.

Conceptually, then, two distinct compartments, with
chemical analyses given in Table II, communicate with
each other through the idealized membrane. Proteins and
certain other large molecules (e.g., complex phosphates)
cannot penetrate, but other ions and molecules pass
through regardless of the mechanism or of the time required.
The membrane is flexible and will not support a pressure
gradient, so the "red cell" may change volume by as much
as 5 percent between arterial and venous blood. Also,
the temperature is supposed uniform throughout.

STATEMENT OF THE PRELIMINARY PROBLEM

Given these basic hypotheses and assumptions (as well
as further assumptions carefully defined as required), the
essential problem of this simulation is to create Table II
from Table I by means of a mathematical model--that is,
given the total composition of a liter of whole blood and
using the general mathematical program, distribute these

"input" substances into the compartment's plasma and red cell so that the "output" duplicates Table II.

FIRST APPROXIMATIONS

The construction of a model of arterial blood could begin with the simulation of ordinary "soda water," a two-phase system of gas and liquid with both inter- and intraphase reactions.[†] The gases, O_2, CO_2, N_2, have determined solubility constants at a given temperature and pressure, and the solvent water has known vapor pressure. One could, therefore, compute the concentrations of each in the liquid phase as well as the partial pressures of H_2O vapor in the gaseous phase. In the liquid phase, the carbonate system reaction constants are well-documented,[‡] so with fixed partial pressures of the gases one could compute the concentrations of HCO_3^-, $CO_3^=$, H^+, OH^-, and H_2O with arbitrary accuracy.

If the gas volume is finite, the formation of the species in solution will, by conservation of mass, alter the gas composition. Therefore, the preliminary model uses a very large gas phase, which also gives better

---

[†] Reference 2 further details this model.

[‡] See, for example Edsall and Wyman, Ref. 8, Chap. 10.

control of independent variables. Using, say, 1000 moles
of gas phase at a determined composition versus one liter
of liquid phase causes the gas phase to remain almost
constant, thus holding the gases in solution at constant
concentration. The gas composition can be varied, of
course, as required.[†]

MODEL A--PRIMITIVE SYSTEM, PLASMA

The first model, Model A, only slightly enlarges the
soda water model which consists of the gases O_2, CO_2, N_2,
H_2O, the solvent H_2O, and two phases, gas and liquid.
Adding more species to the liquid phase without adding
intraphase reactions will change the results for soda
water only slightly. Thus, adding Na^+, Cl^-, K^+, $HPO_4^=$,
Ca^{++}, Mg^{++}, $SO_4^=$, urea, glucose, lactic acid, and protein
up to the approximate concentrations of these substances
in plasma, changes the concer rations of dissolved gases
only slightly although the pH may require adjustment
with NaOH or HCl. The gas concentrations do change be-
cause the solubility constant for the gases differs in

[†]Previous studies--Refs. 1 through 5--describe the
computation procedure employed here.

plasma and in water, and because the actual number of moles of liquid phase, $\bar{x}$, has increased. No new intra-phase reactions are introduced yet. Later the protein will buffer H^+ ion and bind Ca^{++}, Mg^{++}, and Cl^-. Here, the protein makes the solution non-ideal and increases the volume of plasma over the water volume by 6 percent. Otherwise, in the normal viable range, this two-phase preliminary system can be assumed to be well-behaved. Again, concentration curves could be computed for this simple system, but it is not yet of much interest.

MODEL B--OSMOLARITY

A second model, Model B, has a third compartment called "red cells" and several additional conditions. For this model, the total amounts of substances added to the total system will be exactly those of Table I, arterial blood. The problem is to determine how much of each of these substances is distributed into the red cell compartment under various conditions. Such a determination is a solution of the problem under those conditions.

First, for Model b, let the membrane between plasma and red cells be permeable to all species--including protein. In this case, the mathematical solution is not unique, for the membrane could divide the two compartments arbitrarily, and the mixed composition of the two compartments would be identical and uniform except for $\bar{x}_{Pl}$ and $\bar{x}_{RC}$, the total number of moles of all species in each.

Second, Model B a) supposes the membrane impermeable to proteins only, b) ignores the electrical charge on the ions and proteins, and c) supposes (as do subsequent models in Chap. I) that the gases have equal solubility in red cells and plasma.

With the protein distributed and fixed in plasma and red cells, and with the membrane flexible so that hydrostatic pressure gradients cannot arise, all species distribute between the compartments in proportion to the amounts of impermeable proteins in each, a result of the elementary "osmotic" phenomenon: i.e., each substance, including water, will distribute so that it has the same concentration on each side of the membrane, independently of the other species. In addition, since the proteins are impermeable, all other species must move; i.e., the

membrane must move, so that the proteins on each side are equally dilute. Thus, the total moles in each compartment have the ratio

$$\bar{x}_{PL}/\bar{x}_{RC} = 8.706 \times 10^{-4} \Big/ (10.568 \times 10^{-3} + 2.2725 \times 10^{-3}) = 0.0678$$

where the numbers on the right are the moles of protein on each side of the membrane. Table III, a reproduction of the computer results for Model B, illustrates these comments.

MODEL C--ELECTRICAL NEUTRALITY

Model C involves an hypothetical experiment. Suppose that, in addition to the above conditions, each protein now has an electrical charge of -1 per molecule, and the other ions have their normal chemical valence. Suppose, further, that the sum of the charged input substances is such that the whole is neutrally charged. Now apply the mathematical condition that each compartment, plasma and red cells, be neutrally charged, i.e., that the sum over all charged species in each compartment is zero. Under these conditions, no change at all will occur in the computed distribution of the species and the results will be identical to Model B. That is, under the conditions

Table III

ELEMENTARY OSMOLARITY--MODEL B

PRELIMINARY BLOOD MODEL   NEITHER CHARGE OR NA PUMP   DELAND

		AIR OUT	PLASMA	RED CELLS
X-BAR		9.99160E 02	2.97125E 00	4.38209E 01
PH		-0.	7.34527E 00	7.34527E 00
O2	MOLES	1.31507E 02	6.93539E-06	1.02285E-04
	MFRAC	1.31617F-01	2.33416E-06	2.33416E-06
CO2	MOLES	5.26022E 01	7.15457E-05	1.05518E-03
	MFRAC	5.26464E-02	2.40793F-05	2.40793E-05
N2	MOLES	7.54000F 02	2.22640E-05	3.28250E-04
	MFRAC	7.54634F-01	7.49314E-06	7.49314E-06
H20	MOLES	6.10509F 01	2.95582F 00	4.35933E 01
	MFRAC	6.11022E-02	9.94807E-01	9.94807E-01
H+	MOLES	-0.	2.41847E-09	3.56682E-08
	MFRAC	-0.	8.13955E-10	8.13955E-10
OH-	MOLES	-0.	2.83934E-08	4.18755E-07
	MFRAC	-0.	9.55605E-09	9.55605E-09
CL-	MOLES	-0.	5.08309E-03	7.49669F-02
	MFRAC	-0.	1.71076E-03	1.71076E-03
NA+	MOLES	-0.	4.28936E-03	6.32607E-02
	MFRAC	-0.	1.44362E-03	1.44362E-03
K+	MOLES	-0.	2.86063E-03	4.21894E-02
	MFRAC	-0.	9.62769E-04	9.62769E-04
CA++	MOLES	-0.	1.01916E-04	1.50308E-03
	MFRAC	-0.	3.43006F-05	3.43006E-05
MG++	MOLES	-0.	1.02392E-04	1.51011E-03
	MFRAC	-0.	3.44609E-05	3.44609E-05
SO4=	MOLES	-0.	3.33370E-05	4.91653E-04
	MFRAC	-0.	1.12198E-05	1.12198E-05
HPO4=	MOLES	-0.	9.08035E-05	1.33920E-03
	MFRAC	-0.	3.05607E-05	3.05607E-05
UREA	MOLES	-0.	1.99516E-04	2.94249E-03
	MFRAC	-0.	6.71480E-05	6.71480E-05
GLUCOS	MOLES	-0.	2.32787E-04	3.43321E-03
	MFRAC	-0.	7.83665E-05	7.83665E-05
LACTIC	MOLES	-0.	1.29091E-04	1.90391E-03
	MFRAC	-0.	4.34475E-05	4.34475E-05
NH4+	MOLES	-0.	5.51806E-05	8.11813E-04
	MFRAC	-0.	1.85715E-05	1.85715E-05
HCO3-	MOLES	-0.	1.27953E-03	1.88708E-02
	MFRAC	-0.	4.30636F-04	4.30636E-04
H2CO3	MOLES	-0.	1.01787E-07	1.50119E-06
	MFRAC	-0.	3.42574E-08	3.42574E-08
CO3=	MOLES	-0.	1.49518E-06	2.20766E-05
	MFRAC	-0.	5.03039E-07	5.03039E-07
MISC**	MOLES	-0.	8.70600E-04	1.05860E-02
	MFRAC	0.	2.93008E-04	2.41164E-04
HRA	MOLES	-0.	-0.	2.77350E-03
	MFRAC	-0.	-0.	5.10580E-05

for B but with all protein <u>uniformly</u> charged, all sub-
stances are already distributed on both sides of the
membrane such that each compartment is electrically
neutral.

MODEL D--GIBBS-DONNAN AND HAMBURGER SHIFT

Model D supposes that the average charge of the
protein molecules in plasma <u>only</u> is -10 per molecule. The
moles of input substances are identical to Table I, and
the average charges on hemoglobin and the miscellaneous
fixed species in red cells are such that the total inputs
are neutrally charged. Applying the neutral charge re-
straint now to plasma and to red cells, if the average
charge per molecule of the red cell protein happens also
to be -10, the results are again as in Model B or C. Any
other charge on the average, red cell, protein molecule
causes different results.

The average charge for all red cell proteins in
Table I is -3.5, and a comparison of this with -10 for
the average charge of plasma protein indicates that posi-
tive ions should be displaced into plasma and the permeable
negative ions displaced or repelled into red cells. Table
IV, a reproduction of the computer results for Model D,

Table IV

GIBBS-DONNAN PHENOMENON--MODEL D

PRELIMINARY BLOOD MODEL   NO SODIUM PUMP, PL PR CHG -10   DELAND

		AIR OUT	PLASMA	RED CELLS
X-BAR		9.99136E 02	5.95029E 00	4.08829E 01
PH		-0.	7.28065E 00	7.35342E 00
O2	MOLES	1.31507E 02	1.38893E-05	9.54297E-05
	MFRAC	1.31620E-01	2.33422E-06	2.33422E-06
CO2	MOLES	5.26022E 01	1.43282E-04	9.84456E-04
	MFRAC	5.26477E-02	2.40799E-05	2.40799E-05
N2	MOLES	7.54000E 02	4.45874E-05	3.06349E-04
	MFRAC	7.54652E-01	7.49332E-06	7.49332E-06
H2O	MOLES	6.10271E 01	5.91722E 00	4.06557E 01
	MFRAC	6.10799E-02	9.94443E-01	9.94442E-01
H+	MOLES	-0.	5.61819E-09	3.26460E-08
	MFRAC	-0.	9.44188E-10	7.98523E-10
OH-	MOLES	-0.	4.90004E-08	3.98084E-07
	MFRAC	-0.	8.23496E-09	9.73716E-09
CL-	MOLES	-0.	8.77348E-03	7.12765E-02
	MFRAC	-0.	1.47446E-03	1.74343E-03
NA+	MOLES	-0.	1.24538E-02	7.23662E-02
	MFRAC	-0.	2.09298E-03	1.77008E-03
K+	MOLES	-0.	6.61453E-03	3.84355E-02
	MFRAC	-0.	1.11163E-03	9.40135E-04
CA++	MOLES	-0.	2.71376E-04	1.33362E-03
	MFRAC	-0.	4.56072E-05	3.26206E-05
MG++	MOLES	-0.	2.72644E-04	1.33986E-03
	MFRAC	-0.	4.58203E-05	3.27730E-05
SO4=	MOLES	-0.	4.95000E-05	4.75500E-04
	MFRAC	-0.	8.31892E-06	1.16308E-05
HPO4=	MOLES	-0.	1.34829E-04	1.29517E-03
	MFRAC	-0.	2.26592E-05	3.16800E-05
UREA	MOLES	-0.	3.99200E-04	2.74280E-03
	MFRAC	-0.	6.70891E-05	6.70891E-05
GLUCOS	MOLES	-0.	4.65776E-04	3.20022E-03
	MFRAC	-0.	7.82778E-05	7.82778E-05
LACTIC	MOLES	-0.	2.22817E-04	1.81018E-03
	MFRAC	-0.	3.74464E-05	4.42773E-05
NH4+	MOLES	-0.	1.27592E-04	7.41408E-04
	MFRAC	-0.	2.14430E-05	1.81349E-05
HCO3-	MOLES	-0.	2.20822E-03	1.79397E-02
	MFRAC	-0.	3.71111E-04	4.38808E-04
H2CO3	MOLES	-0.	2.03772E-07	1.40006E-06
	MFRAC	-0.	3.42457E-08	3.42457E-08
CO3=	MOLES	-0.	2.38843E-06	2.29434E-05
	MFRAC	-0.	4.01397E-07	5.61198E-07
MISCPR	MOLES	-0.	8.70600E-04	1.05680E-02
	MFRAC	-0.	1.46312E-04	2.58494E-04
HB4	MOLES	-0.	-0.	2.27250E-03
	MFRAC	-0.	-0.	5.55856E-05

shows this actually occurs. Table IV demonstrates that Na^+, say, is now predominantly in plasma, and Cl^- is predominantly in red cells. The total mole ratio of plasma and red cell compartments, $\bar{x}_{PL}/\bar{x}_{RC}$, has changed to 0.1455.

Note that this movement of the positive and negative ions is anomalous. The directions of movement of the Cl^- ion and K^+ ion here are opposite to the standard blood distribution. Thus, the zero-charge restraint plus the impermeable fixed-protein distribution alone are inadequate to establish the desired (Table II) electrolyte distribution. This observation is significant because Model D contains both of the essential elements for the classical Gibbs-Donnan equilibrium [9], i.e., the fixed-protein and the charge restraint.

The Gibbs-Donnan phenomenon is usually explained with an hypothetical system where electrically charged protein is on only one side of a rigid membrane in a water solution containing other electrolytes. The zero-charge constraint is then applied to a compartment on one side of the membrane. Substances move across the rigid membrane, in response to both the osmotic effect of the protein and the charge condition, until a hydrostatic

pressure builds up on the protein side sufficient to stop further flow. Simultaneously, the electrolytes rearrange to satisfy the charge condition. The hydrostatic pressure thus acquired by the system is an empirical measure of the "osmotic pressure" of the system.

In the present case, the membrane is flexible so hydrostatic pressure cannot build up--the complementary compartments simply change size. Replacing the hydrostatic pressure which balances the flow, a second protein is dissolved in the second compartment. Osmotic redistribution will cease when the two proteins are equally dilute, as in Model B. The charge restraint simultaneously redistributes the electrolyte, as in Models C and D. The Gibbs-Donnan phenomenon, however, is basically the same, and the above results show it is insufficient in itself to establish the desired (Table II) distribution of electrolytes for arterial blood.

The Gibbs-Donnan equilibrium phenomenon does, however, contribute an important characteristic to the blood model--namely, the so-called "chloride" or "Hamburger shift" which takes place reversibly at the lung surface and in the body tissue capillary beds [1 . At the body tissue level, CO_2 dissolves in plasma and diffuses into

the red cell, where the enzyme carbonic anhydrase combines it with a molecule of water to become H_2CO_3. The consequent ions HCO_3^- and H^+ are, of course, subject to the charge constraint of the Gibbs-Donnan phenomenon, just as any other ion. Conventionally, the charge constraint affects the concentration of HCO_3^- exactly as it does Cl^-, yielding

$$\frac{[HCO_3^-]_{Pl}}{[HCO_3^-]_{RC}} = k \frac{[Cl^-]_{Pl}}{[Cl^-]_{RC}} \tag{1}$$

where square brackets indicate concentration. In this case $k = 1$; Model G below introduces a difference in solubility for CO_2 between plasma and red cells, so $k \neq 1$. As the concentration of bicarbonate increases in the red cell, the HCO_3^- moves into the plasma under a diffusion gradient. This movement of HCO_3^- would leave a net positive charge in the red cell except that Cl^-, as well as other anions, then shifts into the red cell milieu (the chloride shift). The solvent species H_2O must also shift to maintain Eq. (1). Exactly the opposite set of reactions occurs at the lung surface.

Two important tentative assumptions derive from this discussion. First, since Eq. (1) is accepted in the literature [10] and verified empirically [6,7], neither Cl^- nor HCO_3^- is likely to be subject to active transport (see below, Model E) at or in the cell membrane. If the concentration ratios of either were effected, Eq. (1) could not hold over the range of the Hamburger shift unless both were affected exactly equally by an active transport mechanism, which is unlikely.

The second assumption is that Eq. (1) may be made much stronger. Indeed, any ion not subject to active transport must have the same chemical potential gradient given by the zero-charge constraint, i.e.,

$$\frac{[Cl^-]_{Pl}}{[Cl^-]_{RC}} = k \frac{[HCO_3^-]_{Pl}}{[HCO_3^-]_{RC}} = \frac{[H^+]_{RC}}{[H^+]_{Pl}} = \left(\frac{[SO_4^=]_{Pl}}{[SO_4^=]_{RC}}\right)^{\frac{1}{2}} = \dots \quad (2)$$

where the hydrogen ratio is inverted because of its sign and the $SO_4^=$ ratio is reduced because of its valence.[†] The dots indicate similar ratios for other ions. For example, in the present Model F, Na^+ and K^+ are not subject

---

[†]See Ref. 8, p. 227.

to active transport (see Model E) and therefore they, too,
satisfy Eq. (2), as shown in Table IV.

MODEL E--THE SODIUM PUMP

Model E, again a hypothetical experiment, ignore
the electrical charge of the species in order to simplify
a first simulation of the sodium pump. Because the species
subject to the sodium pump have electrical charge, the
effects of the pump and the effects of the zero-charge
restraint applied in D would otherwise interact. In
order, then, to isolate the function of the sodium pump,
the mathematical zero-charge restraint of the Gibbs-
Donnan phenomena is temporarily suspended. All other
conditions--semipermeable, flexible membrane, etc.--still
apply.

"Sodium pump" is a generic name for the phenomena
whereby living cells, via a biochemical and/or biophysical
mechanism within or at the surface of the membrane of
those cells, selectively excrete or absorb cations. The
sodium pump is a subclass of the more general "active
transport" processes, the exact mechanisms for which are
still generally obscure [11,12].

The present Model E concerns not the biochemical or biophysical mechanism whereby the sodium pump is accomplished, but only the net result. As may be seen in Table II, the sodium pump acting in the erythrocyte membranes causes most of the Na^+ and Ca^{++} ions to concentrate in plasma, and most of the K^+ and Mg^{++} ions to concentrate in the interiors of the red cells. The above examples show clearly that the Gibbs-Donnan forcing functions, osmotic effects, and zero-charge condition cannot account for the disposition of cations in Table II. Additional work on these cations is necessary.

In order to quantize the sodium pump phenomena, we assume that the species Na^+_{PLASMA} and the species $Na^+_{RED\ CELL}$ are not identical. It is convenient to say, instead, that

$$Na^+_{Pl} \overset{\sim}{=} Na^+_{RC} , \quad \Delta F \qquad (3)$$

is a chemical reaction converting one species to the other, an interphase reaction, even though Eq. (3) is not a complete reaction in the thermodynamic sense. Further, the increment of free energy, ΔF, is proportional to the work done on the substance during conversion, although the actual work in vivo is difficult to measure

and may differ considerably from this theoretical minimum value required to maintain a gradient. Thus, though we do not represent the membrane or the mechanism, we postulate a free energy parameter proportional to the difference in concentrations or mole fractions of the two species in Eq. (3) at steady state.

Tables V and VI respectively list the input data and reproduce the computer results for Model E. Table V lists the species to be expected in the three compartments, their respective free energy parameters, and the input components from which the output species originate, as in a chemical reaction.

The "free energy parameters" in Table V have various appropriate meanings. The O_2 species has a free energy parameter -10.94 in the "Air Out" compartment, and zero in "Plasma." This number is the log base e of the solubility constant in mole fractions for O_2 in plasma, 0.02089 cc/cc/atm. The species HCO_3^- in plasma has the free energy parameter -21.35, which is the log base e for the mass action constant in mole fractions for the reaction[+]

$$OH^- + CO_2 \rightleftharpoons HCO_3^- , \quad \Delta F \qquad (4)$$
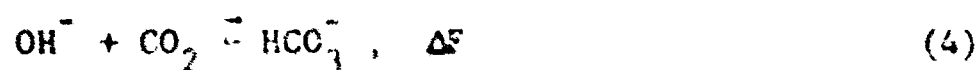
[+] See Ref. 2, p. 15.

Table V

INPUT DATA--ELEMENTARY MODEL

Expected Species	Free Energy Parameter	Input Components		
AIR OUT				
O2	-10.940000	1.000 O2		
CO2	-7.690000	1.000 CO2		
N2	-11.520000	1.000 N2		
H2O	-36.600000	1.000 H+	1.000 OH-	
PLASMA				
O2	0.	1.000 O2		
CO2	0.	1.000 CO2		
N2	0.	1.000 N2		
H+	0.	1.000 H+		
OH-	0.	1.000 OH-		
CL-	0.	1.000 CL-		
NA+	0.	1.000 NA+		
K+	0.	1.000 K+		
CA++	0.	1.000 CA++		
MG++	0.	1.000 MG++		
SO4=	0.	1.000 SO4=		
HPO4=	0.	1.000 HPO4=		
UREA	0.	1.000 UREA		
GLUCOS	0.	1.000 GLUCOS		
LACTIC	0.	1.000 LACTIC		
NH4+	0.	1.000 NH4+		
HCO3-	-21.350000	1.000 CO2	1.000 OH-	
H2CO3	-32.840000	1.000 CO2	1.000 H+	1.000 OH-
CO3=	6.260000	1.000 CO2	-1.000 H+	1.000 OH-
H2O	-39.390000	1.000 H+	1.000 OH-	
MISCPM	0.	1.000 MISCPL		
RED CELLS				
O2	-0.	1.000 O2		
CO2	0.	1.000 CO2		
N2	-0.	1.000 N2		
H+	0.	1.000 H+		
OH-	0.	1.000 OH-		
CL-	0.	1.000 CL-		
NA+	2.191000	1.000 NA+		
K+	-2.761000	1.000 K+		
CA++	2.751700	1.000 CA++		
MG++	-0.457700	1.000 MG++		
SO4=	-0.	1.000 SO4=		
HPO4=	-0.	1.000 HPO4=		
UREA	0.	1.000 UREA		
GLUCOS	0.	1.000 GLUCOS		
LACTIC	0.	1.000 LACTIC		
NH4+	0.	1.000 NH4+		
HCO3-	-21.350000	1.000 CO2	1.000 OH-	
H2CO3	-32.840000	1.000 CO2	1.000 H+	1.000 OH-
CO3=	6.260000	1.000 CO2	-1.000 H+	1.000 OH-
H2O	-39.390000	1.000 H+	1.000 OH-	
MISCPM	0.	1.000 MISCRE		
HB4	0.	1.000 HB4		

Table VI

SODIUM PUMP--MODEL E

PRELIMINARY BLOOD MODEL   NO CHARGE EQUATION   DELAND

		AIR OUT	PLASMA	RED CELLS
X-BAR		9.99136E 02	2.69537E 01	1.98795E 01
PH		-0.	7.34407E 00	7.34487E 00
O2	MOLES	1.31507E 02	6.29158E-05	4.64032E-05
	MFRAC	1.31620E-01	2.33422E-06	2.33422E-06
CO2	MOLES	5.26022E 01	6.49042E-04	4.78697E-04
	MFRAC	5.26477E-02	2.40799E-05	2.40799E-05
N2	MOLES	7.54000E 02	2.01973E-04	1.48964E-04
	MFRAC	7.54652E-01	7.49332E-06	7.49332E-06
H2O	MOLES	6.10271E 01	2.68039E 01	1.97690E 01
	MFRAC	6.10799E-02	9.94442E-01	9.94442E-01
H+	MOLES	-0.	2.19513E-08	1.61900E-08
	MFRAC	-0.	8.14407E-10	8.14407E-10
OH-	MOLES	-0.	2.57334E-07	1.89795E-07
	MFRAC	-0.	9.54725E-09	9.54725E-09
CL-	MOLES	-0.	4.60708E-02	3.39792E-02
	MFRAC	-0.	1.70926E-03	1.70926E-03
NA+	MOLES	-0.	7.83728E-02	6.44721E-03
	MFRAC	-0.	2.90768E-03	3.24314E-04
K+	MOLES	-0.	3.00870E-03	4.20413E-02
	MFRAC	-0.	1.11625E-04	2.11480E-03
CA++	MOLES	-0.	1.48942E-03	1.15576E-04
	MFRAC	-0.	5.52586E-05	5.81380E-06
MG++	MOLES	-0.	7.44583E-04	8.67918E-04
	MFRAC	-0.	2.76245E-05	4.36589E-05
SO4=	MOLES	-0.	3.02151E-04	2.22849E-04
	MFRAC	-0.	1.12100E-05	1.12100E-05
HPO4=	MOLES	-0.	8.23001E-04	6.06999E-04
	MFRAC	-0.	3.05339E-05	3.05339E-05
UREA	MOLES	-0.	1.80630E-03	1.33370E-03
	MFRAC	-0.	6.70891E-05	6.70891E-05
GLUCOS	MOLES	-0.	2.10988E-03	1.55612E-03
	MFRAC	-0.	7.82773E-05	7.82778E-05
LACTIC	MOLES	-0.	1.17004E-03	8.62957E-04
	MFRAC	-0.	4.34094E-05	4.34094E-05
NH4+	MOLES	-0.	5.00131E-04	3.68869E-04
	MFRAC	-0.	1.85532E-05	1.85532E-05
HCO3-	MOLES	-0.	1.15948E-02	8.55131E-03
	MFRAC	-0.	4.30249E-04	4.30249E-04
H2CO3	MOLES	-0.	9.23047E-07	6.80787E-07
	MFRAC	-0.	1.42456E-08	1.42456E-08
CO3=	MOLES	-0.	1.45421E-05	1.07254E-05
	MFRAC	-0.	5.39520E-07	5.39520E-07
H5CP+	MOLES	-0.	8.70600E-04	1.09660E-02
	MFRAC	-0.	3.22986E-05	5.51603E-04
HB+	MOLES	-0.	-0.	2.27250E-03
	MFRAC	-0.	-0.	1.14314E-04

or

$$H_2O + CO_2 \rightleftharpoons H_2CO_3 \rightleftharpoons H^+ + HCO_3^-$$

plus

$$OH^- + H^+ \rightleftharpoons H_2O$$
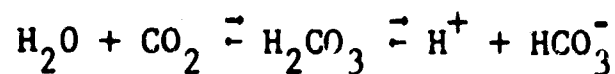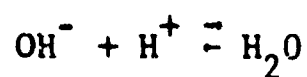
giving

$$\frac{(HCO_3^-)}{(OH^-)(CO_2)} = K . \tag{5}$$

Using the free energy parameters for Na_{Pl}^+ and Na_{KC}^+ in Table V, we may compute from Table VI

$$\ln (\hat{N}a_{Pl}^+)\Big/(\hat{N}a_{RC}^+) = \ln (2.908 \times 10^{-3}\Big/3.243 \times 10^{-4}) = 2.1934 . \tag{6}$$

That is, the cations have acquired the gradients given by their respective free energy parameters, c_j, proportional to ΔF of Eq. (3). Taking their valence into consideration, the other cations satisfy similar equations. References 1

and 3 develop the detailed mathematical background for the procedures and computations involved here.

Note that the distribution of species in Table V1 is not yet that of Table II. From Table VI, because of the new disposition of the solute resulting from the cation pumps, the ratio of $\bar{x}_{PL}/\bar{x}_{RC}$ is now $26.95/19.88 = 1.355$. The pH $= 7.34$ is the same for each compartment since H^+ ion, assumed to be not subject to an active pump, is distributed uniformly throughout. Model F again applies the charge constraint, causing the H^+ ion to shift nearer to that of Table II.

MODEL F--SIMULTANEOUS CONDITIONS

Model F finally applies the conditions of the previous examples simultaneously, i.e., the cation pumps, the zero-charge restraint, and the impermeable protein with average charge -10 per molecule on the plasma proteins.

The input data for this model are, therefore, essentially the same as Table V, except for the equation which computes and imposes the charge constraint. Table VII reproduces the computer results for Model F.

An anomalous shift of electrolytes has important results. Compared with Table III, the charge equation

Table VII

NONLINEARITY--MODEL F

PRELIMINARY BLOOD MODEL   BOTH CHARGE AND NA PUMP   DELAND

		AIR OUT	PLASMA	RED CELLS
X-BAR		9.99136E 02	2.91541E 01	1.76791E 01
PH		-0.	7.40003E 00	7.23496E 00
O2	MOLES	1.31507E 02	6.80521E-05	4.12669E-05
	MFRAC	1.31620E-01	2.33422E-06	2.33422E-06
CO2	MOLES	5.26027E 01	7.02028E-04	4.25711E-04
	MFRAC	5.26477E-02	2.40799E-05	2.40799E-05
N2	MOLES	7.54000E 02	2.18461E-04	1.32475E-04
	MFRAC	7.54652E-01	7.49332E-06	7.49332E-06
H2O	MOLES	6.10271E 01	2.89921E 01	1.75808E 01
	MFRAC	6.10799E-02	9.94442E-01	9.94442E-01
H+	MOLES	-0.	2.09111E-08	1.85442E-08
	MFRAC	-0.	7.17261E-10	1.04893E-09
OH-	MOLES	-0.	3.16040E-07	1.31040E-07
	MFRAC	-0.	1.08403E-08	7.41261E-09
CL-	MOLES	-0.	5.65062E-02	2.34638E-02
	MFRAC	-0.	1.94093E-03	1.32721E-03
NA+	MOLES	-0.	7.71834E-02	7.63458E-03
	MFRAC	-0.	2.64750E-03	4.31842E-04
K+	MOLES	-0.	2.53073E-03	4.25193E-02
	MFRAC	-0.	8.68051E-05	2.40506E-03
CA++	MOLES	-0.	1.41230E-03	1.92703E-04
	MFRAC	-0.	4.84424E-05	1.09000E-05
MG++	MOLES	-0.	5.28749E-04	1.08175E-03
	MFRAC	-0.	1.81343E-05	6.13013E-05
SO4--	MOLES	-0.	4.09024E-04	1.15976E-04
	MFRAC	-0.	1.40297E-05	6.56005E-06
HPO4-	MOLES	-0.	1.11610E-03	3.15836E-04
	MFRAC	-0.	3.82143E-05	1.78683E-05
UREA	MOLES	-0.	1.95393E-03	1.18407E-03
	MFRAC	-0.	6.70891E-05	6.70891E-05
GLUCOS	MOLES	-0.	7.28212E-03	1.38188E-03
	MFRAC	-0.	7.02778E-05	7.02778E-05
LACTIC	MOLES	-0.	1.41710E-03	3.95902E-04
	MFRAC	-0.	4.92931E-05	3.17046E-05
NH4+	MOLES	-0.	4.60968E-04	4.95416E-04
	MFRAC	-0.	1.57974E-05	2.11027E-05
HCO3-	MOLES	-0.	1.42426E-02	5.90572E-03
	MFRAC	-0.	4.88522E-04	1.34051E-04
H2CO3	MOLES	-0.	9.38621E-07	6.75412E-07
	MFRAC	-0.	3.42456E-08	3.42456E-08
CO3-	MOLES	-0.	2.02765E-05	9.74618E-06
	MFRAC	-0.	6.95462E-07	3.25312E-07
PISCPO	MOLES	-0.	8.70605E-04	1.05680E-02
	MFRAC	-0.	7.98620E-05	5.97606E-04
HB	MOLES	-0.	-0.	2.27249E-03
	MFRAC	-0.	-0.	1.28562E-04

effect of Table IV drives a small amount of Na^+ into the plasma compartment. On the other hand, compared with Table VI, the _same_ charge equation effect of Table VII drives a small amount of Na^+ into the red cell compartment. That is, the charge equation applied to Model B results in a different direction of ion movement than would the same charge equation applied to Model E.

Thus, it would be convenient if a stress or forcing constraint applied to the system always gave the same results. But this wish is naive. The result of a stress is clearly a function of the system to which it is applied.

The hematocrit of Table VII is now 44 percent; the pH of plasma is nearly correct at 7.4, but the pH of red cells is still alkaline (compared to Table II). The model requires further modification.

MODEL G--HILL'S EQUATION, MYOGLOBIN

Model G, the final model in this preliminary series, applies three small modifications to Model F. The crude outlines of a simulation of Table II are already apparent in Model F. The _general_ descriptive characteristics of live arterial blood at steady state have been deduced according to the classical principles of the biochemical

structure--i.e., using the fixed proteins and the charge
constraint (to obtain the Gibbs-Donnan phenomena), and
the sodium pump hypothesis. At this point, the model
resembles that of Ref. 1 which was derived from a dif-
ferent point of view.

The first kind of addition to be illustrated con-
cerns additional interphase reactions--or transport. As
an example, consider the $HPO_4^=$ and $SO_4^=$ anions. The total
of these ions, as acid-soluble phosphate and sulfate,
shown in Table I were computed from Edelman [13]; the
distribution shown in Table II was estimated from Spector
[7] and Edelman [13]. The anions considered here do not
include the phosphates and sulfur bound, for exampl , in
the structure of the nucleoproteins and lipids

In Table VII, these acid-soluble anions, in response
to the charge equation, have a greater mole fraction in
plasma than in red cells, just as the chloride ion does.
In fact, however, most of the $HPO_4^=$ in whole blood is in
the red cell interior [7], and we presume the same for
$SO_4^=$ [13], although the evidence for this is meager and
somewhat contradictory.

Ion selectivity of the membrane may cause these
anions to appear mainly in the cell interior; $HPO_4^=$ in

particular may become involved in large complexes with low permeability, giving a choice of methods to insure the approximate distribution: An intraphase, red cell reaction to combine the HPO_4^- and SO_4^- with an impermeable species; or interphase, transport-forcing functions similar to the sodium pump. Either process would hold these red cell anions in a predetermined proportion--a proportion which would vary, however, with the number of other anions present because of the charge equation and Gibbs-Donnan effects.

We choose for this example the interphase pump for distributing the HPO_4^- and SO_4^-. Thus, in Table VIII, the free energy parameters, c_j, for these anions differ by 2.0 between plasma and red cell. As in Eq. (6), this causes a mole fraction gradient between the two compartments: the mole fraction ratio is approximately three, the mole fraction being greater in red cells (Table IX). More detail will be added in later models where the phosphate also ionizes in a buffering reaction.

The second modification gives the atmospheric gases a different solubility coefficient in the red cell milieu than in plasma. Using the data from Roughton [14], Table VIII shows the computed differences in solubility as

Table VIII

INPUT DATA--MODEL G

Expected Species	Free Energy Parameter	Input Species				
AIR OUT						
O2	-10.940000	1.000 O2				
CO2	-7 690000	1.000 CO2				
N2	-11.520000	1.000 N2				
H2O	-36.600000	1.000 H+	1.000 OH-			
PLASMA						
O2	0.	1.000 O2				
CO2	0.	1.000 CO2				
N2	0.	1.000 N2				
H+	0.	1.000 H+	-0.		-0.	1.000 *PLASM
OH-	0.	1.000 OH-	-0.		-0.	-1.000 *PLASM
CL-	0.	1.000 CL-	-0.		-0.	-1.000 *PLASM
NA+	0.	1.000 NA+	-0.		-0.	1.000 *PLASM
K+	0.	1.000 K+	-0.		-0.	1.000 *PLASM
CA++	0.	1.000 CA++	-0.		-0.	2.000 *PLASM
MG++	0.	1.000 MG++	-0.		-0.	2.000 *PLASM
SO4=	0.	1.000 SO4=	-0.		-0.	-2.000 *PLASM
HPO4=	0.	1.000 HPO4=	-0.		-0.	-2.000 *PLASM
UREA	0.	1.000 UREA				
GLUCOS	0.	1.000 GLUCOS				
LACTIC	0.	1.000 LACTIC	-0.		-0.	-1.000 *PLASM
NH4+	0.	1.000 NH4+	-0.		-0.	1.000 *PLASM
HCO3-	-21.350000	1.000 CO2	1.000 OH-		-0.	-1.000 *PLASM
H2CO3	-32.840000	1.000 CO2	1.000 H+	1.000 OH-		
CO3=	6.260000	1.000 CO2	-1.000 H+	1.000 OH-	-2.000 *PLASM	
H2O	-39.390000	1.000 H+	1.000 OH-			
MISCPR	0.	1.000 MISCPL	-0.		-0.	-10.000 *PLASM
RED CELLS						
O2	-0.490000	1.000 O2				
CO2	0.	1.000 CO2				
N2	-0.500000	1.000 N2				
H+	0.	1.000 H+				
OH-	0.	1.000 OH-				
CL-	0.	1.000 CL-				
NA+	2.193399	1.000 NA+				
K+	-2.941575	1.000 K+				
CA++	2.751790	1.000 CA++				
MG++	-0.457703	1.000 MG++				
SO4=	-2.000000	1.000 SO4=				
HPO4=	-2.000000	1.000 HPO4=				
UREA	0.	1.000 UREA				
GLUCOS	0.	1.000 GLUCOS				
LACTIC	0.	1.000 LACTIC				
NH4+	0.	1.000 NH4+				
HCO3-	-21.490000	1.000 CO2	1.000 OH-			
H2CO3	-32.840000	1.000 CO2	1.000 H+	1.000 OH-		
CO3=	6.120000	1.000 CO2	-1.000 H+	1.000 OH-		
H2O	-39.390000	1.000 H+	1.000 OH-			
MISCPR	0.	1.000 MISCRE				
HB4	0.	1.000 HB4				
HB4O2	-15.230000	1.000 O2	1.000 HB4			

Table IX

COMPLETED DISTRIBUTION--MODEL G

PRELIMINARY BLOOD MODEL   STD STATE   NO PROTEIN REACTIONS   DEI AND

		AIR OUT	PLASMA	RED CELLS
X-BAR		9.99127E 02	2.88744E 01	1.79596E 01
PH		-0.	7.39264E 00	7.19424E 00
O2	MOLES	1.31498E 02	6.73954E-05	6.84255E-05
	MFRAC	1.31613E-01	2.33409E-06	3.80997E-06
CO2	MOLES	5.26022E 01	6.95300E-04	4.37470E-04
	MFRAC	5.26487E-02	2.40801E-05	2.40801E-05
N2	ES	7.54000E 02	2.16367E-04	2.21882E-04
	RAC	7.54659E-01	7.49339E-0	1.23545E-05
H2O	MOLES	6.10264E 01	2.87139E 01	1.78598E 0'
	MFRAC	6.10797E-02	9.94440E-01	9.94440E-.
H+	MOLES	-0.	2.10661E-08	2.06905E-08
	MFRAC	-0.	7.29576E-10	1.15206E-09
OH-	MOLES	-0.	3.07724E-07	1.21211E-07
	MFRAC	-0.	1.06573E-08	6.74909E-09
CL-	MOLES	-0.	5.74290E-02	2.26210E-02
	MFRAC	-0.	1.98892E-03	1.25955E-03
NA+	MOLES	-0.	7.64455E-02	8.37448E-03
	MFRAC	-0.	2.64752E-03	4.66295E-04
K+	MOLES	-0.	2.29755E-03	4.27525E-02
	MFRAC	-0.	7.95704E-05	2.38048E-03
CA++	MOLES	-0.	1.37985E-03	2.25154E-04
	MFRAC	-0.	4.77878E-05	1.25367E-05
MG++	MOLES	-0.	4.67237E-04	1.14526E-03
	MFR C	-0.	1.61617E-05	6.37688E-05
SO4=	MOLES	-0.	1.84653E-04	3.40347E-04
	MFRAC	-0.	6.39502E-06	1.89507E-05
HPO4=	MOLES	-0.	5.02959E-04	9.27041E-04
	MFRAC	-0.	1.74188E-05	5.16181E-05
UREA	MOLES	-0.	1.93713E-03	1.20487E-03
	MFRAC	-0.	6.70879E-05	6.70879E-05
GLUCOS	MOLES	-0.	2.26019E-03	1.40581E-03
	MFRAC	-0.	7.82764E-05	7.82764E-05
LACTIC	MOLES	-0.	1.45850E-03	5.74497E-04
	MFRAC	-0.	5.05119E-05	3.19883E-05
NH4+	MOLES	-0.	4.38403E-04	4.30592E-04
	MFRAC	-0.	1.51833E-05	2.39755E-05
HCO3-	MOLES	-0.	1.38678E-02	6.23113E-03
	MFRAC	-0.	4.80280E-04	3.49859E-04
H2CO3	MOLES	-0.	9.88831E-07	6.15043E-07
	MFRAC	-0.	3.42459E-08	3.42459E-08
CO3=	MOLES	-0.	1.94118E-05	5.79988E-06
	MFRAC	-0.	6.72284E-07	3.23133E-07
MISCPR	MOLES	-0.	8.70600E-04	3.75050E-03
	MFRAC	-0.	3.01512E-05	2.08830E-04
HB4	MOLES	-0.	-0.	3.35368E-04
	MFRAC	-0.	-0.	1.86734E-05
HB4O2	MOLES	-0.	-0.	8.75463E-03
	MFRAC	-0.	-0.	4.87452E-04

modified, free energy parameters. The result is the solution of slightly more O_2 and N_2 in the red cell milieu than in plasma. Reference 2 computes these data.

Finally, this preliminary model incorporates an illustrative reaction of hemoglobin with oxygen. Hemoglobin oxygenation has an extensive literature (summarized in Ref. 14) and is, of course, still the subject of much research. This preliminary, illustrative model incorporates one of the earlier theoretical structures of the oxygenation reactions. Studying a simpler theory and its shortcomings clarifies some of the details of, and much of the motivation for, the following two chapters.

In 1910, A. V. Hill [15] proposed that reaction of a solution of hemoglobin with oxygen could be written

$$Hb + nO_2 \rightleftarrows Hb(O_2)_n \ , \ K \tag{7}$$

where both K and n were to be determined from empirical data from the laboratory. Using the Hill equation, as in Ref. 14, the percent saturation of hemoglobin with oxygen, y, can be computed from

$$\frac{y}{100} = y' = \frac{Kp^n}{1 + Kp^n} \tag{8}$$

where p is the oxygen pressure in millimeters. The
saturation can be measured in the laboratory at various
pO_2 by a variety of means. Comparing the laboratory
experimental curve to that given by Eq. (8), one can
attempt to "fit" the laboratory curve by adjusting K and
n [14].

The discussion in the literature centers around the
fact that unique K and n cannot be found to fit the ex-
perimental curve over the entire range of oxygen pressure
from zero to, say, 150 millimeters. A deterrent to fit-
ting the curve under general conditions (i.e., physiologic)
is the difficulty of determining a satisfactory laboratory
experimental curve, particularly at the extreme values of
oxygen pressure [14].

But, for purposes of this comparison, the Dill curves
[16] are satisfactory. They have been the standard for
many years [7], and were obtained under conditions reason-
ably well-controlled for the time.

Table VIII has, in the red cell compartment, a reac-
tion of oxygen with hemoglobin (cf. Table V). The re-
action constant, K, is determined in the model to give a
normal saturation (97 percent) at 100 mm O_2. Figure 1
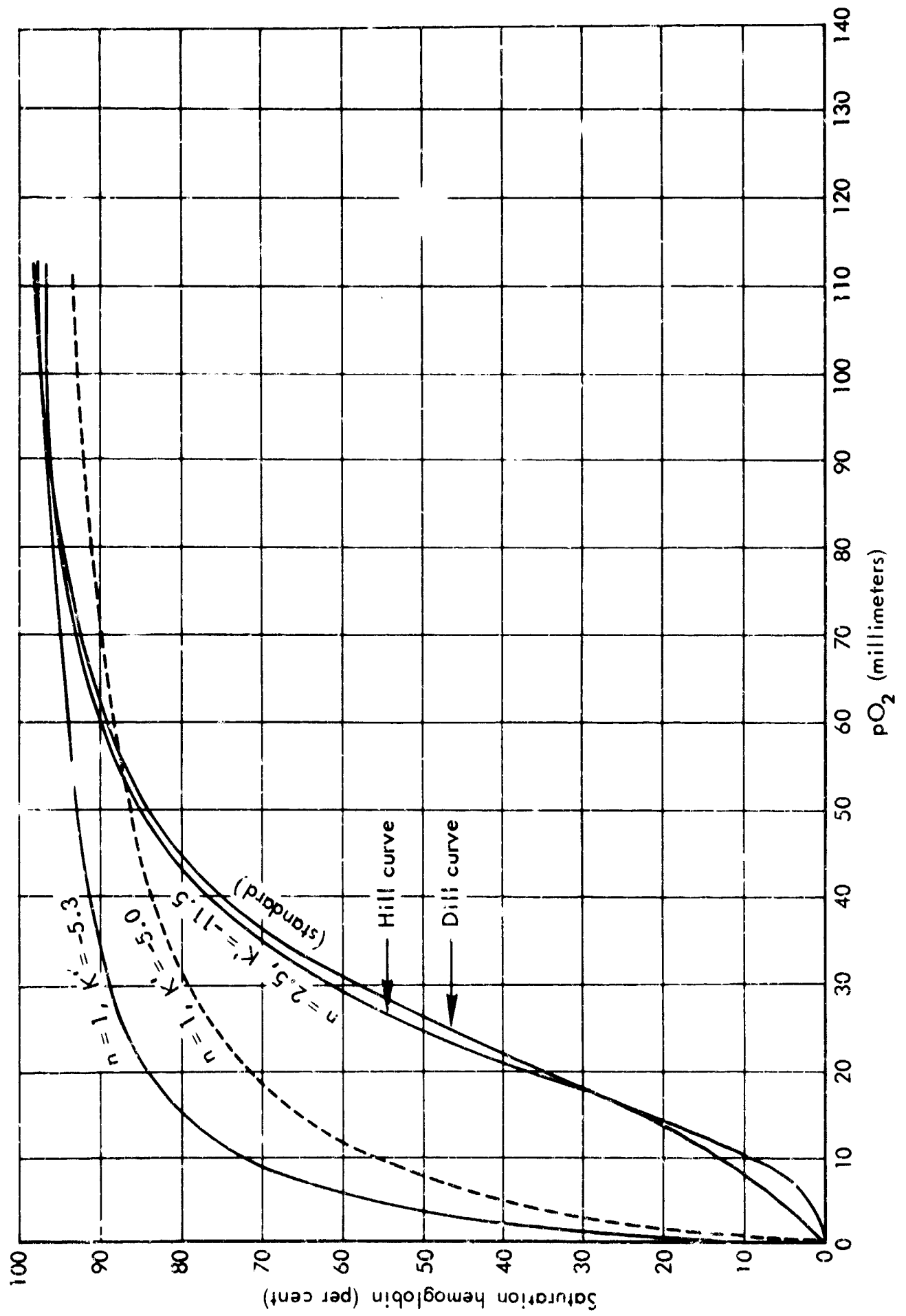shows two cases (computed by varying the rO_2): two curves

Fig. 1.—Experimental hemoglobin saturation hypotheses

for the case n = 1 (as in Table VIII) and a curve for the case n = 2.5 as Hill originally determined. The normal Dill curve also appears. The Dill curve, of course, was determined under general physiologic conditions.

Hemoglobin has four binding sites for oxygen. So for the case n = 1, in order to bind one oxygen per molecule of hemoglobin, the hemoglobin was conceptually broken into four parts, each with a heme, as in Eq. (7). Thus, for the case n = 1, 9.09 rather than 2.2725 moles of hemoglobin combine with oxygen. The reaction constant for this case is $K = 4.98 \times 10^{-3}$, or $\ln_e K = K' = -5.30$. Reducing this constant immediately decreases the maximum saturation without materially shifting the curve toward the Dill curve, as for the curve with $K = 6.74 \times 10^{-3}$, $K' = 5.0$. The pH is 7.39 in plasma, 7.19 in red cells.

The Hill curve with n = 2.5 uses the proper average number of moles of hemoglobin, 2.2725, per liter of blood, but the fixed average number of oxygen molecules, 2.5, attach to each molecule of hemoglobin. Thus, each hemoglobin, Hb_4, has either 2.5 molecules of O_2 attached or none at all. There are no intermediate stages. An equilibrium constant of $K = 1.51 \times 10^{-4}$, $K' = -11.1$ is necessary to give 97 percent saturation at 100 mm O_2 and the same pH as before.

Some of the data for Fig. 1 (the $n = 2.5$ and $n = 1$, $K = 5.3$ curves) are verified in Ref. 14 where similar curves were computed by desk calculator (the values of K are not given). This reasonably validates the present model under varying conditions. But the discrepency between the empirical Dill curve and the Hill curves necessitates better hypothesis and an improved model. Subsequent biochemical hypotheses for the oxygenation reactions are increasingly sophisticated [2] and, also, the presence of CO_2 and H^+ are important. Hemoglobin binds CO_2 in the carbamino reactions as well as buffering the H^+ ion; both of these reactions effect oxygenation. Reference 2 discusses these problems.
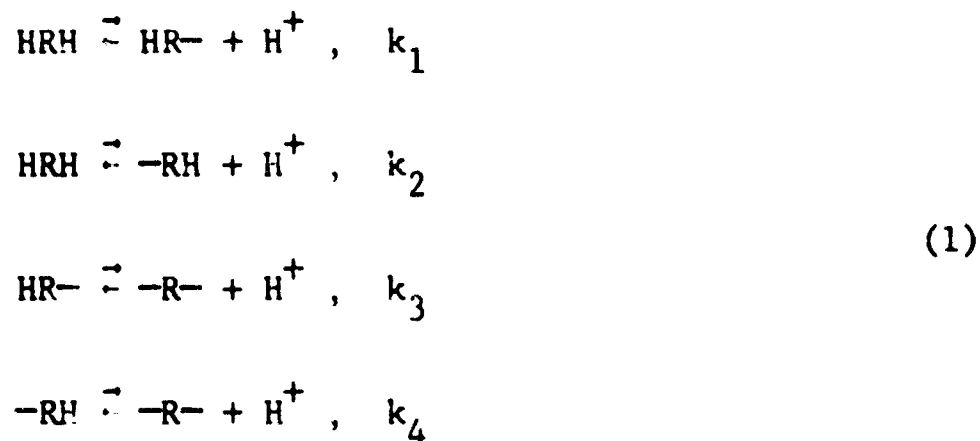
Chapter II

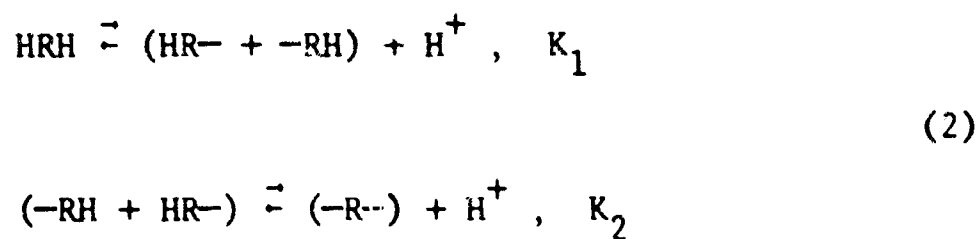## CONCEPTUAL COMPARTMENTS

1. INTRODUCTION

Chemically speaking, by far the most interesting constituents of the blood are the proteins. These species along with other complex constituents--the organic phosphates, the lipids, the carbohydrates--can combine with other blood constituents potentially to create innumerable biochemical reaction products. However, such a model, with lists of possibly thousands of reactions, would be extremely unwieldy; and the thousands of necessary microscopic reaction constants probably could not be determined.

The problem then is to make a model which approximates the more complex real situation but, at the same time, has exactly the same characteristics as the large model wherever possible.

The following elementary example illustrates this remark. Consider a polypeptide having two identical but independent ionizing groups--i.e., the ionization of one does not affect the ionization of the other. Thus, a representative molecule HRH has three ionization states and four reactions

$$\text{HRH} \rightleftharpoons \text{HR--} + \text{H}^+ \;, \quad k_1$$

$$\text{HRH} \rightleftharpoons \text{--RH} + \text{H}^+ \;, \quad k_2$$

$$\text{HR--} \rightleftharpoons \text{--R--} + \text{H}^+ \;, \quad k_3 \qquad\qquad (1)$$

$$\text{--RH} \rightleftharpoons \text{--R--} + \text{H}^+ \;, \quad k_4$$

each with the intrinsic microscopic dissociation constant k_i or intrinsic association constant $1/k_i$. But if the paths of ionization are immaterial, one can instead write [8]

$$\text{HRH} \rightleftharpoons (\text{HR--} + \text{--RH}) + \text{H}^+ \;, \quad K_1$$

$$\qquad\qquad (2)$$

$$(\text{--RH} + \text{HR--}) \rightleftharpoons (\text{--R--}) + \text{H}^+ \;, \quad K_2$$

with constants K_1 and K_2, respectively, where K_1 and K_2 are the apparent titration constants obtained from a laboratory titration curve, and HR-- and --RH are indistinguishable, i.e., a single species. The constants k_i and K_i can be related by the following reasoning: Considering the several mass action equations for Eqs. (1) and (2), we may write, as in Ref. 8,

$$K_1 = \frac{[(-RH) + (HR-)] (H^+)}{(HRH)} = \frac{(-RH)(H^+)}{(HRH)} + \frac{(HR-)(H^+)}{(HRH)}$$

$$\tag{3}$$

$$= k_1 + k_2$$

and

$$K_2 = \frac{(-R-)(H^+)}{[(-RH) + (HR-)]} = \left\{ \frac{[(-RH) + (RH-)]}{(-R-)(H^+)} \right\}^{-1}$$

$$\tag{4}$$

$$= \left\{ \frac{1}{k_3} + \frac{1}{k_4} \right\}^{-1} .$$

The two chemical systems, Eq. (1) and Eq. (2), are thus completely convertible, and equivalent in the sense that the computed ratios of concentrations for $(-R-)/(HRH)$ at equilibrium are identical, as are the concentrations of (H^+) and $(-HR + HR-)$. The first case, however, requires four reactions to represent the system; the second, only two.

This and other types of reductions to be discussed have a common property: They reduce the size of the problem but not the simulation accuracy. Such reductions

are important in the computer model, since both the computing time and the size of the computer required for a solution increase nonlinearly with the problem size. In biological systems, a problem could easily be too large--i.e., have too many chemical reactions in its representation--for even a reasonably large computer.

In the blood, serum albumin has 190 sites for active hydrogen ionization, each of which falls into one of four classes. These classes are independent but not mutually exclusive; i e., ionization in one class does not prohibit ionization in another. Because ionization can occur simultaneously in all four classes, they must be considered as simultaneous events though not with equal probability. Since each site has two possible states and there are 99 sites in the first class, 16 in the second, 57 in the third, and 18 in the fourth, then $2^{99} \times 2^{16} \times 2^{57} \times 2^{18} \approx 10^{60}$ states are possible--each of which must be represented in the model. Obviously, some reduction is necessary.

While an equivalent representation can reduce the size of complex systems, as in Eqs. (1) and (2), conceptual compartmentalization is generally an even more economical device. As will be shown, the conceptual

compartments are artificial compartments created in the chemical milieu of the model to isolate classes of reactions on complex molecules when these reactions can occur simultaneously. As in the example of serum albumin, the reactions of independent classes may occur simultaneously--thus, the same molecule must have multiple representation to show all possible configurations. The procedure suggested here is to identify and characterize the myriad chemical reactions according to class (type of ligand) and interdependence (mutually exclusive, dependent, or independent), in order to represent each _class_ of reaction as an isolated event rather than representing all possible ed-class species. Since the classes of reactions are much fewer than the total possible number of species, the reduction can be considerable.

2.   CONCEPTUAL COMPARTMENTS

PROTEIN IONIZATION--EXAMPLE

The blood macromolecules of principal concern are serum albumin, the various globulins, and hemoglobin. Because serum albumin is perhaps the simplest, most stable, and best known, it will be used extensively as an example. This protein is the most abundant of the plasma proteins, about ten times more numerous than the next most abundant. The pertinent characteristic of serum albumin is its ability to buffer hydrogen ion in the physiological range of pH, but its activity is by no means limited to proton binding. Serum albumin also binds small ions of either sign and even small neutral molecules. To simplify the description of serum albumin for the model, we will deal exclusively with the hydrogen binding activity.

Tanford, et al. [17] and Tanford [18] (sources for much of the factual data on albumin) list among the hydrogen-binding sites of serum albumin, 99 carboxyl radicals with average pK $\approx$ 4.02 at 25°C. The carboxyl groups alone have 99 configurations of the molecule in which it has lost just one hydrogen, 99x98/2 configurations in which it has lost two hydrogens, and so on, in

all 2^{99} species in the milieu. But several ways exist
to reduce this variety to an approximate or an equivalent
system.

Assume first that the 99 sites are equivalent and
independent, that the ionization of one site will not
affect the probability of ionization of any other. An
equivalence can then be drawn between the ionization of
this polybasic acid and 99 monobasic acids, each with the
same pK and the same concentration as the protein. But
this equivalence is immediate if the protein is concep-
tually split into n parts. If $\bar{h}$ is the number of moles
of hydrogen released per mole of protein per site then,
as for a monobasic acid,

$$RH \rightleftharpoons R- + H^+ \ , \quad k \tag{5}$$

or

$$k = \frac{(R-)(H^+)}{(RH)} = \frac{\bar{h}}{1-\bar{h}} (H^+) \ , \tag{6}$$

where k is the microscopic dissociation constant for that
particular site. If this were the only site for ioniza-
tion, then clearly the ideal titration constant determined
in the laboratory would be k. For n identical, independent

sites on each molecule of R, n times as many protons will
be released at the same pH, but of course the ionization
pK remains the same, i.e., -log k. Also, $\bar{\nu} = n\bar{h}$ is the
moles of protons for all sites per mole of R. Therefore,

$$\frac{n\bar{h}}{n(1-\bar{h})} = \frac{(R-)}{(RH)}$$

or

$$k = \frac{\bar{\nu}}{n-\bar{\nu}} (H^+) \ ,$$

where, again, the empirically observed titration constant
in vitro would also be simply k.

For the similar case of n moles of monovalent acid,
each with the same concentration and pK as for R, the
titration constant will equal that of the protein, i.e.,
either system will buffer maximally at the pK of the in-
trinsic ionization groups. Then, in titration or buffering
action, the two systems would be indistinguishable except
for electrostatic concentration effects.

We note for future reference the difference between the titration constants and the dissociation constants. For the monovalent acids, these two constants are the same and are given by the mass action equation, i.e., the pK of the ionizing hydrogen. For the protein, the pK of the ionizing class (Eq. (6)) gives the titration constant; but the dissociation constant, given by mass action equations where the protein is not conceptually split, depend upon the number of hydrogens dissociated (and perhaps the particular configuration of their dissociation). This difference is important because the apparent mass action equation constant for a protein may be difficult to measure, whereas the titration constant can be determined from the in vitro titration curve.[+]

This discussion implies that, under the strong assumption of equivalence and independence of the groups of a given class, for application to the computer model, the simulation of the protein could be obtained by writing down the chemical reaction, Eq. (5), and inserting this in the model with constant k and in amount n times RH, i.e., n monovalent acids. In fact, the simulation is not quite so simple: the milieu would contain n times too much protein and the osmolarity would be in error.

[+]Ref. 8, Chap. 9.

However, in other respects--e.g., the buffering re-
action--this simulation would be perfectly valid. There-
fore, the model may reasonably contain an osmotically
isolated compartment for the monovalent acids. This
conceptual compartment will be impermeable to all species
except H^+ ion and will not be counted in the osmolarity--
it will be a sink or source of H^+ ion, a place to store
H^+ ion effectively out of the milieu in proportion to the
pK of the monovalent acids which are available only with-
in the conceptual compartment.

The example of serum albumin in Sec. 1 permits more
specificity. Table X gives five major classes of ionizing
sites on the protein, each with a distinct number of sites.
There are 17 imidazole groups, 57 ϵ-amino groups, 19 phenolic
groups, and 22 guanidine groups, so that, as on p. 46,
approximately 10^{60} species are possible and an equal number
of intrinsic constants could be required for a chemical
description.

The method of conceptual compartments replaces each
ionizing class with a single monobasic acid having the
"average" pK of that class, but with n times the mole
number of the protein, where n is the number of sites in
the class. Then, to not disturb the osmolarity (or the

Table X[a]

TITRATABLE GROUPS PER 65,000 GRAMS SERUM ALBUMIN

	Found by Titration	Amino Acid Analysis
α-carboxyl	(1)	1
β, γ-carboxyl	99	≥89.9
Imidazole	16	16.8
α-amino	(1)	1
ϵ-amino	57	57.0
Phenolic	19	18.1
Guanidine	22	22.0
Sulfhydryl (free)	(0)	0.7

[a]Adapted from Tanford, et al. [17].

total mole count), an artificial compartment is created
to contain the monobasic acid. This compartment has but
two species, the ionized and un-ionized forms. The dis-
tribution between these two species is determined by the
pK of the acid and the H^+ ion concentration of the liquid
compartment.

Thus, the serum albumin problem is reduced to a
representation containing just eleven species: the protein
in the main compartment and two species in each ionization

class compartment. The remainder of this section shows
in what respect this problem with eleven species (plus
the remaining species in the liquid phase, such as Na^+,
Cl^-, OH^-, H_2O, etc.) is equivalent to the original problem
of 10^{60} species, where "equivalent" means that the solu-
tions of these two problems will be indistinguishable.

Shapiro [4] develops and proves in general an
equivalence theorem adaptable to the particular case of
serum albumin. Suppose, first, that the ionizing sites
on the protein are divisible into classes (e.g., carboxyl,
alpha-amino, etc.) and that within each class each ionizing
site is indistinguishable, the order of ionization im-
material, and the free energy associated with ionization
is strictly additive (i.e., the ionization of one site
does not in any way affect the ionization of any other).

Second, suppose this entire protein-carboxyl system
is replaced in the mathematical model with a single mono-
basic acid having a pK identical to the equivalent hydrogens
of the protein but 99 times the number of moles of the
protein. Preserving the osmolality requires a new phase
or conceptual compartment containing only the monobasic
acid in its two states, ionized and un-ionized the pro-
tein itself remains unreactive in the original milieu

(again, to keep the osmolality correct). The protein and the monobasic acid are related by a conservation of mass equation.

Shapiro then shows that under these conditions the total number of moles of ionized monobasic acid will equal the number of ionized sites in the original large problem, although the number of species has decreased from 2^{99} to just two. The remaining species other than the protein and monobasic acid will be unaffected in concentration or distribution. Further, the total thermodynamic free energy of the system will be unaffected. We forego the details or proof of the more general theorem.

This model then proceeds similarly for the other classes of ionizing sites on the protein (Table X). The pK of each class comes directly from Tanford, et al. [17], who determine the pK from the titration curve with a correction for the static charge on the molecule and for the adsorbed chloride ion. Reference 19 discusses this computer model in detail and shows that it reproduces the titration curve for serum albumin within two ionizing sites over the range of pH from 3.5 to 10. The extreme ends of the curve require a more complex model.

3. BLOOD PROTEINS: PLASMA

The power and flexibility of conceptual compartmentalization permits further development of the elementary and insufficiently accurate blood model of Chap. I. The simulation will continue by incorporating further complexities of the hemoglobin reactions and certain buffering systems of the blood.

᠇m one view, the principal buffering system of the blood ... the bicarbonate. With the loss of each CO_2 molecule at the lung surface, a free hydrogen ion is absorbed in solution by the OH^- ion from the decomposing bicarbonate ion, thus making the blood more basic. At the tissue level, the absorption by the blood of each CO_2 molecule creates hydrogen ions, making the blood more acid.

These two systems--the production and consumption of H ion by the bicarbonate reactions--need not be and perhaps seldom are in exact balance, thus causing respiratory acidosis or alkalosis. However, the very low CO_2 content of the atmosphere relative to the blood permits CO_2 to be easily released at the lungs; the autonomic controls over depth and rate of respiration and blood flow rate tend to balance production and absorption of H^+ ion.

The necessity for this buffering may be easily shown. At a steady resting state, blood coursing through the tissues picks up about 40 ml of CO_2 per liter in changing from arterial to venous. This is equivalent to the release of about 2 mM of hydrogen ion, since CO_2 either combines with H_2O to form HCO_3^- and liberate a H^+ ion, or forms a carbamino compound with hemoglobin and again liberates almost one hydrogen per reaction. Since the hydrogen ion concentration is normally only about 10^{-7} moles per liter of blood, this tremendous excess acidity must be buffered. The net change in pH during the normal transformation from arterial to venous blood is only about 0.03 pH units.

Hemoglobin itself takes up approximately three-quarters of the excess hydrogen in the oxylabile binding of hydrogen on groups which become available on the molecule as the oxygen is removed at the tissue level. The oxygenation of hemoglobin yields this hydrogen at the lung level, thus preventing the blood from going basic from the loss of CO_2.

The remaining excess hydrogen at the tissue level is buffered principally by the plasma proteins, the phosphate ionization systems, and by the non-oxylabile sites on the

hemoglobin [20]. Plasma proteins, however, may account for a major portion of the remaining excess, since the imidazole groups of the serum albumin are at their maximum buffering power in this important range of pH of the viable system. Peferring again to Tanford [17], one millimole of serum albumin buffers approximately one millimole of hydrogen in a change of 0.1 pH point. Since the pH changes about 0.03 points from arterial to venous blood and since there is approximately 0.5 mM of serum albumin per liter of blood, the serum albumin could buffer up to 0.15 mM of H^+ during this change.

Incorporating the plasma protein buffering system into the mathematical model requires modifying the generalized model of plasma protein described in Chap. I. Serum albumin accounts normally for 80 or 90 percent by mole number of the total plasma protein, nd the various globulins for most of the remainder. Fibrinogen is also present, but is not thought to be an important buffer. We assumed that the two principal proteins represent all of the important buffering power of the plasma fraction, and have similar titration curves, particularly in the middle, viable range of pH. This latter assumption is not quite true [18,21], but considering the small

proportion of globulin and the reasonably small difference in the titration curves in the viable range, the error will be insignificant--not more than 2 percent of the maximum buffering power of the plasma proteins.

Finally, the titration curve itself is more sophisticated than indicated in the previous section. Tanford [17] used a solution of serum albumin with salt added to provide an ionic strength 0.15. Thus, the titration curve incorporates the electrostatic charge on the molecule of protein and the competitive binding of chloride ion. The pK of the hydrogen-binding sites thereby varies appropriately through the range of pH. References 19 and 22 detail this problem. Of course, the behavior of the protein in plasma may differ greatly from its behavior in the 0.15 molar NaCl titrating solution. However, this error can temporarily be discounted, since Chap. III will demonstrate with Astrup diagrams and more stringent tests that the simulated blood does buffer properly.

Serum albumin binds anions, cations, and even uncharged particles by incompletely understood mechanisms [8]. However, Cl^- probably binds to the positively charged amine groups; this reaction is a function of the pH and the concentration of chloride ions. Scatchard, et al. [23],

for example, discuss the binding of Cl^-, which is important in the respiratory function of blood; Loken, et al. [24] treat the binding of calcium. These reactions change the net charge on the protein molecule and thus affect the buffering power of the protein; but by tying up permeable ions, they also affect the Gibbs-Donnan equilibrium. Neither of these systems are explicitly in effect in the model, where serum protein may bind up to 50 percent of the calcium, and up to 10 ions of Cl^- per molecule of protein, depending upon the pH.

The binding of these ions by other proteins has not been studied as closely; in particular, hemoglobin's role is not well understood. We presume that hemoglobin and other complexes within the cell may also bind these small ions. Although we may assume that none of the single-valent alkaline cations are bound, both the double-valent Mg^{++} and the double-valent anions are tied up in various ways. The literature regarding these intracellular reactions is not as definite as for Cl^- and Ca^{++}, and no attempt has been made to account for them.

4. BLOOD PROTEINS: RED CELL

Hemoglobin is only one important constituent of the red cell. In fact, the water content is approximately 99.45 percent of the total moles; hemoglobin is only about 1.5 percent of the remainder, or about 2.30 mM per liter of blood. However, hemoglobin is more prominent in terms of mass: each liter of blood contains about 160 grams of hemoglobin--all in the 450 cc occupied by red cells. The hemoglobin protein, minor impermeable constituents, and the membranes of the red cells (which are very thin) increase the volume of the cells over that of the pure water content by about 120 cc per liter of blood.

The physical-chemical structure of the red cell interior may orient the hemoglobin molecules with respect to each other, perhaps linked in a fluid crystalline lattice. In any case, we assume an homogeneous fluid throughout, with reasonably steady composition states (within measurable error) when the cell environment is constant. A change in the environment results in a change in the cell interior--i.e., in the rate of its mechanisms-- and consequently a new steady state.

Besides hemoglobin, inorganic electrolytes, organic permeable molecules and ions, and water the red cell

contains a complex of interesting and active substances, most of which are charged. The kinds of these particles (organic phosphates, enzymes, chelates, etc.) are so numerous and their specific contributions so varied that they are usually lumped together in the electrolyte balance as simply X^-.

The milliequivalents of this total are more easily calculated than the actual millimoles. By assuming that the red cell milieu of a given volume of arterial red cells is neutrally charged, one can compute the total charge attributable to X^---about 10 milliequivalents of negative charge per liter of blood. Then, since the osmolarity of the milieu should equal that of plasma, and the moles of each other substance are report_d, one can determine that there should be about 7.5 millimoles of X, only an approximate calculation.

From this, however, the average charge per average molecule is between one and two, about the average charge of inorganic phosphate or of a hemoglobin molecule near the viable pH. Accordingly, the mathematical model carries 7.5 mM of X^- per liter, but (as Chap. III proves) for the present model the net charge need not be specified. This

is a temporary procedure for handling the mixture of substances denoted by X^-, whose details may be added gradually to the model as specific reactions data become available or important. However, the situation for hemoglobin differs considerably, since its details are important and relatively well-known.

Hemoglobin's chemical reactions important to respiration are the reversible combinations formed with:

1) Oxygen (via the four iron atoms in the heme groups);

2) Carbon dioxide (via $-NH_2$ groups, probably those in heme and lying near the iron atom);

3) Hydrogen ion (via the $-COOH$, $-\alpha NH_2$, and $-\epsilon NH_3^+$ groups, a significant number of which are oxylabile in their ionization; i.e., the oxygen attachment affects the bonding energy).

The Adair [25] equation for the oxygen dissociation of hemoglobin under standard conditions--viz.,

$$y = \frac{y'}{100} = \frac{(a_1 p + 2a_2 p^2 + 3a_3 p^3 + 4a_4 p^4)}{4(a_0 + a_1 p + a_2 p^2 + a_3 p^3 + a_4 p^4)} \qquad (7)$$

where

y' = percent saturation of hemoglobin,

$a_0 = 1$,

$$a_j = \prod_{i=1}^{j} K_i \tag{8}$$

p = oxygen pressure in millimeters,

and

$$[Hb_4(O_2)_i] = K_i\, p[Hb_4(O_2)_{i-1}] \tag{9}$$

--is used in this model, as in Ref. 2, for the generation of the empirical saturation curve.

Given an empirical curve, y vs. p, from the laboratory, the analytic problem is to find the unique set of four parameters, the ratios $a_0: a_1: a_2: a_3: a_4$, or simply the apparent K_j, that enable Eq. (7) to reproduce the curve within the model. Because of the oxylability of the ancillary reactions of hemoglobin, however, these apparent K_j may differ from the intrinsic K_j of Eq. (9). In this circumstance, Pauling [26] correctly wrote K'_j for the apparent constants in the milieu and K_j for the intrinsic constants of "pure" hemoglobin. The solution of this impasse lies in finding analytical transformations,

based upon structural, physical, and chemical hypotheses, which will carry one set of constants into the other,

$$K_j \overset{T}{-} K_j'.$$

The apparent macroscopic K_j',

$$Hb_4(O_2)_{j-1} + O_2 \overset{K_j'}{=} Hb_4(O_2)_j \quad \text{for each } j, \quad (10)$$
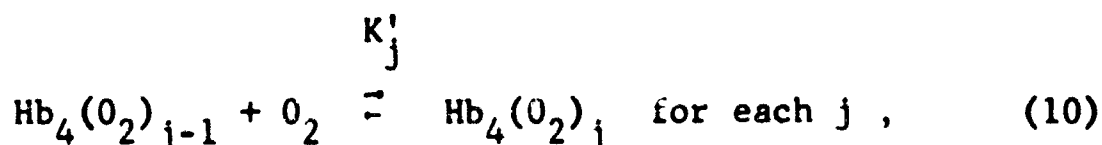
are not identical, and we have

$$y = \frac{y'}{100}$$

$$= \frac{K_1'p + 2K_1'K_2'p^2 + 3K_1'K_2'K_3'p^3 + 4K_1'K_2'K_3'K_4'p^4}{4\left(1 + K_1'p + K_1'K_2'p^2 + K_1'K_2'K_3'p^3 + K_1'K_2'K_3'K_4'p^4\right)} \quad (11)$$

for the Adair Eq. (7).

Reference 2 discusses the use of the computer in the derivation of the oxygenation constants. This study utilizes the ratios derived independently on the computer and by Roughton, et al. [27,28], namely, $K_1' : K_2' : K_3' : K_4' :: 1 : 0.4 : 0.24 : 9.4$. The absolute values are adjusted to give the proper saturation of hemoglobin at p50, the oxygen pressure for half-saturation. Chapter III

discusses the quantitative goodness-of-fit for these constants.

This simulation assumes that the transformation T is affected only by the ancillary oxylabile carbamino and hydrogen ionization reactions. In deriving T, we may reasonably assume [14] two oxylabile hydrogen ionization sites per heme group on hemoglobin, and 16 sites per heme for non-oxylabile ionization. Identification of the position and kind of these sites on the actual molecule is not yet definite [14], but for convenient reference this simulation classifies the oxylabile sites as a carboxyl and an alpha-amino, the non-oxylabile as identical ligands on histidine groups. Further, we assume that the pK's of the oxylabile groups are sufficiently far apart that only three species with respect to the oxylabile heme groups appear in the milieu:

$$R_{NH_3^+}^{COOH} \;\overset{K_2}{\rightleftharpoons}\; R_{NH_3^+}^{COO^-} \;\overset{K_1}{\rightleftharpoons}\; R_{NH_2}^{COO^-} \tag{12}$$
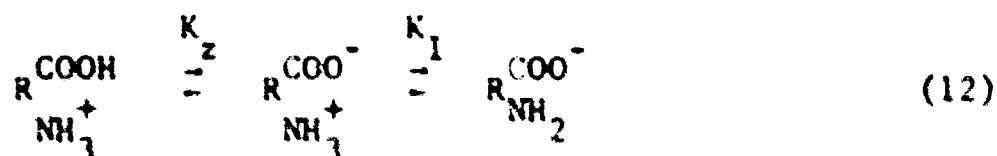
where R is a heme group.

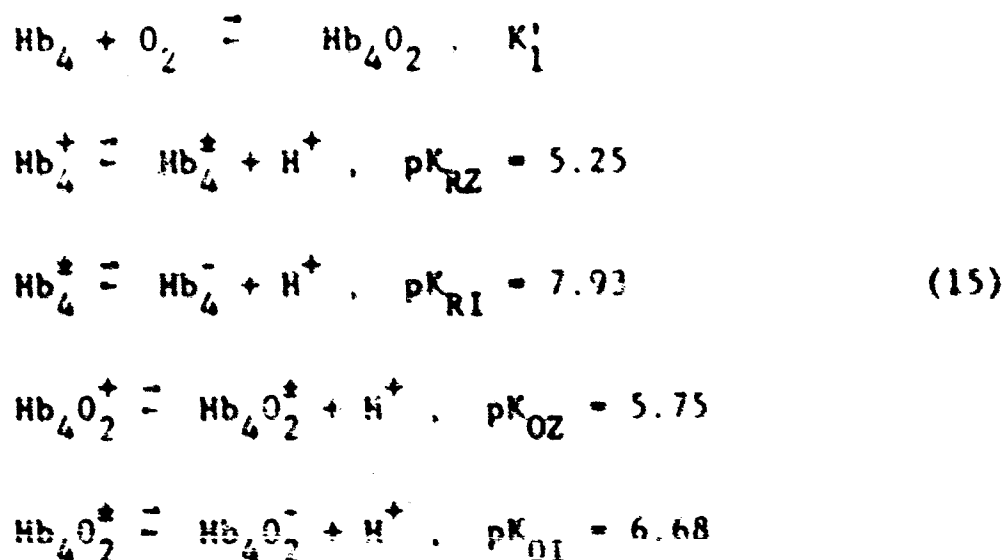Evidently, the CO_2 molecule is bound only by the amphiani he species on the right of Eq. (12), with the

amino in the NH_2 condition. The apparent constants for oxygenated and reduced hemoglobin differ, and therefore the equations for the model are

$$Hb + CO_2 \rightleftharpoons Hb(CO_2) + H^+ , \quad K_{RC} = 6.4 \times 10^{-6} \tag{13}$$

and

$$HbO_2 + CO_2 \rightleftharpoons HbO_2(CO_2) + H^+ , \quad K_{OC} = 2.5 \times 10^{-6} \tag{14}$$

where the symbol Hb indicates a 1/4 hemoglobin molecule, and/or a reactive group on an amphanionic heme. Similarly, the pK_1 for hydrogen ionization will have subscripts referring to oxygenated or reduced hemoglobin, and the apparent pK_1 may correspond to any number of H^+ equivalents ionized. The equations relating to the first stage of oxygenation are:

$$Hb_4 + O_2 \rightleftharpoons Hb_4O_2 \quad K_1'$$

$$Hb_4^+ \rightleftharpoons Hb_4^{\pm} + H^+ , \quad pK_{RZ} = 5.25$$

$$Hb_4^{\pm} \rightleftharpoons Hb_4^- + H^+ , \quad pK_{RI} = 7.93 \tag{15}$$

$$Hb_4O_2^+ \rightleftharpoons Hb_4O_2^{\pm} + H^+ , \quad pK_{OZ} = 5.75$$

$$Hb_4O_2^{\pm} \rightleftharpoons Hb_4O_2^- + H^+ , \quad pK_{OI} = 6.68$$

where K_1 in the first equation is the intrinsic reaction constant for the attachment of O_2 on any of the four hemes. K_1' is the apparent constant measured in the laboratory in the presence of H^+ or CO_2 reactions. Equations (13), (14), and (15) specify the interrelated reactions with respect to the first oxygenation state. Computing the ratio (in moles) of oxygenated to reduced molecules yields (suppressing the square concentration brackets)

$$\frac{Hb_4 O_2}{Hb_4} = K_1'[O_2]$$

$$= \frac{Hb_4 O_2^{\pm} + Hb_4 O_2^{+} + Hb_4 O_2^{-} + Hb_4 O_2 (CO_2)}{Hb_4^{\pm} + Hb_4^{+} + Hb_4^{-} + Hb_4 (CO_2)} \quad . \tag{16}$$

Alternatively, using the equilibrium constants from the individual mass action equations, Eqs. (9), (13), (14), and (15), pO_2 in millimeters, and concentrations of each species (suppressing the square brackets), yields

$$\frac{Hb_4 O_2}{Hb_4} = K_1'p = \frac{K_1 p + K_1 p \dfrac{H^+}{K_{OZ}} + K_1 p \dfrac{K_{OI}}{H^+} + K_1 p \dfrac{CO_2}{H^+} \dfrac{K_{OI}}{H^+} K_{OC}}{1 + \dfrac{H^+}{K_{RZ}} + \dfrac{K_{RI}}{H^+} + \dfrac{CO_2}{H^+} \dfrac{K_{OI}}{H^+} K_{RC}}$$

or

$$K_1'p = K_1p \; \frac{\dfrac{H^+}{K_{OZ}} + 1 + \dfrac{K_{OI}}{H^+} + \dfrac{CO_2}{(H^+)^2} K_{OC} K_{OI}}{\dfrac{H^+}{K_{RZ}} + 1 + \dfrac{K_{RI}}{H^+} + \dfrac{CO_2}{(H^+)^2} K_{RC} K_{OI}} \;, \qquad (17)$$

where numerator and denominator are divided by $[Hb_4]$ and multiplied by 760 mm. Thus, a complex ratio modifies the intrinsic constant K_1 to give K_1', the apparent constant for first-stage oxygenation in the presence of ancillary reactions. This result, Eq. (17), resembles derivations elsewhere, e.g., Pauling [26].

Equation (11), corresponding to the Adair formulation for the dissociation of hemoglobin--i.e.,

$$Y = \frac{a_1'p + 2a_2'p^2 + 3a_3'p^3 + 4a_4'p^4}{4 \left(a_0' + a_1'p + a_2'p^2 + a_3'p^3 + a_4'p^4 \right)} \qquad (18)$$

--shows the constant $a_1' = K_1'$. Now, if

$$a_2' = K_1' \, K_2' \, ,$$

$$a_3' = K_1' \, K_2' \, K_3' \, ,$$

$$a_4' = K_1' \, K_2' \, K_3' \, K_4' \, ,$$

where the K_j' are the apparent j^{th}-stage oxygenation constants in the milieu of reactions, then

$$a_j' = a_j \frac{\left(\dfrac{H^+}{K_{OZ}} + 1 + \dfrac{K_{OI}}{H^+} + \dfrac{CO_2}{(H^+)^2} K_{OI} \, K_{OC} \right)^j}{\left(\dfrac{H^+}{K_{RZ}} + 1 + \dfrac{K_{RI}}{H^+} + \dfrac{CO_2}{(H^+)^2} K_{OI} \, K_{RC} \right)^j} , \qquad (19)$$

gives a_j for $j=1,\ldots,4$, the intrinsic Adair constants, by an argument similar to that yielding Eq. (17).

This mathematical model incorporates Eqs. (19). A different model may result, however, if the relations of the several reactions of hemoglobin are eventually determined to be dependent in other ways. Some of the H^+ ionization must be oxylabile, but certainly not all; and

the oxygen absorption will depend on H^+ lability. Similarly, remote areas of the protein and heme groups may bind CO_2 as non-oxylabile carbamino, although carbamino formation always depends on the pH. Also, some of these reactions may be mutually exclusive--e.g., the CO and O_2 reactions, and the Ca^{++} and H^+ reactions, not considered here.

In the format of the mathematical model, each stoichiometric chemical reaction requires a separate entry in the matrix of reactions. Thus, if five ways exist for O_2 to combine with Hb_4 and four ways for H^+ ionization, and if these reactions are not mutually exclusive, then 20 entries would represent the possible combinations. However, conceptual compartments convert this "multiplicative" model into an equivalent "additive" model of nine entries. In addition to the principal red cell compartment, the latter model computes carbamino reactions and the H^+ ionization of reduced and oxygenated heme in separate but dependent conceptual compartments.

Equations (19) relate to a model which computes the carbamino reactions of oxygenated or reduced heme in the corresponding ionization compartments. This procedure is efficient and does not yield multiplicative combinations

because Hb^+, $Hb^\pm$, Hb^-, and $HbCO_2^-$ are assumed to be mutually exclusive species, CO_2 combining only with the amphanion form. Also, the present model regards the product of Eqs. (13) and (14) as completely ionized, an assumption which is probably not much in error at viable pH.

Finally, the computer program incorporates Eqs. (9), (13), (14), and (15) as lists of the expected chemical reactions and species in appropriate compartments. Table XI shows the red cell and subsidiary conceptual compartments for the current mathematical model. In the red cell, the Adair formulation has four stages of oxygenation of hemoglobin. The coefficients of the terms reduced heme, oxy heme, and histidine give the number of equivalents assumed in n_j moles of hemoglobin for subsequent reactions in the conceptual compartments. Thus, the coefficients in the red cell compartment count the moles of reduced and oxygenated hemes and the number of oxystable H^+ ionization sites, which are assumed to be on histidines. The two subsidiary compartments each contain the two stages of ionization and a carbamino reaction. The amounts of reduced heme, oxy heme, and histidine

Table XI[a]

HEMOGLOBIN REACTIONS AND HEMOGLOBIN CONCEPTUAL COMPARTMENTS

species in the conceptual compartments derive from the red cell via conservation-of-mass equations called "transfer rows." In all cases, the free energy parameters are the natural logs of the several pK's in the mole fraction scale which give the best fit to the hemoglobin titration curve and to the amount of carbamino formed in the oxygenated and reduced cases.

It now remains to show that the results of the conceptual compartments and transfer rows in the model are simply mass action equations similar to Eqs. (15) and (17); i.e., that H^+ ion and CO_2 reactions with hemoglobin have the hypothesized effect upon the oxygenation reactions.

Write the mass action equations from the model treating the transfer coefficients as a species (see Table XI). Consider the first-stage oxygenation of Hb_4, the row "Hb4O2" in Table XI:

$$\frac{(Hb_4O_2)(RHeme)^3 (OHeme)}{(Hb_4)(O_2)} = e^{-15.7665} \quad , \tag{20}$$

where the symbol RHeme stands for a reduced heme of which Hb_4O_2 contains three, and OHeme represents an oxygenated heme. The concentrations are in mole fractions and the exponent is log base e of the equilibrium constant, i.e., the intrinsic constant K_1'. Equation (20) is, then, the first-stage oxygenation with extra terms which transform the apparent oxygenation (as measured by the actual concentrations) into the intrinsic equilibrium. Equation (20) shows this more clearly if written

$$\frac{(Hb_4O_2)}{(Hb_4)(O_2)} = \frac{1}{(RHeme)^3(OHeme)} e^{-15.7665} , \qquad (21)$$

where the concentrations on the left are measured.

Investigating the nature of the transformation on the right side of Eq. (21) via the mass action equations for the chemical equations in the conceptual compartments (Table XI) yields, comparing Eqs. (15):

$$K_{RZ} = \frac{(RHeme)(H^+)}{(H_2Hb^+)} = e^{-22.4397} , \qquad (22)$$

where

$$(RHeme) = (HHb^{+\ -}) \quad (\text{the zwitterion}) \ ,$$

$$K_{RI} = \frac{(Hb^-)(H^+)}{(RHeme)} = e^{-21.0582} \ ,$$

$$K_{RC} = \frac{(Hb^-)(H^+)^2}{(RHeme)(CO_2)} = e^{-31.4723} \ ,$$

and a similar set from the oxyheme compartment. These exponents are in natural logs and mole fraction scale.

Considering that the mole fractions of all species in a conceptual compartment must sum to one,

$$(RHeme)\left[\frac{(H^+)}{K_{RZ}} + 1 + \frac{K_{RI}}{(H^+)} + K_{OI}\frac{K_{RC}(CO_2)}{(H^+)^2}\right] = 1 \qquad (23)$$

and, similarly,

$$(OHeme)\left[\frac{(H^+)}{K_{OZ}} + 1 + \frac{K_{OI}}{(H^+)} + K_{OI}\frac{K_{OC}(CO_2)}{(H^+)^2}\right] = 1 \ .$$

In addition, the condition that one hemoglobin yields
four conceptual hemes with no change in free energy gives

$$Hb_4 \rightleftharpoons 4(RHeme) \; . \tag{24}$$

Substituting Eqs. (23) and (24) into Eq. (21) immediately
results in Eq. (17). A similar development yields Eq.
(19). The ancillary reactions in the model thus affect
the oxygenation reactions in the hypothesized way, i.e.,
Eq. (19).

Chapter III

VALIDATION OF THE MODEL

1. INTRODUCTION

The addition of the serum albumin buffering and
hemoglobin reactions permits further testing of the mathe-
matical model begun in Chap. I. These tests will subject
the improved model to varied chemical stresses and note
in detail the qualitative and quantitative responses.
Generally, these computer validation experiments will be
similar to laboratory experiments, so that results in the
two facilities may be compared. Emphasis is therefore
placed on reproducing laboratory conditions as nearly
as possible, so that the experiments are comparable.
The subsequent discussions of particular experiments will
further illustrate this point.

2. THE STANDARD STATE

The standard reference state for the blood simulation continues to be the arterial blood of a resting, adult male, as in Tables I and II of Chapter I, where various stages of an increasingly complex model approximated these reference data. The incorporation of serum protein buffering and hemoglobin chemistry--the final stages in this series of experiments--requires another comparison of these standard data with those from the present model.

Tables XII and XIII list the input for this model, called "Standard Model BFFR-1." In comparison to Model G, Chap. I, it contains several important additions. The species protein (PROTN) in the plasma compartment now has subcategories associated with the conceptual compartments Site 1, Site 2, Site 3, and Site 4, where the carboxyl, imidazole, ϵ-amino, and phenolic groups, respectively, are ionized. The miscellaneous protein (sometimes called "X^-") in the red cells also is ionized at an average pK of 6.79. The hemoglobin is oxygenated in the four Adair stages and undergoes ionization and carbamino reactions according to the data developed in Chap. II. (Table XIII also shows the subcompartments of the red cell.)

Table XII

STANDARD MODEL INPUTS

(Species in Liquid Phase Given in Moles per Liter Blood, Gas in Mole Fractions)[a]

EXPERIMENTAL HUMAN BLOOD BFFR-1 NIH-DELAND '64

ROWS	LIQUID PHASE	FRESH AIR	GAS (ARTERIAL)	GAS (VENOUS)
O2	6.3300000E-03	2.0990000E-01	1.3150000E-01	5.2600000E-07
CO2	2.3490000E-02	3.0000000E-04	5.2600000E-07	6.0500000E-02
N2	4.3700000E-04	7.8980000E-01	7.5400000E-01	8.2580000E-01
H+	4.6500000E 01	-0.	6.1099999E-07	6.1099999E-07
OH-	4.6552121E 01	-0.	6.1099999E-02	6.1099999E-07
CL-	8.0050000E-02	-0.	-0.	-0.
NA+	8.4820000E-02	-0.	-0.	-0.
K+	4.5050000E-02	-0.	-0.	-0.
CA++	1.6050000E-03	-0.	-0.	-0.
MG++	1.6125000E-03	-0.	-0.	-0.
SO4=	5.2500000E-04	-0.	-0.	-0.
HPO4=	1.4300000E-03	-0.	-0.	-0.
NH4+	8.6900000E-04	-0.	-0.	-0.
LACTIC	7.0330000E-03	-0.	-0.	-0.
UREA	3.1420000E-03	-0.	-0.	-0.
GLUCOSE	3.6660000E-03	-0.	-0.	-0.
MISCPLASMA	5.3800000E-04	-0.	-0.	-0.
MISCREDCELL	7.5000000E-03	-0.	-0.	-0.
MB6	2.2750000E-03	-0.	-0.	-0.
RED MEME RNA	-0.	-0.	-0.	-0.
OXY MEME CHR	-0.	-0.	-0.	-0.
MISTIO IMID	-0.	-0.	-0.	-0.
PLASMA	-0.	-0.	-0.	-0.
RCOO-	-0.	-0.	-0.	-0.
ANH3+	-0.	-0.	-0.	-0.
HAM3+	-0.	-0.	-0.	-0.
S4	-0.	-0.	-0.	-0.

[a] The symbol "E±OX" gives the power of 10 multiplying each number.

Table XIII

EXPECTED OUTPUT SPECIES

Expected Species	Free Energy Parameter	Input Components

```
PLASMA
     O2         0.000000      1.000 O2
     CO2        0.000000      1.000 CO2
     N2         0.000000      1.000 N2
     H2O      -39.390000      1.000 H+       1.000 OH-
     H+         0.000000      1.000 H+      -0.000          -0.000           1.000 HPLASM
     OH-        0.000000      1.000 OH-     -0.000          -0.000          -1.000 HPLASM
     CL-        0.000000      1.000 CL-     -0.000          -0.000          -1.000 HPLASM
     NA+        0.000000      1.000 NA+     -0.000          -0.000           1.000 HPLASM
     K+         0.000000      1.000 K+      -0.000          -0.000           1.000 HPLASM
     CA++       0.000000      1.000 CA++    -0.000          -0.000           2.000 HPLASM
     MG++       0.000000      1.000 MG++    -0.000          -0.000           2.000 HPLASM
     SO4=       0.000000      1.000 SO4=    -0.000          -0.000          -2.000 HPLASM
     HPO4=      0.000000      1.000 HPO4=   -0.000           0.000          -2.000 HPLASM
     H2PO4-   -20.570000      1.000 H+       1.000 HPO4=    -0.000          -1.000 HPLASM
     NH4+       0.000000      1.000 NH4+    -0.000          -0.000           1.000 HPLASM
     NH3       24.461000     -1.000 H+       1.000 NH4+
     LACTIC     0.000000      1.000 LACTIC  -0.000          -0.000          -1.000 HPLASM
     UREA       0.000000      1.000 UREA
     GLUCOS     0.000000      1.000 GLUCOS
     HCO3-    -21.190000      1.000 CO2      1.000 OH-      -0.000          -1.000 HPLASM
     H2CO3    -17.840000      1.000 CO2      1.000 H+        1.000 OH-
     CO3=       6.260000      1.000 CO2     -1.000 H+        1.000 OH-      -2.000 HPLASM
     PROTN      0.000000      1.000 HISCPL -99.000 HCCO-   -16.000 AMN3+  -17.000 [illegible]
     PROTN     -0.000000    -14.000 SS

RED CELLS
     O2        -0.490000      1.000 O2
     CO2        0.000000      1.000 CO2
     N2        -0.900000      1.000 N2
     H2O      -39.390000      1.000 H+       1.000 OH-
     H+         0.000000      1.000 H+
     OH-        0.000000      1.000 OH-
     CL-        0.000000      1.000 CL-
     NA+        2.112951      1.000 NA+
     K+        -3.012029      1.000 K+
     CA++       2.087593      1.000 CA++
     MG++      -0.671946      1.000 MG++
     SO4=      -2.000000      1.000 SO4=
     HPO4=     -2.000000      1.000 HPO4=
     H2PO4-   -22.570000      1.000 H+       1.000 HPO4=
     NH4+       0.000000      1.000 NH4+
     NH3       24.461000      1.000 H+       1.000 NH4+
     LACTIC     0.000000      1.000 LACTIC
     UREA       0.000000      1.000 UREA
     GLUCOS     0.000000      1.000 GLUCOS
     HCO3-    -21.490000      1.000 CO2      1.000 OH-
     H2CO3     12.840000      1.000 CO2      1.000 H+        1.000 OH-
     CO3=       6.120000      1.000 CO2     -1.000 H+        1.000 OH-
     PROTN      0.000000      1.000 HISCRB
     PROTN-    19.440300      1.000 HISCRB  -1.000 H+
     HB4        [illegible]  -0.000          1.000 HB4      -4.000 [illegible]
     HB4        [illegible]  -0.000         -3.000         -16.000 HISTID
     [illegible]  1.000 O2       1.000 HB4      -3.000 [illegible]   -1.000 [illegible]
     [illegible] -0.000         -3.000         -16.000 HISTID
     [illegible]  2.000 O2       1.000 HB4      -2.000 [illegible]   -2.000 [illegible]
     [illegible] -0.000         -0.000         -16.000 HISTID
     [illegible]  3.000 O2       1.000 HB4      -1.000 [illegible]   -3.000 [illegible]
     [illegible] -0.000         -0.000         -16.000 HISTID
     [illegible]  4.000 O2       1.000 HB4      -0.000               -4.000 [illegible]
     [illegible] -0.000         -0.000         -16.000 HISTID

[illegible]
     [illegible]  1.000 H+      -0.000           1.000 [illegible]
     [illegible] -0.000         -0.000           1.000 [illegible]
     [illegible] -1.000 H+      -0.000           1.000 [illegible]
     [illegible] -2.000 H+       1.000 CO2       1.000 [illegible]

[illegible]
     [illegible]  1.000 H+      -0.000          -0.000           1.000 [illegible]
     [illegible] -0.000         -0.000          -0.000           1.000 [illegible]
     [illegible] -1.000 H+      -0.000          -0.000           1.000 [illegible]
     [illegible] -2.000 H+       1.000 CO2      -0.000           1.000 [illegible]

[illegible]
     [illegible] -0.000         -0.000           1.000 HISTID
     [illegible] -1.000 H+      -0.000           1.000 HISTID

[illegible]
     [illegible]    1.000 [illegible]
     [illegible] -0.000          1.000 [illegible]  -0.000        -1.000 HPLASM

[illegible]
     [illegible]  0.000          1.000 [illegible]
     [illegible]  1.000 H+       1.000 [illegible]  -0.000         1.000 HPLASM

[illegible]
     [illegible] -0.000          1.000 [illegible]  -0.000         1.000 HPLASM
     [illegible]  1.000 H+       1.000 [illegible]

[illegible]
     [illegible] -0.000         -0.000           1.000 SS      1.000 HPLASM
     [illegible] -1.000 H+      -0.000           1.000 SS
```

Table XII gives the total of species in the liquid
phase in moles-per-liter-of-blood. The species H^+ and OH^-
are combined in the model according to $(H^+)(OH^-)/(H_2O) = K_w$
to give water. The total moles of miscellaneous macro-
molecular species and protein for plasma and red cells
come from Documenta Geigy [29]. Table XII also shows the
gas phases for equilibration.

The free energy parameters of Table XIII resemble those
of the previous models (Chap. I). Each additional chemical
reaction, however, also requires a parameter. For example,
consider the carboxyl ionization of serum protein given
in Site 1, Table XIII. The conceptual compartment Site 1
shows two reactions. The symbol $RCOO^-$ represents a carboxyl
site on a serum protein molecule. This site has two pos-
sible expected states related by

$$\frac{(RCOO^-)(H^+)}{(RCOOH)} = K \tag{1}$$

where $\ln_e K = -12.40503$ with the concentrations in mole
fractions, or $-\log_{10} X = pK_{COOH} = 3.64$, a "best fit" average
value from the titration data for carboxyl ionization sites.

Similarly, the remaining ionization parameters are
derived on a mole fraction scale from the best laboratory
estimates as discussed in the previous chapter.

The oxygenation equilibrium constants have the (Roughton) ratios derived in the previous chapter. Table XIII expresses them in the mole fraction scale for all constituents of the mass action equations. While the ratios of the oxygenation constants are fixed, the absolute values are adjusted empirically to give the correct oxygenation at p50, the oxygen pressure at half-saturation. This empirical fitting is the best procedure presently available.

Table XIV prints the computer output for the standard arterial state. All species appear in moles, mole fractions, and moles-per-liter of water in each compartment.

Similarly, Table XV is a computer solution for the distribution of species in standard venous blood. The differences between arterial and venous result entirely from a change in gas pressures. For arterial blood, pO_2 = 100 mm, pCO_2 = 40 mm; and for venous, pO_2 = 40 mm, pCO_2 = 46 mm. Table XVI summarizes these data for some of the important species, and compares them with similar data from the reference literature.

Table XVI has few important discrepencies. The mathematical model uses a slightly higher (5 percent) solubility

EXPERIMENTAL HUMAN BLOOD BFFR-1 NIH-OFLAND '64

		PLASMA	RED CELLS	AIR OUT
X-BAR		2.886917 01	1.79896E 01	9.99128E 02
PH		7.39478 00	7.23255E 00	-0.
O2	MOLES	6.71828F-05	6.05395E-05	1.31498E 02
	MFRAC	2.31404F-06	3.80996F-06	1.31613E-01
	M/LH2O	1.29530E-04	2.11434E-04	1.14914E 02
CO2	MOLES	6.05145E-04	4.31174E-04	5.26002E 01
	MFRAC	2.40747E-05	2.40292E-05	5.26461F-02
	M/LH2O	1.13628F-03	1.13628F-03	4.75667F 01
N2	MOLES	2.16127E-04	2.22252E-04	7.54000F 02
	MFRAC	7.49338E-06	1.23545E-05	7.54658E-01
	M/LH2O	4.15844E-04	6.95614E-04	6.81846E 02
H2O	MOLES	2.87104E 01	1.78907E 01	6.10303E 01
	MFRAC	9.94502F-01	9.94502E-01	6.10835F-02
	M/LH2O	5.51900E 01	5.51900E 01	5.51900E 01
I+	MOLES	2.07601E-08	1.89759E-08	-0.
	MFRAC	7.26037E-10	1.05483E-09	-0.
	M/LH2O	4.02915E-08	5.85379E-08	-0.
OH-	MOLES	3.09186E-07	1.32612E-07	-0.
	MFRAC	1.07099E-08	7.37163F-09	-0.
	M/LH2O	5.94349E-07	4.09089E-07	-0.
CL-	MOLES	5.60718E-02	2.40282E-02	-0.
	MFRAC	1.94054E-03	1.33567E-03	-0.
	M/LH2O	1.07641E-01	7.41233F-02	-0.
NA+	MOLES	7.64511E-02	8.36888E-03	-0.
	MFRAC	2.64827E-03	4.65095E-04	-0.
	M/LH2O	1.46986E-01	2.58105E-02	-0.
K+	MOLES	2.29975E-03	4.27502E-02	-0.
	MFRAC	7.96613E-05	2.37639E-03	-0.
	M/LH2O	4.42082E-03	1.31878E-01	-0.
CA++	MOLES	1.37994E-03	2.25362E-04	-0.
	MFRAC	4.77999E-05	1.25107E-05	-0.
	M/LH2O	2.65266E-03	6.94289E-04	-0.
MG++	MOLES	4.87391E-04	1.16511E-03	-0.
	MFRAC	1.61301E-05	6.36539E-05	-0.
	M/LH2O	8.94710E-04	3.53246E-03	-0.
SO4=	MOLES	1.65023E-04	3.59977E-04	-0.
	MFRAC	5.71626E-06	2.00103E-05	-0.
	M/LH2O	1.17224E-04	1.11047E-03	-0.
HPO4=	MOLES	2.67480F-04	5.39845E-04	-0.
	MFRAC	4.57244E-06	3.00088E-05	-0.
	M/LH2O	4.75731E-04	1.66534E-03	-0.
H2PO4-	MOLES	1.54147E-04	4.84528E-04	-0.
	MFRAC	5.33955E-06	2.71562E-05	-0.
	M/LH2O	2.96318E-04	1.50703E-03	-0.
NH4+	MOLES	4.43692E-04	4.01692E-04	-0.
	MFRAC	1.53691E-05	2.23291E-05	-0.
	M/LH2O	8.52910E-04	1.23916E-03	-0.
NH3	MOLES	1.45494E-05	9.06436E-06	-0.
	MFRAC	5.03979E-07	5.01979E-07	-0.
	M/LH2O	2.79684E-05	2.79684E-05	-0.
LACTIC	MOLES	1.42277E-03	6.10235E-04	-0.
	MFRAC	4.92833E-05	3.39216E-05	-0.
	M/LH2O	2.73498E-03	1.88248E-03	-0.
UREA	MOLES	1.73575E-03	1.20425E-03	-0.
	MFRAC	6.70927E-05	6.70527E-05	-0.
	M/LH2O	3.72110E-03	3.72110E-03	-0.
GLUCOS	MOLES	2.25854E-03	1.40742E-03	-0.
	MFRAC	7.82392E-05	7.82357E-05	-0.
	M/LH2O	4.34167E-03	4.34167E-03	-0.
HCO3-	MOLES	1.39312E-02	6.87408E-03	-0.
	MFRAC	4.82637E-04	3.82115E-04	-0.
	M/LH2O	2.67833E-02	2.12055E-02	-0.
H2CO3	MOLES	9.98671E-07	6.16084E-07	-0.
	MFRAC	3.47467E-08	3.47467E-08	-0.
	M/LH2O	1.90057E-06	1.90053E-06	-0.
CO3=	MOLES	1.95984E-05	6.65520E-06	-0.
	MFRAC	6.79869E-07	3.69946E-07	-0.
	M/LH2O	3.76739E-05	2.05103E-05	-0.
PROTH	MOLES	5.38000E-04	1.98685E-03	-0.
	MFRAC	1.86358E-05	1.10446E-04	-0.
	M/LH2O	1.03429E-03	6.12913E-03	-0.
PROTN-	MOLES	-0.	5.51315E-03	-0.
	MFRAC	-0.	3.06463E-04	-0.
	M/LH2O	-0.	1.70072E-02	-0.
HB4	MOLES	-0.	4.75063E-06	-0.
	MFRAC	-0.	3.19665E-07	-0.
	M/LH2O	-0.	1.77398E-05	-0.
HB4O2	MOLES	-0.	2.37521E-05	-0.
	MFRAC	-0.	1.32033F-06	-0.
	M/LH2O	-0.	7.32716F-05	-0.
HB4O4	MOLES	-0.	8.13020E-05	-0.
	MFRAC	-0.	4.63507E-06	-0.
	M/LH2O	-0.	2.57221E-04	-0.
HB4O6	MOLES	-0.	2.58114E-05	-0.
	MFRAC	-0.	1.43591E-06	-0.
	M/LH2O	-0.	7.96461E-05	-0.
HB4O8	MOLES	-0.	2.13379E-03	-0.
	MFRAC	-0.	1.18612E-04	-0.
	M/LH2O	-0.	6.58241E-03	-0.

Table XIV

STANDARD ARTERIAL BLOOD

HEMOGLOBIN REACTIONS

		REOHFPE RHR	JXYHFPE OHR	OXYSTABLE HR
X-BAR		2.86854E-04	6.80315E-03	1.61600F-02
H2HB+	MOLES	2.10142E-04	-0.	-0.
	MFRAC	7.32975F-01	-0.	-0.
HHS+-	MOLES	3.58008E-05	-0.	-0.
	MFRAC	1.24805E-01	-0.	-0.
HB-	MOLES	2.42801E-05	-0.	-0.
	MFRAC	8.46426E-02	-0.	-0.
HCARB+	MOLES	1.66312E-05	-0.	-0.
	MFRAC	5.79778E-02	-0.	-0.
H2HBO+	MOLES	-0.	1.28505E-03	-0.
	MFRAC	-0.	1.45977E-01	-0.
HHBO+-	MOLES	-0.	4.36835E-03	-0.
	MFRAC	-0.	4.96226E-01	-0.
HBO2-	MOLES	-0.	1.86931E-03	-0.
	MFRAC	-0.	2.12346F-01	-0.
HCARB+	MOLES	-0.	1.28043E-03	-0.
	MFRAC	-0.	1.45451E-01	-0.
IPID+	MOLES	-0.	-0.	1.11130E-02
	MFRAC	-0.	-0.	3.05639E-01
IHID	MOLES	-0.	-0.	2.52469E-02
	MFRAC	-0.	-0.	6.94361F-01

SERUM ALBUMIN REACTIONS

		SITE1 SERUM	SITE2 SERUM	SITE3 SERUM	SITE4 SERUM
X-BAR		5.32620E-02	8.60800E-03	1.06660E-02	1.02720E-02
RCOOH	MOLES	9.43687E-06	-0.	-0.	-0.
	MFRAC	1.77141E-04	-0.	-0.	-0.
RCOO-	MOLES	5.32526E-02	-0.	-0.	-0.
	MFRAC	9.99823E-01	-0.	-0.	-0.
RANH2	MOLES	-0.	6.77078E-03	-0.	-0.
	MFRAC	-0.	7.80760F-01	-0.	-0.
RANH3+	MOLES	-0.	1.88722E-03	-0.	-0.
	MFRAC	-0.	2.19240E-01	-0.	-0.
RENH3+	MOLES	-0.	-0.	3.06495E-07	-0.
	MFRAC	-0.	-0.	9.99441E-01	-0.
RENH2	MOLES	-0.	-0.	1.65201E-05	-0.
	MFRAC	-0.	-0.	5.38712E-04	-0.
R++	MOLES	-0.	-0.	-0.	1.02710E-02
	MFRAC	-0.	-0.	-0.	9.99900F-01
R++-	MOLES	-0.	-0.	-0.	1.02503E-06
	MFRAC	-0.	-0.	-0.	1.00396E-04

EXPERIMENTAL HUMAN BLOOD 8FFR-1 NIH-DELAND '64

		PLASMA	RED CELLS	AIR OUT
X-BAR		7.87266E 01	1.81815E 01	9.99977E 02
PH		7.16969E 00	7.22081E 00	-0.
O2	MOLES	2.67976E-05	2.75359E-05	5.25999E 01
	MFRAC	9.12852E-07	1.52271E-06	5.26011E-02
	M/LH2O	5.17716E-05	8.45073E-05	4.75284E 01
CO2	MOLES	7.35499E-04	5.00192E-04	6.04982E 01
	MFRAC	2.76712E-05	2.76712E-05	6.04996E-02
	M/LH2O	1.53569E-03	1.53569E-03	5.46652E 01
N2	MOLES	2.15557E-04	2.44479E-04	8.25800E 02
	MFRAC	8.19997E-06	1.35195E-05	8.25819E-01
	M/LH2O	4.55081E-04	7.50107E-04	7.46179E 02
H2O	MOLES	2.45672E 01	1.79832E 01	6.10790E 01
	MFRAC	9.34451E-01	9.94451E-01	6.10804E-02
	M/LH2O	5.51900E 01	5.51900E 01	5.51900E 01
H+	MOLES	2.20957E-08	1.95971E-08	-0.
	MFRAC	7.61172E-10	1.08370E-09	-0.
	M/LH2O	4.20875E-08	6.01432E-08	-0.
OH-	MOLES	2.90191E-07	1.29747E-07	-0.
	MFRAC	1.01088E-08	7.17487E-09	-0.
	M/LH2O	5.61018E-07	3.98191E-07	-0.
CL-	MOLES	5.55290E-02	2.47210E-02	-0.
	MFRAC	1.92606E-03	1.36704E-03	-0.
	M/LH2O	1.06892E-01	7.58643E-02	-0.
NA+	MOLES	7.66064E-02	8.21314E-03	-0.
	MFRAC	2.66678E-03	4.54178E-04	-0.
	M/LH2O	1.48000E-01	2.52059E-02	-0.
K+	MOLES	2.14502E-03	4.27050E-02	-0.
	MFRAC	8.16325E-05	2.36154E-03	-0.
	M/LH2O	4.53044E-03	1.31061E-01	-0.
CA++	MOLES	1.18968E-03	2.15325E-04	-0.
	MFRAC	4.41760E-05	1.19072E-05	-0.
	M/LH2O	2.68477E-03	6.60827E-04	-0.
MG++	MOLES	4.86490E-04	1.12791E-03	-0.
	MFRAC	1.68690E-05	6.21723E-05	-0.
	M/LH2O	9.36197E-04	3.46153E-03	-0.
SO4=	MOLES	1.57033E-04	3.47967E-04	-0.
	MFRAC	5.46649E-06	2.03462E-05	-0.
	M/LH2O	1.03379E-03	1.12928E-03	-0.
HPO4=	MOLES	2.11330E-04	5.42062E-04	-0.
	MFRAC	8.05281E-06	2.93759E-05	-0.
	M/LH2O	4.46918E-04	1.66358E-03	-0.
H2PO4-	MOLES	1.52649E-04	5.03960E-04	-0.
	MFRAC	5.31386E-06	2.78685E-05	-0.
	M/LH2O	2.94908E-04	1.54664E-03	-0.
NH4+	MOLES	4.48549E-04	3.97828E-06	-0.
	MFRAC	1.56144E-05	2.19949E-09	-0.
	M/LH2O	8.66589E-04	1.22092E-03	-0.
NH3	MOLES	1.18836E-05	8.71993E-06	-0.
	MFRAC	4.43309E-07	4.33309E-07	-0.
	M/LH2O	2.68227E-05	2.68227E-05	-0.
LACTIC	MOLES	1.40517E-03	6.27810E-04	-0.
	MFRAC	4.49154E-05	3.47184E-05	-0.
	M/LH2O	2.71470E-03	1.92680E-03	-0.
UREA	MOLES	1.92819E-03	1.71381E-03	-0.
	MFRAC	6.71223E-05	6.71273E-05	-0.
	M/LH2O	3.72515E-03	3.72515E-03	-0.
GLUCOS	MOLES	2.24978E-03	1.41624E-03	-0.
	MFRAC	7.81165E-05	7.81165E-05	-0.
	M/LH2O	4.36640E-03	4.36440E-03	-0.
HCO3-	MOLES	1.50383E-02	7.72882E-03	-0.
	MFRAC	5.23498E-04	4.27398E-04	-0.
	M/LH2O	2.90533E-02	2.37196E-02	-0.
H2CO3	MOLES	1.11049E-06	7.11648E-07	-0.
	MFRAC	3.93536E-08	3.93536E-08	-0.
	M/LH2O	2.19603E-06	2.18431E-06	-0.
CO3=	MOLES	1.93666E-05	7.28338E-06	-0.
	MFRAC	6.99057E-07	4.02763E-07	-0.
	M/LH2O	3.85743E-05	2.23525E-05	-0.
PROTN	MOLES	5.18000E-04	2.02654E-03	-0.
	MFRAC	1.47283E-05	1.12065E-04	-0.
	M/LH2O	1.03753E-03	6.21940E-03	-0.
PROTN-	MOLES	-0.	5.47366E-06	-0.
	MFRAC	-0.	3.02677E-04	-0.
	M/LH2O	-0.	1.67979E-02	-0.
HB4	MOLES	-0.	1.59877E-04	-0.
	MFRAC	-0.	8.84107E-06	-0.
	M/LH2O	-0.	4.90658E-04	-0.
HB4O2	MOLES	-0.	2.60901E-04	-0.
	MFRAC	-0.	1.44276E-05	-0.
	M/LH2O	-0.	8.00699E-04	-0.
HB4O4	MOLES	-0.	3.61868E-04	-0.
	MFRAC	-0.	2.00109E-05	-0.
	M/LH2O	-0.	1.11056E-03	-0.
HB4O6	MOLES	-0.	4.42925E-05	-0.
	MFRAC	-0.	2.44913E-06	-0.
	M/LH2O	-0.	1.35911E-04	-0.
HB4O8	MOLES	-0.	1.44556E-03	-0.
	MFRAC	-0.	7.99181E-05	-0.
	M/LH2O	-0.	4.43640E-03	-0.

Table XV

STANDARD VENOUS BLOOD

HEMOGLOBIN REACTIONS

		REDHEME HMB	OXYHEME OHP	OXYSTABLE HP
X-BAR		2.11024E-03	6.84974E-01	1.63600E-02
H2HB+	MOLES	1.61146E-03	-0.	-0.
	MFRAC	7.55746E-01	-0.	-0.
HHB+	MOLES	2.67122E-04	-0.	-0.
	MFRAC	1.27006E-01	-0.	-0.
HB-	MOLES	1.76401E-04	-0.	-0.
	MFRAC	8.05398E-02	-0.	-0.
RCARB+	MOLES	1.39155E-04	-0.	-0.
	MFRAC	6.17082E-02	-0.	-0.
H2HBO+	MOLES	-0.	1.02376E-03	-0.
	MFRAC	-0.	1.48304E-01	-0.
HHBO+	MOLES	-0.	6.18576E-01	-0.
	MFRAC	-0.	4.40704E-01	-0.
HBO2-	MOLES	-0.	1.41024E-01	-0.
	MFRAC	-0.	2.04390E-01	-0.
OCARB+	MOLES	-0.	1.08050E-01	-0.
	MFRAC	-0.	1.56600E-01	-0.
IP10+	MOLES	-0.	-0.	1.13225E-02
	MFRAC	-0.	-0.	5.11400E-01
IH10	MOLES	-0.	-0.	2.50379E-02
	MFRAC	-0.	-0.	6.86600E-01

SERUM ALBUMIN REACTIONS

		SITE1 SERUM	SITE2 SERUM	SITE3 SERUM	SITE4 SERUM
X-BAR		5.37620E-02	8.60800E-03	1.06660E-02	1.02220E-02
RCOOH	MOLES	9.49530E-06	-0.	-0.	-0.
	MFRAC	1.87663E-04	-0.	-0.	-0.
RCOO-	MOLES	5.32920E-02	-0.	-0.	-0.
	MFRAC	9.49817E-01	-0.	-0.	-0.
RANH2	MOLES	-0.	6.63436E-03	-0.	-0.
	MFRAC	-0.	7.70721E-01	-0.	-0.
RANH3+	MOLES	-0.	1.97366E-03	-0.	-0.
	MFRAC	-0.	2.29279E-01	-0.	-0.
RENH3+	MOLES	-0.	-0.	3.06504E-07	-0.
	MFRAC	-0.	-0.	9.99491E-01	-0.
RENH2	MOLES	-0.	-0.	1.55942E-05	-0.
	MFRAC	-0.	-0.	5.08516E-04	-0.
R+	MOLES	-0.	-0.	-0.	1.02210E-02
	MFRAC	-0.	-0.	-0.	9.99905E-01
R++	MOLES	-0.	-0.	-0.	9.68312E-07
	MFRAC	-0.	-0.	-0.	9.47282E-05

Table XVI

COMPARISON OF LITERATURE AND COMPUTED VALUE MODEL BFFR-1

One Liter, Young, Adult, Male, Human Blood[a]

Item	Literature Arterial Blood Plasma	Literature Arterial Blood Red Cell	Computer Arterial Blood Plasma	Computer Arterial Blood Red Cell	Computer Venous Blood Plasma	Computer Venous Blood Red Cell
O_2	6.33×10^{-5}	6.43×10^{-5}	6.74×10^{-5}	6.85×10^{-5}	2.68×10^{-5}	2.75×10^{-5}
CO_2	7.01×10^{-4}	4.76×10^{-4}	6.95×10^{-4}	4.33×10^{-4}	7.94×10^{-4}	5.00×10^{-4}
N_2	2.20×10^{-4}	2.20×10^{-4}	2.16×10^{-4}	2.22×10^{-4}	2.36×10^{-4}	2.44×10^{-4}
H_2O	28.50	18.00	28.71	17.89	28.56	17.99
Cl^-	56.65 Meq	23.40 Meq	56.02 Meq	24.03 Meq	55.3 Meq	24.75 Meq
Na^+	76.45 "	8.37 "	76.45 "	8.37 "	76.61 "	8.20 "
K^+	2.36 "	42.69 "	2.30 "	42.75 "	2.34 "	42.70 "
Ca^{++}	2.86 "	0.34 "	2.76 "	0.45 "	2.78 "	0.43 "
Mg^{++}	0.94 "	2.30 "	0.93 "	2.29 "	0.97 "	2.26 "
HCO_3^-	13.84 "	6.03 "	13.94 "	6.88 "	15.08 "	7.76 "
Volume	550 cc	450 cc	553 cc	447 cc	540 cc	460 cc
pH	7.39	7.19	7.395	7.23	7.37	7.22
HCT	45.1%		44.7%		46.0%	
Hb Sat.	97%		96.6%		73.7%	
Total O_2	8.83×10^{-3}		8.9×10^{-3}		6.74×10^{-3}	
Total CO_2	22.8×10^{-3}		23.26×10^{-3}		25.34×10^{-3}	
Carb. CO_2	0.86×10^{-3}		1.28×10^{-3}		1.21×10^{-3}	

[a] In moles unless otherwise specified.

constant for oxygen than did the calculations of the
standard reference.[†] This slightly increased solubility
causes a small rise in the saturation of hemoglobin, but
the absolute level of the oxygenation constants for
hemoglobin are adjusted empirically to fit the saturation
curve. The carbamino CO_2 is also more abundant, in ac-
cordance with what are believed to be better laboratory
data.[†] The hematocrit is computed using volume factors
(cc of water per cc of plasma or red cells) of 94 percent
for plasma and 72 percent for red cells.

In addition to comparing the data of Table XVI with
the literature, many other criteria exist for evaluating
a model of blood chemistry. From Table XIV, one can
compute, for example, the ratio of Cl^{-1} ion mole-fractions
between plasma and red cell,

$$\frac{(Cl^-)_{PL}}{(Cl^-)_{RC}} = 1.94 = 1.45 , \tag{2}$$

while Bernstein [30] gives 1.44 for this ratio. Since

Cl^- ions are assumed not actively pumped, the Cl^- gradient is a measure of the Gibbs-Donnan gradient and of the specific ion potential across the cell membrane. In this connection, as in Chap. I,

$$\frac{(Cl^-)_{PL}}{(Cl^-)_{RC}} = k\,\frac{(HCO_3^-)_{PL}}{(HCO_3^-)_{RC}} = \frac{(NH_4^+)_{RC}}{(NH_4^+)_{PL}} = \frac{(H^+)_{RC}}{(H^+)_{PL}} = \frac{(OH^-)_{PL}}{(OH^-)_{RC}} \quad (3)$$

for the ratio for all single-valent ions having the identical apparent level of the active pump mechanism. This study assigns a zero-level active pump to species satisfying Eq. (3), and names these ions the "free" ions in contrast to ions associated with a non-zero-level active pump. The simpler models of Chap. I could also show this ratio equal to the square root of the sulfate ratio, but it does not hold here, as will be demonstrated below. The constant before the bicarbonate ratio is, here, 1.15. The HCO_3^- ratio is not the same as the Cl^-, owing to the increased solubility of red cell CO_2 over plasma and a slight difference in apparent pK for the red cell bicarbonate reactions. This Memorandum thus postulates a zero-level active pump for the bicarbonate ion and accounts

for the anomalous bicarbonate ratio by differences in intracellular ionic activity--although these two phenomena may be difficult to distinguish.

One of the major discrepancies in this model of human blood arises from an inconsistency in the variable biological data. Whereas the literature [29,30] gives the Cl^- ion concentration ratio as 1.44, it usually gives the H^+ ion concentration ratio at around 1.57. This H^+ ion ratio is computed from the difference in pH between plasma (pH 7.39) and red cells (pH 7.19), a difference of 0.2 pH [7,31]. If neither of these ions is actively pumped, the cause of the difference in concentration ratios, if it exists, is not clear. Of course, a change in the activity of H^+ ion or of Cl^- ion is possible, e.g., by interaction with the proteins.

In Table XIV, the model has the "correct" Cl^- ion concentration ratio [30]. In Table XVII, the model has the "correct" H^+ ion ratio [7]. In each table, the other ion of the two has an error in the quoted ratio. The change in gradient of the free ions was obtained, in this case, by increasing or decreasing the average negative charge on the serum proteins by 4 percent, the lower average negative charge giving the higher chloride ratio.

EXPERIMENTAL HUMAN BLOOD BFFR-1 NIH-DELANO '64

		PLASMA	RED CELLS	AIR OUT

Table XVII

MODIFIED ARTERIAL BLOOD

HEMOGLOBIN REACTIONS

		RFDHEME RHB	OXYHEME OHR	DRYSTABLE HP

SERUM ALBUMIN REACTIONS

		SITE1 SERUM	SITE2 SERUM	SITE3 SERUM	SITE4 SERUM

This small inconsistency has not been resolved. The model with the correct chloride ion was chosen for further computation, since it also has the "correct" hematocrit [7].

For the free ions, Eq. (3) holds and permits the following definition of specific free ion potential:

$$RT \; ln \; \frac{(Cl^-)_{PL}}{(Cl^-)_{RC}} = RT(0.3716) = z_{Cl^-} \; F^* E \; , \qquad (4)$$

where:

R = Gas constant = 1.987 cal deg^{-1} $mole^{-1}$,

T = Absolute temperature = 310°,

z_{Cl^-} = Valence of ion = -1,

F^* = One Faraday = 23,060 cal $volt^{-1}$ $mole^{-1}$,

E = Specific ion potential;

or

$$E = \frac{615.9(0.3716)}{(-1)(23,060)}$$

$$= -9.9 \; millivolts \qquad (5)$$

for the red cell free specific ion potential.

The specific ion potential as measured by Cl^- ion gradient differs from that which could be computed simi-larly from Na^+ or K^+ gradients, because of the active cation pumps. The direction of the observed Na^+ gradient, and hence the model gradient, is opposite to that given by the Cl^- specific ion potential. That specific ion potential would, in fact, concentrate the positive ions in the interior of the cell (see Chap. I), just as the negative Cl^- ion is concentrated externally. Therefore, the Na^+ pump must overcome the (Donnan) electrostatic gradient, as well as raise Na^+ ions up to the concentra-tion ratio observed. Analytically,

$$\frac{(Na^+)_{PL}}{(Na^+)_{RC}} \times \frac{(Cl^-)_{PL}}{(Cl^-)_{RC}} = 5.69 \times 1.45 = 8.25 = e^{2.113} , \quad (6)$$

where the exponent on the right is exactly the free energy parameter, in Table XIII, for the Na^+ pump. Taking the log of both sides,

$$\ln \frac{(Na^+)_{PL}}{(Na^+)_{RC}} = 2.11 - \ln \frac{(Cl^-)_{PL}}{(Cl^-)_{RC}} = 1.739 . \quad (7)$$

Or, if we write

$$\Delta F' = RT \ln \frac{(x)_1}{(x)_2} , \qquad (8)$$

then

$$\Delta F'_{Na^+} = RT \ln \frac{(Na^+)_{PL}}{(Na^+)_{RC}} = 615.9(1.739) \text{ cal/mole}$$

$$= 1071 \text{ cal/mole} . \qquad (9)$$

The interpretation of Eq. (8) in this context is actually
not as clear as Eq. (9) would suggest. Thus $\Delta F'$ replaces
the usual ΔF, because the ideal equation (9) gives only
the theoretical work required to move an infinitesimal
increment of Na^+ ions (plus the concomitant negative ions)
from one concentration to the other while maintaining the
system in the present state; but it ignores any energy
losses in the membrane, the concentration effects in each
phase, or any mechanism which maintains the gradient.
Particularly, Eq. (9) does not measure the work required
to obtain the present distribution from classical equi-
librium.

The K^+ ion is concentrated in the cell interior, so the Gibbs-Donnan gradient aids its active pump. Therefore,

$$\ln \frac{(K^+)_{PL}}{(K^+)_{PC}} = -3.0220 - \ln \frac{(Cl^-)_{PL}}{(Cl^-)_{RC}} = -3.3945 , \qquad (10)$$

where -3.0220, from Table XIII, is the free energy parameter representing the work per mole to maintain the observed potassium gradient.

Computing the "potential" of the K^+ ion from Eq. (4) gives

$$RT \ln \frac{(K^+)_{PL}}{(K^+)_{RC}} = z_{K^+} F' E_{K^+} ,$$

$$E_{K^+} = - \frac{615.9(-3.3945)}{(+1)23,060}$$

$$= -9.07 \text{ millivolts} ;$$

and for Na^+,

$$E_{Na^+} = \frac{615.9(1.798)}{(+1)23,060}$$

$$= +4.64 \text{ millivolts} .$$

However, neither of these last two "potentials" are significant for the activity of the cell, since the cation mobilities are so low in relation to those of the anions. For example, the "membrane potential" of the cell, given by Ref. 32,

$$E_m = \frac{RT}{F^*} \ln \frac{P_k(K^+)_{RC} + P_{Na}(Na^+)_{RC} + P_{Cl}(Cl^-)_{PL}}{P_k(K^+)_{PL} + P_{Na}(Na^+)_{PL} + P_{Cl}(Cl^-)_{RC}} , \qquad (11)$$

where the P_j are permeability coefficients, reduces to just Eq. (4) since $P_{Na} < P_k \ll P_{Cl}$.

Tables XIV and XV show a somewhat misleading distribution of the species SO_4^- and HPO_4^-, as well as Ca^{++} and Mg^{++}. These species represent the so-called acid-soluble phosphates, the non-protein sulphate, and the double-valent cations obtained by precipitation. While the distributions of these species in the model correspond to results quoted in the literature (cf. Table XVI), the "distribution" as

such is not well-defined. These species are much more likely to combine in various forms, as well as bind to the protein, than are the singly-charged species of either sign. But these reactions have not yet been incorporated into the present mathematical model, which imposes theoretical concentration gradients on these ions to create in the two compartments the moles of each species observed in chemical analysis.

While Tables XIV and XV give a detailed distribution of species for arterial and venous blood, Table XVIII graphically presents the differences between arterial and venous as percent change from the arterial standard for both the plasma and red cells. These data present several interesting facts requiring, for explanation, complex intercompartmental relationships. For example, in changing to venous blood from arterial, the hydrogen ion concentration increases proportionately more in the plasma than in the red cells, whereas Na^+, K^+, Ca^{++}, and Mg^{++} move from red cells to plasma, and Cl^- moves from plasma to red cells. Since in the model the gas pressure change alone initiates this pattern of movement, i.e., pO_2 changing from 100 mm to 40 and pCO_2 changing from 40 mm to 46, it requires explanation.

Table XVIII

VENOUS BLOOD ST NDARD MODEL BFFR-1, MOLE FRACTION
CHANGE FROM ARTERIAL

COMPARTMENT   MOLE FRACTION PERCENT CHANGE FROM STANDARD

	-40	-30	-20	-10	-0	10	20	30	40

PLASMA   PH= 7.17   VOL H2O= 0.518 L.   VOL= 0.551 L.

	MM/ H2O	MILLIMLS	PERCENT
O2			-60.0
CO2			14.5
N2			9.4
H2O			-0.0
He			5.9
OH-			-5.6
CL-			-0.7
NA+			0.7
K+			7.5
CA++			1.2
MG++			4.7
SO4=			-4.4
HPO4=			-4.1
H2PO4-			-0.5
NH4+			1.6
NH3			-4.1
LACTIC			-0.7
UREA			0.1
GLUCOS			0.1
HCO3-			8.5
H2CO3			14.9
CO3=			7.4
PROTN			0.9

RED CELLS   PH= 7.22   VOL H2O= 0.326 L.   VOL= 0.450 L.

	MM/L H2O	MILLIMLS	PERCENT
O2			-60.0
CO2			14.9
N2			9.4
H2O			-0.0
He			7.7
OH-			-2.7
CL-			2.7
NA+			-7.5
K+			-0.6
CA++			-4.8
MG++			-2.0
SO4=			1.7
HPO4=				
H2PO4-			7.6
NH4+			-1.5
NH3			-4.1
LACTIC			2.5
UREA			0.1
GLUCOS			0.1
HGB-			11.9
H2CO3			14.9
CO3=			8.9
PROTN			1.5
PROTN-			-1.2
HBO			464.7
HBO2			992.7
HB+			331.7
HB-			10.6
HBH+			-32.6

Table XVIII lists concentrations of species computed in millimoles per liter of H_2O, although the plot is in percent change in mole fractions. In either case, the change in the water concentration appears as zero because, even on the mole fraction scale, the molality of the solution (and consequently the mole fraction of H_2O) is practically constant and is the same in each compartment. Water moves, of course, under the influence of various stresses applied to the blood; when ions cross the membrane, a proportionate amount of water goes along to maintain the equal osmolality. The changing concentration of fixed protein in both compartments shows that water moves from plasma to red cells in the change from arterial to venous; the concentration of plasma protein increases and that of red cell protein decreases. Tables XIV and XV, where the water movement is also evident, demonstrate this more clearly.

Blood plasma is less buffered than the red cell milieu (evident also from the Astrup diagram studies of separated fractions [33]). When the pCO_2 rises, the pH of the plasma shifts proportionately more than that of red cells. Thus, as the CO_2 accumulates in the blood and

(via carbonic anhydrase in the red cell) forms HCO_3^- and H^+, the hydrogen ion is buffered--principally by protein-- while the bicarbonate ion redistributes according to the Gibbs-Donnan relations and in indirect response to the cation pumps.

In the system model, the bicarbonate ion is just another permeable, single-valent, negative ion, though subject to intraphase reactions. Hence, it finally acquires the gradient of Eq. (3), i.e., before and after the CO_2 accumulation. In this view, the apparent Cl^- shift (Hamburger shift) is merely a redistribution of the total negative ion pool in response to an additional increment of permeable negative ion whose corresponding positive ion is buffered. Most of the additional HCO_3^- ion, however, is found in the red cell because the increment in acidic pH shift is smaller than that of plasma. By the Henderson-Hasselbach equation, the product $(H^+)(HCO_3^-)$ is directly proportional to pCO_2; but with a positive increment in pCO_2, if the (H^+) does not increase, then the (HCO_3^-) must. Thus, as Tables XIV and XV demonstrate, a large proportion of the produced HCO_3^- stays in the red cell where the H^+ ion is highly buffered.

Actually, these statements depend more completely upon the intercompartmental mechanisms than has been suggested. Fixed proteins in the red cell and plasma plus the active cation pumps are the principal determinants of electrolyte and water distribution, because of the interplay between the fixed charge on the protein and the active pumps. As the pCO_2 changes, protein buffers the H^+ ion, altering the net fixed charge. Now a proportionate change in the charge on the plasma versus the red cell protein exists for which the Donnan gradient would remain constant, but such an exact proportional change would be coincidental. Generally, in the physiological range, the hemoglobin buffers better than serum albumin; the charge increment thus differs for the two proteins, and ions must move. As ions move across the membrane, taking along osmotic water, the cation gradients also shift (the Na^+ gradient increasing and K^+ decreasing) since the apparent activity of the cation pumps is a function of the ion reservoirs from and into which they transport ions.

In addition, the hemoglobin oxygenation changes slightly with pH and pCO_2 (the "Bohr effect"), causing a slight shift of all other species. Table XVIII also

shows the changes in the oxygenated species of hemoglobin
in venous b·ood relative to arterial blood, although these
changes exceed the graph boundaries. The fully oxygenated
species Hb_4O_8 decreases considerably while the remaining
species, insignificant at high saturation, increase greatly
at low pO_2.

THE MATRIX OF PARTIAL DERIVATIVES

Blood in a normal unchanging steady state is probably
very rare. Blood is a viable system, so that even when
held in a bottle it changes chemical composition as it
metabolizes. In the body, it also has a constantly chang-
ing chemical composition, at least cyclic with the cir-
culation time. Blood composition reflects even small
inputs or losses around the vascular tree, since every
species in the blood is--at least via some series of mass
action equations--related to every other.

We may nevertheless assume instantaneous steady
states at various and particular points in the circula-
tion and compute the chemical composition at these points.
In addition, given a particular steady-state composition,
and given an increment in any one of the input components,
the expected response of each output species is comput-
able. If b_i, i=1,.....,m are the input moles of species,

and x_j, $j=1,\ldots,n$ are the output moles, then we compute the partial derivative, $\partial x_j/\partial b_i$, for each i and all j's.

Tables XIXA and B compile these partial derivatives. Tables XIXA show the expected change in the output species (left column) per unit change in the input species (column headings). Similarly, Table XIXB gives the expected change in total moles in each compartment. Generally speaking, small input increments cause additive responses, i.e., the response to two small simultaneous inputs equals the sum of the two responses when the inputs are added separately to the same reference state. Consequently, this matrix may be used to predict the systematic response to small mixed inputs--e.g., the addition of NaCl in water solution.

As an example of the matrix's use, first consider the addition of 1 meq of Na^+ ion to a liter of arterial blood. Reading under the Na^+ column, 9.13×10^{-1} meq of the added Na^+ will appear in plasma and the remainder, 8.65×10^{-2} meq, will appear in red cells. The addition also causes 5.99×10^{-1} meq of Cl^- ion and 2.06×10^{-2} mM of water to move from the red cells to the plasma. Every other species will also change. H^+ ion decreases in both compartments, but in the red cell compartment the OH^- ion

Table XIXA

OUTPUT SPECIES INCREMENTS PER UNIT INCREASE

IN INPUT SPECIES

JACOBIAN, CYCLE   1

	02	CO2	N2	H+	OH-	CL-	NA+	K+
PLASMA	-3.86288E-02	-4.57208E-02	-3.87604E-02	1.23863E 01	-3.17648E 01	-4.49981E 01	2.08010E 02	-2.03773E 02
02	3.50443E-07	-1.78462E-07	-1.62267E-07	7.55178E-05	-7.41141E-05	-1.04953E-04	4.85624E-04	-4.75524E-04
CO2	-1.67051E-06	1.13718E-05	-1.67371E-06	7.86018E-04	-7.71542E-04	-1.08163E-03	5.00861E-03	-4.90601E-03
N2	-5.19958E-07	-5.73010E-05	-2.34050E-07	2.42415E-04	-2.37909E-04	-3.36936E-04	1.55905E-03	-1.52663E-03
H+	-5.82811E-11	1.91926E-10	-6.02888E-11	4.36637E-07	-4.35932E-07	1.72196E-07	-5.40025E-04	-2.44890E-07
OH-	1.05833E-11	-3.81737E-09	5.73972E-11	-5.75058E-06	5.75310E-06	-3.51308E-06	5.24810E-06	-7.57554E-07
CL-	7.48611E-06	-4.03765E-05	6.57637E-06	2.00330E-01	-2.00392E-01	3.55664E-01	5.99547E-01	-1.97515E-01
NA+	-1.76327E-06	9.81571E-06	-1.53574E-06	-4.51779E-02	4.51922E-02	9.11779E-02	9.13472E-01	-1.90748E-01
K+	-5.10370E-07	2.84110E-06	-4.44513E-07	-1.30765E-02	1.30807E-02	2.63910E-02	3.50309E-02	-4.15957E-01
CA++	-1.10908E-07	6.09440E-07	-9.69279E-08	-2.89067E-03	2.89158E-03	5.48769E-03	-2.98242E-03	-6.20420E-03
MG++	-1.90321E-07	1.04667E-06	-1.66332E-07	-4.96047E-03	4.96203E-03	9.41703E-03	-5.11799E-03	-1.06467E-02
SO4=	8.87606E-08	-4.81023E-07	7.78762E-08	2.36019E-03	-2.36093E-03	-4.15588E-03	5.95858E-03	-5.62078E-04
HPO4=	2.71489E-07	-1.79495E-06	2.68073E-07	7.66106E-04	-7.66456E-04	-6.24987E-03	9.02335E-03	-9.42034E-04
H2PO4-	-5.34453E-08	5.57990E-07	-6.96338E-08	1.51388E-03	-1.51336E-03	-2.38430E-03	4.11022E-03	-1.29995E-03
NH4+	-7.48901E-08	3.94070E-07	-5.98643E-08	-9.77045E-04	9.77585E-04	2.57639E-03	2.97407E-04	-5.32950E-03
NH3	1.88931E-08	-1.43507E-07	2.03868E-08	-3.19162E-04	3.18994E-04	-5.77641E-05	1.52103E-04	-1.07431E-04
LACTIC	1.90122E-07	-1.02543E-06	1.67018E-07	5.08770E-03	-5.08929E-03	-8.73901E-03	1.52265E-02	-5.01622E-03
UREA	7.85131E-08	-4.08410E-07	6.96145E-08	2.19995E-03	-2.20063E-03	-3.10976E-03	1.38431E-02	-1.37638E-02
GLUCOS	9.16070E-08	-4.76522E-07	8.12744E-08	2.56684E-03	-2.56763E-03	-3.62839E-03	1.61518E-02	-1.60590E-02
HCO3-	-1.14691E-05	7.81347E-05	-1.22613E-05	-2.59020E-01	2.59113E-01	-1.58275E-01	2.36498E-01	-3.41267E-02
H2CO3	-2.38287E-09	1.61629E-08	-2.38745E-09	1.17811E-06	-1.10711E-06	-1.55726E-06	7.10037E-06	-6.99917E-06
CO3=	9.37409E-09	-1.00896E-07	1.28646E-08	-7.51440E-04	7.51346E-04	-4.16593E-04	5.24760E-04	4.28352E-05
H2O	-3.86190E-02	-4.57800E-02	-3.87510E-02	1.24955E 01	-3.18941E 01	-4.53003E 01	2.06193E 02	-2.05279E 02
PROTN	-6.26315E-14	7.51577E-13	-7.30762E-13	-4.20723E-08	3.79677E-08	7.30011E-08	-7.59354E-08	-3.20369E-08

RED CELLS	-2.59742E-02	-1.86066E-02	-2.58409E-02	-3.30729E 01	3.34642E 01	4.72378E 01	-2.05401E 02	2.06196E 02
02	3.49752E-07	-1.43895E-07	-1.71489E-07	-1.26082E-04	1.27572E-04	1.80052E-04	-7.82760E-04	7.83697E-04
CO2	-1.08683E-06	7.32501E-06	-1.08364E-06	-7.92516E-04	8.01932E-04	1.13862E-03	-4.94787E-01	4.56544E-01
N2	-5.57737E-07	-4.66616E-07	-7.61304E-07	-4.08074E-04	4.13706E-04	5.83058E-04	-2.53025E-03	2.54776E-03
H+	-4.83229E-11	1.49053E-10	-5.07119E-11	5.08860E-07	-5.08258E-07	-7.34104E-08	-7.93187E-08	2.57996E-07
OH-	-4.59559E-11	-1.31920E-09	-2.72721E-11	-4.04821E-06	4.04979E-06	1.20824E-06	-2.47972E-06	1.23347E-06
CL-	-7.48610E-06	4.03765E-05	-6.57637E-06	-2.00130E-01	2.00392E-01	4.44335E-01	-5.99547E-01	1.97515E-01
NA+	1.76327E-06	-9.81569E-06	1.53595E-06	4.51779E-02	-4.51922E-02	-9.11779E-02	8.65277E-02	1.90748E-01
K+	5.10369E-07	-2.84110E-06	4.44975E-07	1.30765E-02	-1.30807E-02	-2.63910E-02	-3.50300E-03	1.00416E 00
CA++	1.10908E-07	-6.09440E-07	9.69285E-08	2.89067E-03	-2.89158E-03	-5.48769E-03	2.98246E-01	6.20420E-03
MG++	1.90322E-07	-1.04667E-06	1.66332E-07	4.96047E-03	-4.96203E-03	-9.41703E-03	5.11798E-03	1.06467E-02
SO4=	-8.87604E-08	4.81024E-07	-7.78761E-08	-2.36019E-03	2.36093E-03	4.15588E-03	-5.95858E-03	5.62077E-04
HPO4=	1.68786E-07	-1.62113E-06	2.13294E-07	-9.60043E-03	9.59883E-03	8.70043E-03	-8.75348E-03	6.27424E-04
H2PO4-	-3.86829E-07	2.87809E-06	-4.11733E-07	5.32245E-03	-5.31901E-03	2.43369E-03	-4.38009E-03	1.61434E-03
NH4+	3.51813E-08	-1.46115E-07	2.76224E-08	1.52197E-03	-1.52224E-03	-2.52259E-03	-3.75437E-04	5.33584E-03
NH3	1.08158E-08	-8.44480E-08	1.18553E-08	-2.25760E-04	2.25663E-04	1.96444E-06	-7.41523E-05	1.01071E-04
LACTIC	-1.90122E-07	1.02543E-06	-1.67017E-07	-5.08770E-03	5.08929E-03	8.73901E-03	-1.52265E-02	5.01622E-03
UREA	-7.85127E-08	4.08411E-07	-6.96143E-08	-2.19995E-03	2.20063E-03	3.10976E-03	-1.38431E-02	1.37638E-02
GLUCOS	-9.16065E-08	4.76522E-07	-8.12400E-08	-2.56684E-03	2.56763E-03	3.62839E-03	-1.61518E-02	1.60590E-02
HCO3-	-9.70967E-06	5.50611E-05	-8.74145E-06	-2.09781E-01	2.09863E-01	6.24087E-02	-1.28539E-01	6.19551E-02
H2CO3	-1.55010E-09	1.04111E-08	-1.54558E-09	-1.12099E-06	1.13445E-06	1.60762E-06	-7.05157E-06	7.04865E-06
CO3=	-2.04494E-09	-5.93853E-09	-2.17630E-10	-3.94386E-04	3.94398E-04	1.04000E-04	-1.72792E-04	4.76731E-05
H2O	-2.59577E-02	-1.86970E-02	-2.58275E-02	-3.27120E 01	3.31031E 01	4.66356E 01	-2.04771E 02	2.04671E 02
PROTN	-1.61264E-06	1.29559E-05	-1.80740E-06	4.18424E-02	-4.18478E-02	-9.48552E-03	1.05683E-02	3.13053E-03
PROTN-	1.61264E-06	-1.29559E-05	1.80740E-06	-4.18424E-02	4.18478E-02	9.48552E-03	-1.05683E-02	-3.13092E-03
HB4	-1.91103E-07	1.90564E-07	1.49005E-09	6.56286E-04	-6.56056E-04	-1.48740E-04	1.65637E-04	4.90378E-05
HB4O2	-5.63361E-07	5.61537E-07	4.39074E-09	1.93895E-03	-1.93321E-03	-4.38294E-04	4.88083E-04	1.44500E-04
HB4O4	-1.23878E-07	1.23477E-07	9.65481E-09	4.25243E-03	-4.25094E-03	-9.63765E-04	1.07329E-03	3.17741E-04
HB4O6	-1.71107E-07	1.70553E-07	1.33357E-09	5.87369E-04	-5.87164E-04	-1.33121E-04	1.48243E-04	4.38882E-05
HB4O8	2.16442E-06	-2.15740E-06	-1.68696E-06	-7.42989E-03	7.42730E-03	1.68390E-03	-1.87519E-03	-5.55162E-04

REDHEME RHB	-5.10347E-06	5.08695E-06	3.97759E-08	1.75190E-02	-1.75129E-02	-3.97049E-03	4.42153E-03	1.30902E-03
H2HB+	-3.84143E-06	4.43915E-06	-8.92373E-08	1.58981E-02	-1.58926E-02	-3.60304E-03	4.01264E-03	1.18809E-03
HHB+-	-6.11931E-07	4.10492E-07	3.29923E-08	1.59400E-03	-1.59344E-03	-3.61303E-04	4.02266E-04	1.19046E-04
HB-	-3.86135E-07	4.35281E-08	5.51112E-08	3.24053E-04	-3.23939E-04	-7.35091E-05	8.17111E-05	2.41413E-05
RCARB-	-2.61970E-07	1.93777E-07	-0.00097E-08	-2.97185E-04	2.97082E-04	6.73676E-05	-7.51344E-05	-2.22812E-05

OXYHEME OMB	5.10347E-06	-5.08694E-06	-3.97766E-08	-1.75190E-02	1.75128E-02	3.97048E-03	-4.42192E-03	-1.30902E-03
H2HBO+	-9.77179E-07	1.13737E-05	-1.99590E-06	4.72834E-02	-4.72669E-02	-1.07144E-02	1.19374E-02	3.53602E-03
HHBO+-	1.48577E-06	-4.07289E-06	-1.27363E-06	3.59911E-02	-3.59788E-02	-8.15777E-03	9.08821E-03	2.69182E-03
HBO2-	2.69619E-06	-1.66050E-05	1.76326E-06	-3.80598E-02	3.80465E-02	8.62280E-03	-9.60739E-03	-2.84602E-03
OCARB+	1.89869E-06	1.85112E-07	1.42965E-06	-6.27339E-02	6.27120E-02	1.42201E-02	-1.58398E-02	-4.69084E-03

OXYSTABLE HP	-9.86204E-12	2.85586E-11	-7.93224E-12	1.03232E-07	-8.58947E-08	-2.37440E-08	2.02133E-08	9.90507E-09
1H1O+	-8.52078E-06	8.86143E-05	-9.54984E-06	2.21190E-01	-2.21113E-01	-5.01191E-02	5.58400E-02	1.65409E-02
1H1O	8.52077E-06	-8.86142E-05	9.54983E-06	-2.21190E-01	2.21113E-01	5.01190E-02	-5.58400E-02	-1.65409E-02

SITE1 SERUM	-3.04213E-11	1.73614E-10	-3.00095E-11	-1.21907E-06	1.24447E-06	1.98099E-06	-2.19877E-06	-8.00015E-07
RCOOH	-1.36147E-08	1.01314E-07	-1.44753E-08	1.85941E-04	-1.85020E-04	9.21974E-05	-9.22407E-05	-4.36671E-05
RCOO-	1.35834E-08	-1.01137E-07	1.44452E-08	-1.87145E-04	1.87056E-04	-9.02335E-05	9.00937E-05	4.28694E-05

SITE2 SERUM	-2.09615E-12	1.45305E-11	-2.18623E-12	-1.35452E-07	1.39557E-07	2.05231E-07	-2.21649E-07	-8.00400E-08
RANH3+	-2.12711E-06	1.58289E-05	-2.26157E-06	2.90507E-02	-2.90319E-02	1.44044E-02	-1.44113E-02	-6.02239E-03
RANH2	2.12711E-06	-1.58289E-05	2.26157E-06	-2.90509E-02	2.90320E-02	-1.44044E-02	1.44111E-02	6.02231E-03

SITE3 SERUM	1.98023E-11	-1.08439E-10	1.86727E-11	5.84908E-07	-5.35662E-07	-1.03021E-06	1.03821E-06	4.53303E-07
RENH3+	-2.38355E-08	1.77411E-07	-2.53444E-08	3.26392E-04	-3.26151E-04	1.60492E-04	-1.60577E-04	-7.60536E-05
RENH2	2.38555E-08	-1.77521E-07	2.53635E-08	-3.25804E-04	3.25592E-04	-1.61347E-04	1.61623E-04	7.65130E-05

SITE4 SERUM	3.56999E-12	-2.21637E-11	3.17952E-12	7.31134E-08	-7.31134E-08	-1.51101E-07	1.41353E-07	6.82392E-08
R+4	-1.47790E-09	1.10046E-38	-1.57701E-09	2.01398E-05	-2.03066E-05	9.87176E-06	-9.88151E-06	-4.67757E-06
R+4-	1.45198E-09	-1.10282E-08	1.57566E-09	-2.02400E-05	2.02266E-05	-1.00356E-05	1.00405E-05	4.75321E-06

AIR OUT	1.06462E 00	1.06420E 00	1.06462E 00	1.23708E 00	-1.23000E 00	-1.16203E 00	-1.61724E 00	-1.44684E 00
02	9.99974E-01	5.40003E-06	3.71223E-07	1.75672E-02	-1.75640E-02	-4.04500E-03	4.71784E-03	9.98043E-04
CO2	2.42949E-05	9.99448E-01	2.22745E-05	5.32985E-01	-5.33181E-01	8.15927E-02	-9.07650E-02	-2.52634E-02
N2	1.08624E-06	1.03138E-06	1.00000E 00	1.44625E-04	-1.55793E-04	-2.47232E-04	9.73306E-04	-1.02179E-03
H2O	6.45999E-02	6.45447E-02	6.45977E-02	6.86359E-01	-6.79069E-01	-1.23937E 00	-1.53040E 00	-1.42156E 00

Table XIXA--continued

JACOBIAN, CYCLE 2

	CA++	MG++	SO4=	HPO4=	NH4+	LACTIC	UREA	GLUCOSE
PLASMA	2.03346E 02	-5.59031E 01	-1.80986E 02	-1.88631E 02	2.59062E 01	-4.49981E 01	1.44443E 00	1.44443E 00
O2	6.61483E-04	-1.30374E-04	-4.22356E-04	-4.40162E-04	6.05103E-05	-1.04953E-04	3.47598E-06	3.47598E-06
CO2	6.82157E-03	-1.34602E-03	-4.35636E-03	-4.54345E-03	6.24231E-04	-1.08163F-03	3.58553F-05	3.58553E-05
N2	2.12362E-03	-4.18561E-04	-1.35594E-03	-1.41309E-03	1.94450E-04	-1.36937E-04	1.11594F-05	1.11594E-05
H+	-2.30103E-07	-2.47501E-07	-2.99067E-09	-2.46998F-07	-1.22643E-07	1.72196F-07	1.44318E-09	1.44318E-09
OH-	9.46236E-06	2.4495RE-06	-3.64083E-06	-4.02858E-07	2.16226E-06	-3.51308E-06	3.19816F-09	3.19816E-09
CL-	1.02424E 00	1.82742E-01	-4.59135E-01	-4.68300E-01	2.45370E-01	-3.44101E-01	-9.06984E-05	-9.06985E-05
NA+	-7.59318E-02	-1.60107E-01	-4.23178E-02	-4.88991E-02	-7.68284E-02	9.11779E-02	7.01726E-05	7.01224E-05
K+	-2.19798E-02	-4.63470E-02	-1.22647E-02	-1.41536E-02	-2.22376E-02	2.61910E-02	5.82447E-06	5.82442E-06
CA++	8.51006E-01	-7.21213E-03	1.01218E-03	8.11634E-04	-4.36767E-03	5.48769E-03	1.29598E-06	1.29597E-06
MG++	-1.51232E-02	2.77566E-01	1.73694E-03	1.39279F-03	-7.49503E-03	9.41703E-03	2.22396E-06	2.22395E-06
SO4=	1.09041E-02	3.04483E-03	3.09803E-01	-4.35829E-03	3.05205E-03	-4.15589E-03	-1.06608E-06	-1.06608E-06
HPO4=	1.66681E-02	4.55209E-03	-6.55353E-03	1.67678E-01	4.50627E-03	-6.26962E-03	-3.41369E-06	-3.41369E-06
H2PO4-	7.04779E-03	1.29961E-03	-3.13593E-03	1.03576E-01	1.76370E-03	-2.38430E-03	7.51146E-07	7.51446E-07
NH4+	-2.19853E-03	-4.49766E-03	-1.17323E-03	-1.47286E-03	5.08442E-01	2.57939E-03	7.66410E-07	7.66405E-07
NH3	2.10665E-04	-3.75609E-06	-1.27014E-04	2.82021E-05	1.67799E-02	-5.77641E-05	-2.46852F-07	-2.46852E-07
LACTIC	2.50122E-02	4.64103E-03	-1.16605E-02	-1.18932E-02	6.23156E-03	6.91027E-01	-2.30344E-06	-2.30345E-06
UREA	1.88881E-02	-3.85203E-03	-1.22297E-02	-1.27565E-02	1.63543E-03	-3.10976E-03	6.16065F-01	-1.01236E-06
GLUCOS	2.20381E-02	-4.49445E-03	-1.42697E-02	-1.48839E-02	1.90818E-03	-3.62839E-03	-1.18117E-06	6.16065E-01
HCO3-	4.26388E-01	1.10390E-01	-1.73050F-01	-1.81818E-02	1.06462E-01	-1.58275E-01	1.63258E-04	1.63258E-04
H2CO3	4.67649E-06	-1.93722E-06	-6.21531E-06	-6.48637E-06	8.65640E-07	-1.55728E-06	3.00500E-08	3.00500E-08
CO3=	1.00813E-03	3.49154E-04	-3.63746E-04	7.75389E-05	2.8247RE-04	-4.14593E-04	-1.36788E-07	-1.36788E-07
H2O	2.81047E 02	-5.62592E 01	-1.80557E 02	-1.88303E 02	2.51198E 01	-4.53003E 01	8.33220E-01	8.33220E-01
PROTN	-1.19034E-07	-4.30985E-06	5.23134E-08	5.20723E-08	-4.10462E-08	6.15692F-08	9.00631F-12	6.01262E-12
RED CELLS	-2.80660E 02	5.84107E 01	1.83264E 02	1.91253E 02	-2.34455E 01	4.72379E 01	9.27796E-01	9.27796E-01
O2	-1.06917E-03	2.22653E-04	6.98311E-04	7.28785E-04	-8.92215E-05	1.80052E-04	3.62936E-06	3.62937E-06
CO2	-6.75873E-03	1.40653E-03	4.41388E-03	4.60635E-03	-5.64280E-04	1.13862E-03	2.29351E-05	2.29351E-05
N2	-3.46609E-03	7.21905E-04	2.76441E-03	2.36324E-03	-2.84322E-04	5.81856E-04	1.17689E-05	1.17689E-05
H+	-1.73321E-08	1.78579E-07	1.03718E-07	-1.00620E-07	8.20012E-08	-7.34104E-08	1.25578E-09	1.25578E-09
OH-	-4.02310E-06	-3.91140E-07	1.97542E-06	1.52281E-06	-9.22840E-07	1.20424E-06	2.08793E-09	2.08793E-09
CL-	-1.02424E 00	-1.82742E-01	4.59135E-01	4.68300E-01	-2.45370E-01	3.44101F-01	9.06981E-05	9.06985E-05
NA+	7.59378E-02	1.60107E-01	4.23178E-02	4.88991E-02	7.68284E-02	-9.11779E-02	-2.01210E-05	-2.01229E-05
K+	2.19798E-02	4.63420E-02	1.22686E-02	1.41536E-02	2.22376E-02	-2.61910E-02	-5.82455E-06	-5.82451E-06
CA++	1.48994E-01	7.21214E-03	-1.01219E-03	-8.11636E-04	4.36767E-03	-5.48769E-03	-1.29600E-06	-1.29599E-06
MG++	1.51212E-02	7.22444E-01	-1.73694E-03	-1.39279E-03	7.49503E-03	-9.41703E-03	-2.22396E-06	-2.22396E-06
SO4=	-1.09041E-02	-3.04483E-03	6.90107E-01	4.35829E-03	-3.05205E-03	4.15589E-03	1.06608E-06	1.06608E-06
HPO4=	-1.41158E-02	-4.44508E-03	6.29812E-03	3.86782E-04	-4.73593E-03	6.20045E-03	-2.36098E-06	-2.36097E-06
H2PO4-	-7.40009E-03	-1.18663E-03	3.39135E-03	3.41944E-01	-1.53401E-03	2.43369E-03	5.02151E-03	5.02152E-06
NH4+	2.05469E-03	4.45674E-03	1.21014E-03	1.27136E-03	4.64341E-01	-2.52260E-03	-3.78081E-07	-3.78077E-07
NH3	-8.68303E-05	4.46839E-05	7.01291E-05	1.73304E-04	1.04373E-02	1.96444E-06	-1.41481E-07	-1.41481E-07
LACTIC	-2.60122E-02	-4.64103E-03	1.16605E-02	1.18932E-02	-6.23156E-03	3.08973E-01	2.30342E-06	2.30343E-06
UREA	-1.88881E-02	3.85203E-01	1.22297E-02	1.27565E-02	-1.63543E-03	3.10976E-03	1.83935E-01	1.01235E-06
GLUCOS	-2.20381E-02	4.49445E-03	1.42697E-02	1.48839E-02	-1.90818E-03	3.62839E-03	1.18116E-06	1.81935E-01
HCO3-	-2.08553E-01	-2.02743E-02	1.02414E-01	1.82594E-01	-4.78319E-02	6.26487E-02	1.17674E-04	1.17674E-04
H2CO3	-9.62858E-06	1.98620E-06	6.26551E-06	6.53332E-06	-8.16368E-07	1.60762E-06	1.95665E-08	1.95665E-08
CO3=	-2.99961E-04	-6.07760E-05	1.30671E-04	2.83147E-04	-8.38563E-05	1.04008E-04	1.63395E-08	1.61196E-08
H2O	-2.79578E 02	5.76759E 01	1.81904E 02	1.89759E 02	-2.37179E 01	4.66356E 01	5.43637E-01	5.43637E-01
PROTN	2.14417E-02	9.00909E-03	-6.88675E-03	-2.32676E-02	8.21615E-03	-9.48552E-03	2.13934E-05	2.13934E-05
PROTN-	-2.14417E-02	-9.00909E-03	6.88674E-03	2.32676E-02	-8.21615E-03	9.48552E-03	-2.13934E-05	-2.13934E-05
HB4	3.36096E-04	1.41194E-04	-1.08000E-03	-3.64487E-04	1.28764E-04	-1.48740E-04	2.96807E-07	2.96807E-07
HB4O2	9.90378E-04	4.16058E-04	-3.18244E-04	-1.07498E-03	3.79430E-04	-4.38294E-04	8.74605E-07	8.74605E-07
HB4O4	2.17774E-03	9.14870E-04	-6.99788F-04	-2.36378E-03	8.34330E-04	-9.63765E-04	1.92317E-06	1.92317E-06
HB4O6	1.00802E-04	1.26367E-04	-9.66567E-05	-3.26698E-04	1.15242E-04	-1.33121F-04	2.65639E-07	2.65639E-07
HB4O8	-3.80498E-03	-1.59846E-03	1.22267E-03	4.13002E-03	-1.45775E-03	1.68390E-03	-3.36020E-06	-3.36019E-06
REDHEME RHB	8.97180E-03	3.76905E-03	-2.88297E-03	-9.71822E-03	3.41125E-03	-3.97049E-03	7.92302E-06	7.92302E-06
H2HB+	8.14205E-03	3.42057E-03	-2.61612E-03	-8.83710E-03	3.11944E-03	-3.60304E-03	7.35223E-06	7.35223E-06
HHB+-	8.16284E-04	3.42899E-04	-2.62352E-04	-8.86089E-04	3.17708E-04	-3.61303E-04	6.82941E-07	6.82914E-07
HB-	1.65874E-04	6.96427E-05	-5.33942E-05	-1.80198E-04	6.35060E-05	-7.35092E-05	7.62278E-08	7.62278E-08
RCARB+	-1.52401E-04	-6.40545E-05	4.49012E-05	1.65173E-04	-5.84123E-05	6.73670E-05	-1.88351E-07	-1.88351E-07
OXYHEME OHB	-8.97178E-03	-3.76905E-03	2.88296E-03	9.73819E-03	-3.43724E-03	3.97048E-03	-7.92300E-06	-7.92301E-06
H2HBO+	2.42197E-02	1.01762E-02	-7.77914E-03	-2.62811E-02	9.28049E-03	-1.07146E-02	2.40589E-05	2.40589E-05
HHBO+-	1.84392E-02	7.74711E-03	-5.92278E-03	-2.00058E-02	7.06514E-03	-8.15777E-03	1.80362E-05	1.80362E-05
HBO2-	-1.94921E-02	-8.19001E-03	6.26034E-03	2.11534E-02	-7.46928E-03	8.62280E-03	-1.96029E-05	-1.96029E-05
OCARB=	-3.21386E-02	-1.35026E-02	1.03246E-02	3.48716E-02	-1.23136E-02	1.42201E-02	-3.04152E-05	-3.04152E-05
OXYSTABLE HB	4.77597E-08	2.20723E-08	-1.53801E-08	-6.04750E-08	1.62570E-08	-2.69956E-08	1.02160E-10	5.94319E-11
IM10+	1.13293E-01	4.76017E-02	-3.63878E-02	-1.22940E-01	4.34120E-02	-5.01119E-02	1.13037E-04	1.13037E-04
IM10	-1.13292E-01	-4.76017E-02	3.63874E-02	1.22940E-01	-4.34120E-02	5.01190E-02	-1.13037E-04	-1.13037E-04
SITE1 SERUM	-4.26679E-06	-2.03178E-06	1.39685E-06	1.39685E-06	-1.57463E-06	2.00639E-06	4.15434E-10	3.33276E-10
RCOOH	-1.96104E-04	-9.11359E-05	5.77682E-05	-4.95605E-05	-6.37493E-05	9.21974E-05	1.76156E-07	1.76156E-07
RCOO-	1.91843E-04	9.10967E-05	-5.61847E-05	5.09443E-05	6.21870E-05	-9.02206E-05	-1.75741E-07	-1.75822E-07
SITE2 SERUM	-4.35089E-07	-2.13440E-07	1.47766E-07	1.51871E-07	-1.60080E-07	2.09335E-07	3.15662E-11	2.93135E-11
RANH3+	-1.06385E-02	-1.45512E-02	9.02549E-03	-7.74315E-03	-9.95995E-03	1.44046E-02	2.75219E-05	2.75219E-05
RANH2	1.06380E-02	1.45510E-02	-9.02534E-03	7.74331E-03	9.95979E-01	-1.44044E-02	-2.75219E-05	-2.75219E-05
SITE3 SERUM	2.31038E-06	9.65097E-07	-6.58021E-07	-6.72644E-07	7.75002E-07	-1.02359E-06	-2.21340E-10	-2.72212E-10
RENH3+	-3.41270E-04	-1.62210E-04	1.00557E-04	-8.75171E-05	-1.10919E-04	1.60529E-04	3.01446E-07	3.04381E-07
RENH2	3.43610E-04	1.63191E-04	-1.01221E-04	8.68393E-05	1.11701E-04	-1.61547E-04	-3.08658E-07	-3.08658E-07
SITE4 SERUM	3.41196E-07	1.26730E-07	-8.28619E-08	-8.77361E-08	1.07233E-07	-1.36478E-07	-1.56994E-11	-6.21774E-11
R+	-2.09717E-05	-9.99604E-06	6.19492E-06	-5.49027E-06	-6.82000E-06	9.88394E-06	1.91144E-08	1.91088E-08
R++	2.15461E-05	1.01340E-05	-6.28815E-06	5.39476E-06	6.93920E-06	-1.00588E-05	-1.91749E-08	-1.91740E-08
AIR OUT	-1.06376E 00	-1.58065E 00	-1.22019E 00	-1.81091E 00	-1.50369E 00	-1.16203E 00	-1.37747E 00	-1.17747E 00
O2	9.17804E-03	3.67631E-03	-3.15837E-03	-1.00254E-02	3.46542E-03	-4.04501E-01	8.24739E-07	8.22825E-07
CO2	-1.86315E-01	-7.68976E-02	6.04380E-02	-1.99871E-01	-4.85162E-02	8.19277E-02	-1.00046E-04	-3.09047E-04
N2	1.13206E-03	3.07472E-04	-9.04467E-04	-9.38336E-04	3.08603E-04	-2.42254E-04	-2.29517E-05	-2.29318E-05
H2O	-1.68817E 00	-1.90713E 00	-1.77657E 00	-1.62004E 00	-1.46071E 00	-1.23933E 00	-1.17714E 00	-1.17714E 00

Table XIXA--continued

JACOBIAN, CYCLE 5

	MISCPLASMA	MISCREDCELL	HR4
PLASMA	-2.11419E 05	-2.04686E 02	1.73977E 02
O2	-4.98147E-03	-4.77711E-04	4.01587E-04
CO2	-5.11850E-02	-4.92340E-03	4.26248E-03
N2	-1.54923E-02	-1.53367E-03	1.30168E-03
H+	2.42164E-06	6.46793E-08	5.16762E-06
OH-	-8.14985E-05	-5.34622E-06	-7.25492E-05
CL-	-1.10663E 01	-9.80837E-02	2.24303E 00
NA+	2.05690E 00	-2.16144E-01	-7.64121E-01
K+	5.95360E-01	-6.83507E-02	-2.21171E-01
CA++	1.42799E-01	-8.52305E-01	-4.23052E-02
MG++	2.45046E-01	-1.46258E-02	-7.25969E-02
SO4=	-1.27087E-01	7.81697E-04	2.83643E-02
HPO4=	-1.81678E-01	-9.78589E-04	7.95122E-03
H2PO4-	-8.34039E-02	9.58732E-04	4.20241E-02
NH4+	5.73367E-02	-6.38571E-03	-1.78041E-02
NH3	-8.77988E-04	-3.57679E-04	-4.08761E-03
LACTIC	-2.81048E-01	-2.49100E-01	5.69670E-02
UREA	-1.43147E-01	-1.38037E-02	1.19063E-02
GLUCOS	-1.67020E-01	-1.61058E-02	1.38919E-02
HCO3-	-3.67255E 00	-2.40816E-01	-3.26788E 00
H2CO3	-7.30833E-05	-7.01654E-06	6.16175E-06
CO3=	-8.88683E-03	-5.38587E-04	-9.32034E-03
H2O	-2.12248E 03	-2.01971E 02	1.75965E 02
PROTN	1.00000E 00	-5.54123E-08	-4.92554E-07
RED CELLS	2.11526E 03	2.06598E 02	-1.79803E 02
O2	8.13514E-03	7.87171E-04	-6.87573E-04
CO2	5.14181E-02	4.97798E-03	-4.28385E-03
N2	2.63800E-02	2.55252E-03	-2.22342E-03
H+	-2.98039E-06	6.52381E-07	6.59935E-06
OH-	5.23646E-05	-1.51975E-06	-4.88289E-05
CL-	1.10663E 01	9.80837E-02	-2.24309E 00
NA+	-2.05690E 00	2.16144E-01	7.64121E-01
K+	-5.95360E-01	6.83507E-02	2.21171E-01
CA++	-1.42799E-01	8.52306E-01	4.23052E-02
MG++	-2.45046E-01	1.46258E-02	7.25969E-02
SO4=	1.27087E-01	-7.81698E-04	-2.83643E-02
HPO4=	2.10218E-01	-5.86790E-01	-1.18065E-01
H2PO4-	5.53617E-02	5.88775E-03	6.80892E-02
NH4+	-5.76591E-02	6.79779E-03	2.45844E-02
NH3	1.20034E-03	-5.43942E-05	-2.69276E-03
LACTIC	2.81048E-01	2.49099E-03	-5.69670E-02
UREA	1.43147E-01	1.38017E-02	-1.19063E-02
GLUCOS	1.67020E-01	1.61058E-02	-1.38919E-02
HCO3-	2.71441E 00	-7.87256E-02	-2.53036E 00
H2CO3	7.31289E-05	7.07108E-06	-6.02951E-06
CO3=	4.46880E-03	-2.29056E-04	-4.83809E-03
H2O	2.12350E 03	2.05204E 02	-1.76979E 02
PROTN	-4.02749E-01	2.98227E-01	5.22693E-01
PROTN-	4.02749E-01	7.01773E-01	-5.22693E-01
HR4	-6.31368E-03	5.24561E-04	1.11270E-02
HR4O2	-1.86052E-02	1.54573E-03	3.58061E-02
HR4O4	-4.09110E-02	3.39891E-03	9.74958E-02
HR4O6	-5.65086E-03	4.69477E-04	1.90833E-02
HR4O8	7.14802E-02	-5.93862E-03	8.41489E-01
REDHEME RHB	-1.68544E-01	1.40027E-02	3.56001E-01
H2HB+	-1.57952E-01	1.27074E-02	2.99020E-01
HHR+-	-1.53356E-02	1.27403E-03	3.70402E-02
HB-	-1.11755E-03	2.58940E-04	1.56777E-02
RCARB+	2.86089E-03	-2.17609E-04	4.26261E-03
OXYHEME OH4	1.68544E-01	-1.40027E-02	3.44400E 00
H2HRO+	-4.54921E-01	3.77960E-02	1.13367E 00
HHRO+-	-3.46325E-01	2.87699E-02	2.36566E 00
HRO2-	3.66140E-01	-3.04230E-02	3.45428E-01
OCARB+	6.03650E-01	-5.01456E-02	-2.20755E-01
OXYSTABLE HB	-7.90423E-07	1.32760E-07	1.60000E 01
IH1O+	-2.12802E 00	1.76808E-01	7.64941E 00
IH1O	2.12802E 00	-1.76808E-01	8.35059E 00
SITE1 SERUM	9.90001E 01	-1.65082E-06	-1.58479E-05
RCOOH	1.93146E-02	9.59597E-05	2.26898E-03
RCOO-	9.89807E 01	-9.75972E-05	-2.28469E-03
SITE2 SERUM	1.60000E 01	-1.80603E-07	-1.77319E-06
RANH3+	3.78558E 00	1.49924E-02	3.54497E-01
RANH2	1.22144E 01	-1.49926E-02	-3.54499E-01
SITE3 SERUM	5.70000E 01	8.33493E-07	7.48682E-06
RENH3+	5.69724E 01	1.68980E-04	3.98321E-03
RENH2	2.75918E-02	-1.68140E-04	-3.97568E-03
SITE4 SERUM	1.40000E 01	1.12107E-07	9.35852E-07
R+4	1.89983E 01	1.05687E-05	2.48015E-04
R+4-	1.71326E-03	-1.04454E-05	-2.46982E-04
AIR OUT	1.22695E-01	-5.27070E-01	9.21070E 00
O2	-1.71673E-01	1.16915E-02	-3.64374E 00
CO2	3.56011E-01	3.70638E-01	6.02892E 00
N2	-1.01870E-02	-1.03394E-03	6.72636E-04
H2O	-5.09858E-02	-9.10396E-01	6.82372E 00

Table XIXB

INCREMENTS IN TOTAL MOLES IN EACH COMPARTMENT
PER UNIT INCREASE IN INPUT SPECIES

JACOBIAN, CYCLE 1

	O2	CO2	N2	H2	OH-	LI-	NA+	K+
PLASMA	-3.862RRE-02	-4.57208F-02	-3.87604E-02	1.21863E 01	-1.17848E 01	-4.53781E 01	2.04310E 02	-2.03773E 02
RED CELLS	-2.59742E-02	-1.86066E-02	-2.58409F-02	-1.30729F 01	1.34442E 01	4.72478E 01	-2.05481E 02	2.04196E 02
REDHERE RHB	-5.10347E-06	5.08695E-06	1.97753E-08	1.75190E-02	-1.75129E-02	-3.97043E-03	4.42153E-03	1.30902E-03
OXYHEME OHB	5.10347E-06	-5.08696E-06	-1.97766E-08	-1.75190E-02	1.75128E-02	3.97044E-03	-4.42152E-03	-1.30902E-03
OXYSTABLE HB	-9.86204E-12	2.85586E-11	-7.93724E-12	1.01212E-07	-8.58947E-08	-2.37448E-08	2.42133E-08	3.90507E-09
SITE1 SERUM	-3.04213E-11	1.71614E-10	-3.00095E-11	-1.21907E-06	1.24447E-06	1.98099E-06	-2.15877E-06	-8.00015E-07
SITE2 SERUM	-2.09815E-12	1.53305E-11	-2.18623E-12	-1.35452E-07	1.19557E-07	2.05231E-07	-2.21649E-07	-8.00400E-08
SITE3 SERUM	1.98023E-11	-1.08419E-10	1.86727E-11	5.34904E-07	-5.55662E-07	-1.03421E-06	1.03821E-06	4.53303E-07
SITE4 SERUM	3.56999E-12	-2.21647E-11	3.17952E-12	7.31134E-08	-7.31134E-08	-1.51101E-07	1.51353E-07	6.82392E-08
AIR OUT	1.06462E 00	1.06420E 00	1.06462E 00	1.23708E 00	-1.23000E 00	-1.16203E 00	-1.61724E 00	-1.44684E 00

JACOBIAN, CYCLE 2

	CA++	MG++	SO4=	HPO4=	NH4+	LACTIC	UREA	GLUCOSE
PLASMA	2.83342E 02	-5.59031F 01	-1.80996E 02	-1.88611E 02	2.59062E 01	-4.45981E 01	1.44941E 00	1.44943E 00
RED CELLS	-2.80660E 02	5.84107E 01	1.43264E 02	1.91253E 02	-2.34455E 01	4.72379E 01	9.27796E-01	9.27796E-01
REDHERE RHB	8.97180E-03	3.76905E-03	-2.88797E-03	-9.73822E-03	3.43725E-03	-3.97049E-03	7.92302E-06	7.92302E-06
OXYHEME OHB	-8.97178E-03	-3.76905E-03	2.88296E-03	9.71819E-03	-3.43725E-03	3.97048E-03	-7.92300E-06	-7.92301E-06
OXYSTABLE HB	4.77597E-08	2.30723E-08	-1.53801E-08	-6.04779E-08	1.62570E-08	-2.64956E-08	1.02160E-10	5.98319E-11
SITE1 SERUM	-4.26675E-06	-2.05178E-06	1.39685E-06	1.39685E-06	-1.57463E-06	2.00639E-06	4.13434E-10	1.33278E-10
SITE2 SERUM	-4.35089E-07	-2.13440E-07	1.47766E-07	1.51871E-07	-1.60080E-07	2.04335E-07	1.15662E-11	2.91115E-11
SITE3 SERUM	2.31038E-06	9.65091E-07	-6.58021E-07	-6.72644E-07	7.75002E-07	-1.02359E-06	-2.21160E-10	-2.72212E-10
SITE4 SERUM	3.41196E-07	1.26730E-07	-8.28619E-08	-8.17361E-08	1.07233E-07	-1.36478E-07	-1.56719E-11	-6.21774E-11
AIR OUT	-1.86376E 00	-1.58065E 00	-1.22019E 00	-1.83091E 00	-1.50369E 00	-1.16203E 00	-1.37747E 00	-1.37747E 00

JACOBIAN, CYCLE 3

	MISCPLASMA	MISCREDCELL	HB+
PLASMA	-3.13419E 03	-2.04686E 02	1.73977E 02
RED CELLS	2.13526E 03	2.06598E 02	-1.79803E 02
REDHERE RHB	-1.68544E-01	1.40027E-02	1.56001E-01
OXYHEME OHB	1.68544E-01	-1.40027E-02	3.64400E 00
OXYSTABLE HB	-7.90423E-07	1.32760E-07	1.60000E 01
SITE1 SERUM	9.90001E 01	-1.65082E-06	-1.58479E-05
SITE2 SERUM	1.60000E 01	-1.80663E-07	-1.77319E-06
SITE3 SERUM	5.70000E 01	8.33493E-07	7.48682E-06
SITE4 SERUM	1.90000E 01	1.12107E-07	9.35842E-07
AIR OUT	1.22695E-01	-5.27070E-01	9.21070E 00

decreases considerably more. In response to Na^+ alone, then, the red cells would go very acidic and the plasma alkaline. Also, partly in response to the pH change, hemoglobin oxygenation decreases.

This experiment cannot be performed in the laboratory since a negative ion must also be added. If 1 meq of Cl^- is added simultaneously, however, the total response is the sum of the two responses shown in the columns headed Na^+ and Cl^-. Thus, there is still a net Na^+ transfer to plasma; and although almost two-thirds of the added Cl^- remains in the red cell--including the Cl^- transferred in the Na^+ column (5.99×10^{-1} meq) and the distribution of the added Cl^- (6.44×10^{-1} meq in plasma)--there is a net increase of 9.57×10^{-1} meq of Cl^- in the plasma compartment as well as a net transfer of water to plasma.

These predicted effects will be proved[*] when dry NaCl is added as an experimental stress. Other details of the response to NaCl can be predicted from the matrix as well as the response of the system to other small stresses. For large stresses, such calculations must be

----

[*] In the doctoral thesis of Eugene Magnier, M.D., Temple University Medical Cent_r, Department of Physiology, Philadelphia (unpublished).

validated, since the partial derivatives are valid for only that system state for which they were calculated.[†]

OXYGEN DISSOCIATION CURVES

Any simulation of the respiratory chemistry of blood should reproduce the standard oxygen dissociation curves-- the oxygen-loading and -unloading functions of normal blood--when the pressure of oxygen to which it is subjected varies from, say, 1 to 100 mm. This test is fundamental.

Since 1942, the data of Dill [16] on oxygen dissociation, from the Mayo Aero-Medical Unit have been the best available for human blood. However, improved techniques (the pH and oxygen electrodes) and more careful attention to detail (especially at very low and very high hemoglobin saturation) may prod_e an improved curve [34].[‡] The new data may modify the presently best available saturation curve by as much as 2 percent of its value in some regions of pO_2. This amount is negligible for clinical applications where calculations are seldom within

---

[†]See the discussion of Model F in Chap. I, Sec. 3, p. 31.

[‡]F.J.W. Roughton, F.R.S., private communication, 1965.

5 percent; but in biochemistry, a 2 percent saturation error in the curve-fitting procedure may modify the oxygen association constants by 100 percent or more, and lead to an entirely different hypothetical microchemistry, particularly in the associated reactions of hemoglobin.

The present model, as Ref. 2, uses the Dill data for validation. The solid lines of Fig. 2 are the Dill curves for human blood; the plotted points are various experiments with the model. The points marked by circles result from a series of computer experiments (described in detail below) wherein the pCO_2 was determined empirically to give the stated pH of the Dill curves at 100 mm of O_2. These points reasonably fit the laboratory data--with less than 1 percent error. This order of error may not even be detectable clinically, but may be crucial for a research hypothesis.

The "normal" curve (pCO_2 = 40 mm, plasma pH = 7.4) of Fig. 2 is, of course, generated with all "normal" values in the liter of simulated blood, e.g., normal buffer base hemoglobin, and gas pressures--all variables with standard values from the literature. The circle data points show the standard computer results holding pH constant over the range of pO_2. The laboratory report [16]
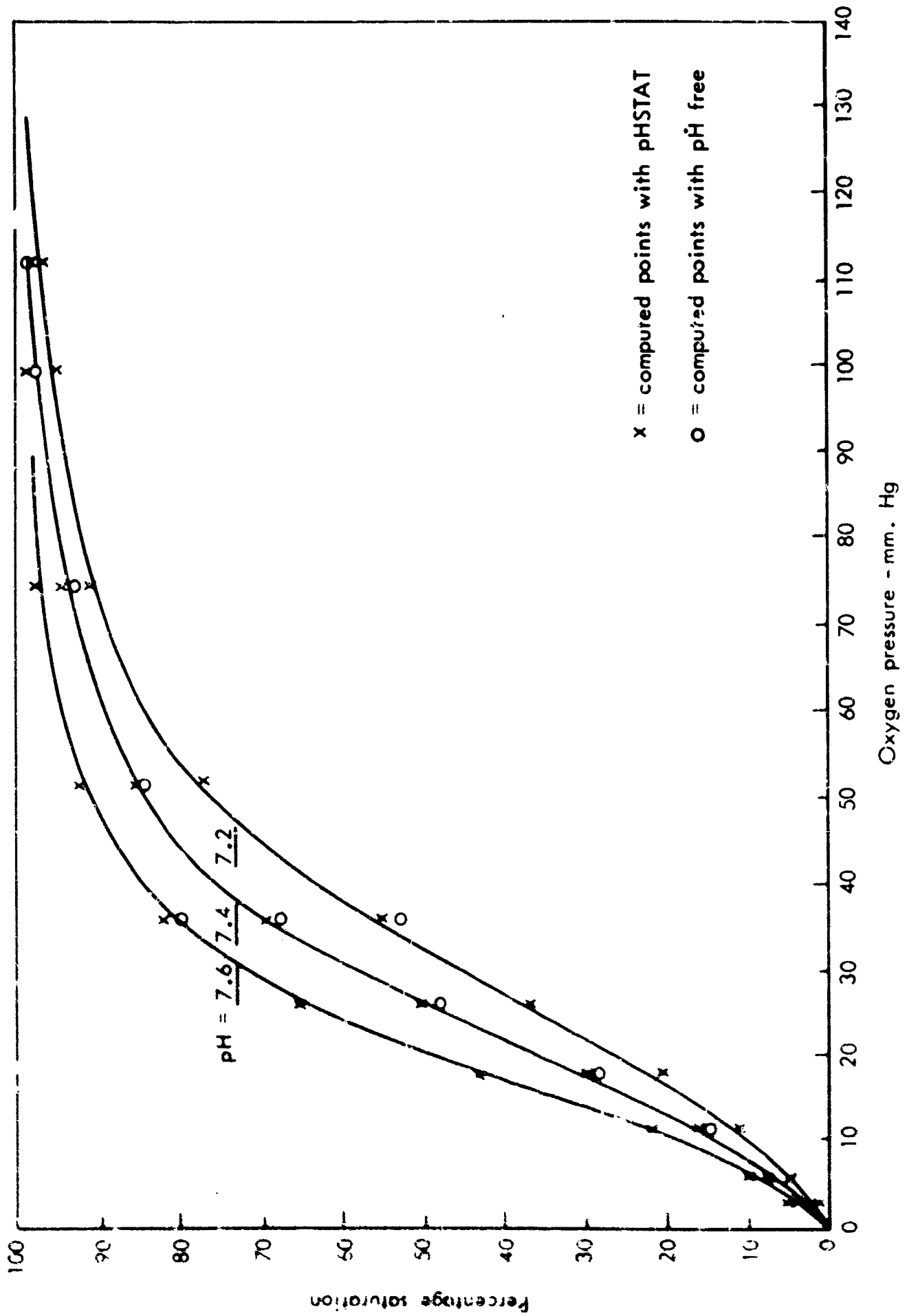
Fig.2—Oxygen dissociation curves for human blood*

x = computed points with pHSTAT

o = computed points with pH free

Oxygen pressure - mm. Hg

Percentage saturation

*Solid lines are from Dill, Ref.16

does not indicate whether the pH and pCO_2 were monitored throughout the range of pO_2 in the wet experiments. The maintenance of both these parameters is now known to be critical in obtaining an accurate saturation curve.

Dill computed the pCO_2 for given pH values and varying pO_2, assuming constant HCO_3^- content. In fact, the HCO_3^- varies uniformly with pH which, in turn, varies with pO_2. Consequently, to maintain a constant pH over the range of pO_2 in the saturation curve experiment, either the pCO_2 or the non-carbonate base must gradually change to hold pH and HCO_3^- constant. If pCO_2 is held constant, either NaOH or HCl must be added to hold the pH.

Conversely, to obtain the extreme pH ranges of 7.2 and 7.6 indicated in Fig. 2 by varying pCO_2 only, pCO_2 values different from those quoted by Dill are necessary. Whereas Dill computed a pCO_2 of 25.5 for pH 7.6 and 61.3 for a pH of 7.2, the corresponding pCO_2 values are in fact closer to 20 mm and 85 mm, respectively. The Henderson-Hasselbach equation also verifies these latter figures, when HCO_3 varies in the presence of a protein buffer having pK 7.2.[*] The crossed points lying on or

_____

[*] See Edsall and Wyman, Ref. 8, p. 569.

near the corresponding Dill curves were obtained by
changing the pCO_2 to these new values and recalculating
the saturation curves at pH 7.2 and 7.6.

For all three of the curves represented by the
crossed points, the computer results are satisfactory,
i.e., practically indistinguishable from the Dill curves.
This is important to several pertinent theoretical ques-
tions. For example, the interaction of CO_2 and H^+ with
oxygenation is evidently simulatable, if not in exact
detail than in overall effect. Again, note that the
oxygenation parameters were determined for hemoglobin in
solution and not for whole blood [2]. Yet when the
parameters were incorporated in the whole blood, they
gave the same curve; i.e., probably no unaccountable
change occurs in the oxygenation of hemoglobin incorporated
into whole blood compared to hemoglobin solution.

A further implication of the goodness of fit concerns
the effect of pH on the saturation curve. From pO_2 = 100 mm
to pO_2 = 1 mm, the pH along the saturation curve drifts
basic by about 0.1 pH unit. (This amount of drift is less
than that predicted from hemoglobin solution experiments--
0.2 pH units [14]--because the blood is more highly buf-
fered.) However, the reasonable fit to the Dill curve

indicates that the pH was not controlled in the wet experiments, and must have drifted approximately the same amount.

With constant non-carbonate base in the blood and constant pCO_2, the pH of normal blood goes basic when the blood deoxygenates, and vice-versa [14]. The exact amount of this effect varies both with the absolute saturation and the absolute pH. Beginning at 100 mm pO_2 and pH 7.4, deoxygenation causes the non-constant pH curve to deviate from the constant pH curve, but by an amount different than for the 7.2 or 7.6 curves [35]. The oxylabile side reactions of the protein produce this phenomenon, related to the Bohr effect. Certain ionizing groups, as yet not precisely specified, change pK according to the state of a nearby oxygen site. Generally speaking, the pK of nearby sites decreases as oxygen attaches, although for certain sites it may rise with oxygenation [36]. Also, some of these sites are evidently carbamino sites, since the absence of CO_2 reduces the shift in pH effect [35].

To test the difference between a curve run at constant pH and one in which the pH drifted, HCl or NaOH was added as though a laboratory pHStat had been used in

the wet experiment. The circle points plotted in Fig. 2 indicate the results.

While the error from the Dill curves is biochemically important at low pO_2, the absolute amounts of these effects are difficult to verify in the literature, because of the absence of definitely comparable experiments. In several published experiments which study the pH effects on oxygenation, principal results are on hemoglobin solution [14,28,36,37]. Since the whole blood is buffered more heavily than hemoglobin solution, the quantitative values for whole blood are not evident from these experiments. Several other papers note that for whole blood the decrease in pH shifts the saturation curve to the right, i.e., decreased oxygen saturation at the s... pO_2 (as expected); but generally this shift in pH is accomplished by changing pCO_2 [38,39]. In short, a careful test of this computer experiment would be interesting.

THE "ASTRUP" EXPERIMENTS

Figure 3 reproduces an Astrup-type chart[*] for clinical determinations of the state of whole blood. The straight
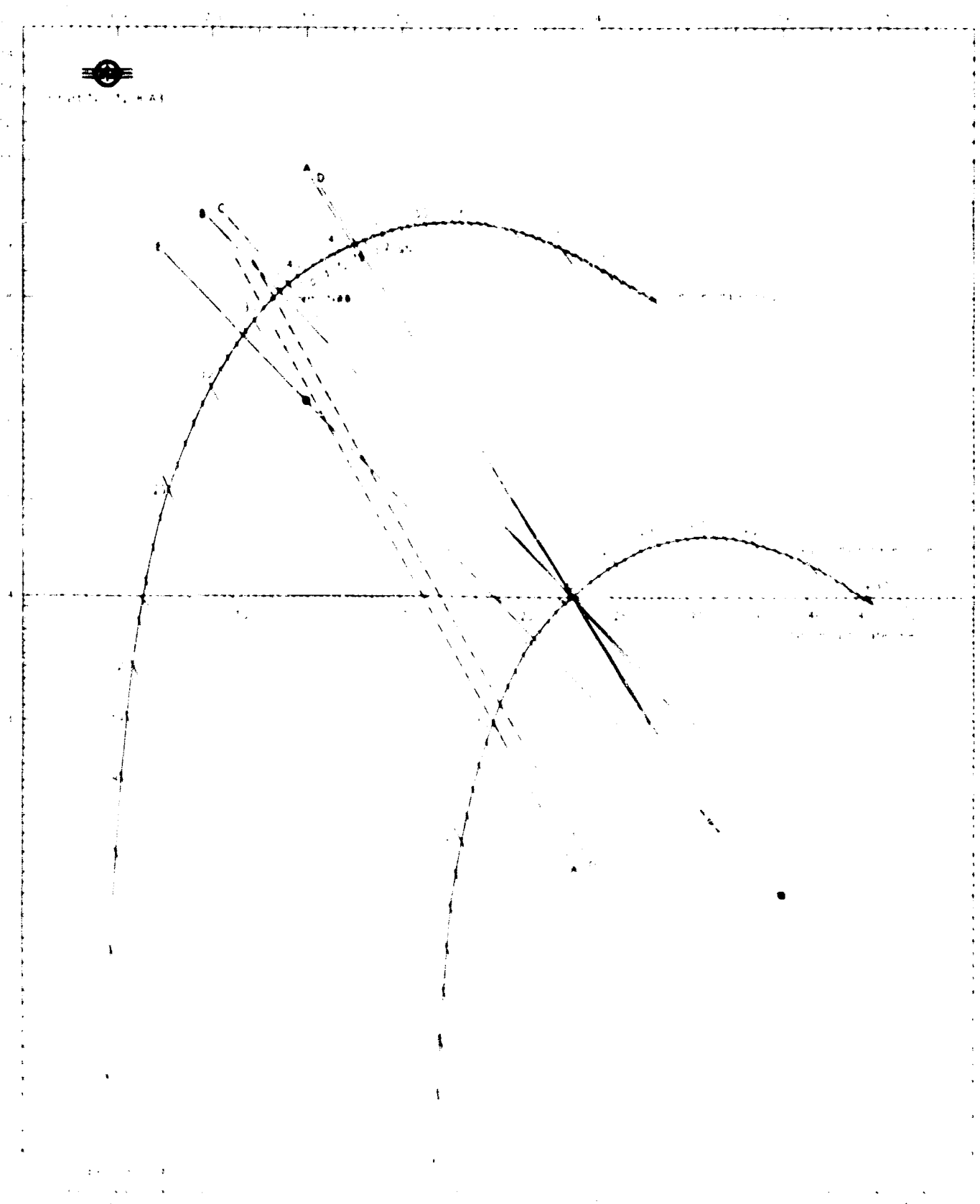

Fig.3—Astrup-type experiments

line A (from the literature [40]) represents an experiment with normal adult male blood; D is a comparable experiment computed from the present model.

Generally speaking, the slope of the lines drawn on the Astrup chart from blood samples is proportional to the buffer power of the blood in respiratory acidosis. The steeper the line, the better the blood will buffer or increase in pCO_2 (i.e., H^+ ion). Thus, the line A-- or the line D (since they differ insignificantly)--gives the normal buffer slope for blood with the standard amounts of buffering constituents. In Fig. 3, blood at pH 7.38 and at 40 mm pCO_2 contains the amount of "standard" bicarbonate given by the Henderson-Hasselbach equation, here 23.8 meq/L blood. With other conditions constant, but changing pCO_2, the buffered blood will normally follow line A (or D) intersecting the hemoglobin content curve at 16 (17) grams percent.

The buffering constituents are, in decreasing order of importance, the carbon dioxide system itself, hemoglobin, plasma proteins, organic and inorganic phosphates, and subsidiary systems. Together, these several constituents represent the anions capable of binding hydrogen ion in the viable pH range and, except for the CO_2 system,

are called the "buffer base" of the blood. The carbonate system is not part of the buffer base because it is (indirectly) the CO_2 which is to be buffered. "Buffer base" is an imprecisely defined term, since the hydrogen-binding capacity of the proteinate and phosphate factors varies so considerably with pH, their "buffer power" being directly proportional to the slope of their titration curves at a particular pH. Nevertheless, the term "buffer base" is useful for the narrow range of pH in clinical applications. At normal concentrations of protein and at viable pH and pCO_2, the imidazole ionizing groups of protein plus the carbamino reactions and phosphate complexes normally buffer as though about 45 to 46 meq per liter of ionizing sites existed.

Additions of acids or bases, as in metabolic acidosis or alkalosis without respiratory compensation, should change an available buffer base of the blood by just the amount of acid or base added. Because the solvent water has a low ionization constant, the added excess of hydrogen or hydroxyl ion can not stay in solution in ionized form; these ions must essentially either bind to a hydrogen-binding site or remove a bound hydrogen--thus reducing or increasing, respectively, the available buffer base.

When the buffer base is non-normal, indicating a
metabolic alkalosis or acidosis, the buffering reactions
of the blood to increased pCO_2 are approximately the same
as for the normal. However, the buffer line on the Astrup
diagram will shift to the new range of pH corresponding
to the new value of the buffer base. Lines A' and D' of
Fig. 3 are, respectively, the ideal responses of whole
blood in the Astrup experiment and the response of the
computer model to changes in pCO_2 after addition of 10
meq of HCl per liter. The slope of the buffer lines has
steepened slightly because the lower pH is closer to the
middle of the range of imidazole ionization, so the
buffering is more efficient. The lines D' did not move
a full ten units on the base excess curve, although 10
meq of acid was added.

This discrepancy is difficult to rationalize. The
literature notes that the standard curves are based on
blood samples from 12 persons, and that the same titra-
tion results were obtained with hydrochloric, lactic, or
acetic acids [40]. Yet at constant pCO_2, the computer
blood buffers HCl better than real blood; i.e., for
constant pCO_2, 10 meq of HCl changes the pH less in the
model than the same amount added to human blood.

The discrepancy is large--about 10 percent of the buffering capacity in this central pH range; and its direction indicates that the model is already buffering too well--i.e., the model does not need an additional buffer system. On the other hand, the blood used to construct the chart was probably not viable blood; it was probably damaged by centrifugation, changes in temperature and gas pressures, and by the addition of a fluoride stabilizing agent [40]. Some denaturation of the protein by physical forces, plus slight hemolosis, plus fluoride agents' interference with cell glycolysis could easily make the blood a 10-percent-less-efficient buffer.

Line B in Fig. 3 is the iso-bicarbonate line, i.e., the line along which pH + log pCO_2 = K is constant, and the HCO_3^- concentration is consequently also constant. Edsall and Wyman [8] give line E for the pCO_2/pH relationship in 0.02 M sodium bicarbonate solution; the HCO_3^- concentration is nearly constant. They also remark that, for this simple solution case, the total CO_2, T, carried is relatively invariant with pCO_2, the change being only from 17.1 to 22.0 mM per liter, with a change in pCO_2 from 0.45 to 63.0 mm.

Blood, however, for efficient action must have a different property. Relatively large amounts of CO_2 must be picked up or lost with small increments of pCO_2 between venous and arterial blood. This is accomplished through better buffering of the blood than the simple solution affords. If the pH is almost constant, then, by the Henderson-Hasselbach equation, as pCO_2 increases HCO_3^- must increase proportionately. Thus, buffering the hydrogen ion is essential to CO_2 transport.

From an earlier mathematical model of human blood [2] not containing the imidazole reactions in plasma and red cell protein, line C in Fig. 3 indicates the buffer power-- and hence CO_2-transport capacity. Rotating this line to the present increased buffer capacity (line D) was a matter of including the titration reactions of plasma protein and of hemoglobin. Of these two groups of proteins, that of the red cell is more important because of the carbamino reactions of hemoglobin with CO_2, oxylabile ionizing groups, and the large group of non-oxylabile sites.

REFERENCES

1. Dantzig, G. B., J. C. DeHaven, I. Cooper, S. M. Johnson, E. C. DeLand, H. E. Kanter, and C. F. Sams, "A Mathematical Model of the Human External Respiratory System," Perspectives Biol. & Med., Vol. 4, No. 3, Spring 1961, pp. 324-376; also, The RAND Corporation, RM-2519-PR, September 28, 1959.

2. DeHaven, J. C., and E. C. DeLand, Reactions of Hemoglobin and Steady States in the Human Respiratory System: An Investigation Using Mathematical Models and an Electronic Computer, The RAND Corporation, RM-3212-PR, December 1962.

3. Shapiro, N. Z., and L. S. Shapley, Mass Action Laws and the Gibbs Free Energy Function, The RAND Corporation, RM-3935-1-PR, September 1964.

4. Shapiro, N. Z., A Generalized Technique for Eliminating Species in Complex Chemical Equilibrium Calculations, The RAND Corporation, RM-4205-PR, September 1964.

5. Clasen, R. J., The Linear-Logarithmic Programming Problem, The RAND Corporation, RM-3707-PR, June 1963.

6. Dittmer, D. S. (ed.), Blood and Other Body Fluids, Prepared under the auspices of the Committee on Biological Handbooks, Federation of the American Society for Experimental Biology, Washington, D.C., 1961.

7. Spector, W. S. (ed.), Handbook of Biological Data, Wright Air Development Center, U.S. Air Force, October 1956.

8. Edsall, J. T., and J. Wyman, Jr., Biophysical Chemistry, Vol. 1, Academic Press, Inc., New York, 1958.

9. Maxwell, M. H., and C. R. Kleeman, Clinical Disorders of Fluid and Electrolyte Metabolism, McGraw-Hill Company, Inc., New York, 1962.

10. Harris, F. J., Transport and Accumulation in Biological Systems, Academic Press, Inc., New York, 1960.

11. Bland, J. H., M.D. (ed.), Clinical Metabolism of Body Water and Electrolytes, W. B. Saunders Company, Philadelphia, 1963; especially Chap. 8, J. H. Bland, M.D., "General Clinical Considerations in Water, Electrolyte and Hydrogen Ion Metabolism."

12. Conway, E. J., "A Redox Pump for the Biological Performance of Osmotic Work, and Its Relation to the Kinetics of Free Ion Diffusion Across Membranes," Internat. Rev. of Cytol., Vol. 2, 1953, pp. 419-445.

13. Edelman, I. S., and J. Leibman, "Anatomy of Body Water and Electrolytes," Am. J. Med., Vol. 27, No. 2, August 1959, pp. 256-277.

14. Roughton, F.J.W., "Respiratory Functions of Blood," Chap. 5 in Walter M. Boothby, M.D. (ed.), Handbook of Respiratory Physiology, USAF School of Aviation Medicine, Randolph Air Force Base, September 19.4, pp. 51-102.

15. Hill, A. V., "The Possible Effects of Aggregation of Molecules of Haemoglobin on its Dissociation Curves," J. Physiol. (Proceedings of the Physiological Society), Vol. 40, January 22, 1910, pp. iv-vii.

16. Dill, D. B., "Oxygen Dissociation Curves of Normal Human Blood," Chart B-1, Sec. B. in Handbook of Respiratory Data in Aviation, National Academy of Sciences, Committee on Aviation Medicine, National Research Council, Washington, D.C., 1944.

17. Tanford, C., S. A. Swanson, and W. S. Shore, "Hydrogen Ion Equilibria of Bovine Serum Albumin," J. Am. Chem. Soc., Vol. 72, No. 13, December 20, 1955, pp. 6414-6421.

18. Tanford, C., "The Interpretation of Hydrogen Ion Titration Curves of Protein," Advances in Protein Chemistry, Vol. 17, C. B. Anfinsen, Jr., K. Bailey, M. L. Anson, J. T. Edsall (eds.), Academic Press, Inc., New York, 1962, pp. 69-165.

19. DeLand, E. C., and R. Heirschfeldt, Computer Titration of Serum Albumin, The RAND Corporation (in preparation).

20. Ruch, T. C., and J. F. Fulton (eds.), Medical Physiology and Biophysics, 18th ed., W. B. Saunders Company, Philadelphia, 1960.

21. Tanford, C., The Physical Chemistry of Macromolecules, J. Wiley and Sons, Inc., New York, 1963.

22. Tanford, C., "The Electrostatic Free Energy of Globular Protein Ions in Aqueous Salt Solution," J. Physical Chem., Vol. 59, No. 6, August 1955, pp. 788-793.

23. Scatchard, G., I. H. Scheinberg, and S. H. Armstrong, Jr., "Physical Chemistry of Protein Solutions. IV. The Combination of Human Serum Albumin with Chloride Ion," J. Am. Chem. Soc., Vol. 72, No. 1, January 1950, pp. 535-540.

24. Loken, H. F., R. J. Havel, G. S. Gordan, and S. L. Whittington, "Ultracentrifugal Analysis of Protein-Bound and Free Calcium in Human Serum," J. Biol. Chem., Vol. 235, No. 12, December 1960, pp. 3654-3658.

25. Adair, G. S., "The Hemoglobin System," J. Biol. Chem., Vol. 63, No. 2, March 1925, pp. 529-545.

26. Pauling, L., "The Oxygen Equilibrium of Hemoglobin and Its Structural Interpretation," Proc. National Academy of Sciences, Vol. 21, No. 4, April 15, 1935, pp. 186-191.

27. Roughton, F.J.W., "The Intermediate Compound Hypothesis in Relation to the Equilibria and Kinetics of the Reactions of Haemoglobin with Oxygen and Carbon Monoxide," No. 5 of "II. Reversible Reactions with Oxygen and Carbon Monoxide," in Haemoglobin, F.J.W. Roughton and J. C. Kendrew (eds.), Interscience Publishers, Inc., New York, 1949, pp. 83-93.

28. Roughton, F.J.W., A. B. Otis, and R.L.J. Lyster, "The Determination of the Individual Equilibrium Constants of the Four Intermediate Reactions between Oxygen and Sheep Hemoglobin," Proc. Royal Soc. of London, Ser. B, Vol. 144, No. 914, August 16, 1955, pp. 29-54.

29. Diem, K. (ed.), Documenta Geigy: Scientific Tables, 6th ed., Geigy Pharmaceuticals, Division of Geigy Chemical Corporation, Ardsley, New York, 1962.

30. Bernstein, R. E., "Potassium and Sodium Balance in Mammalian Red Cells," Science, Vol. 120, No. 3116, September 17, 1954, pp. 459-460.

31. Henderson, L. J., Blood, A Study in General Physiology, Yale University Press, New Haven, Connecticut, 1928.

32. Bard, P. (ed.), Medical Physiology, 11th ed., C. V. Mosby Company, St. Louis, 1961.

33. Anderson, Ole Siggaard, _The Acid-Base Status of the Blood_, 2d ed., H. Cowan, B.Sc. (trans.), Villadson og Christensen, Copenhagen, 1964.

34. Severinghaus, J. W., "Oxygen Dissociation Curve Slide Rule with New pH Base Excess and Temperature Corrections," The American Physiological Society, 17th Autumn Meeting, University of California, Los Angeles, August 23-27, 1965 (unpublished).

35. Rossi, L., and F.J.W. Roughton, "The Difference of pH (ΔpH) between Reduced Human Haemoglobin and Oxyhaemoglobin when Equilibrated with the Same Pressure of Carbon Dioxide," _J. Physiol_ (Communication, Proc. Physiol. Soc., February 1962), Vol. 162, June-August 1962, pp. 17-18P.

36. German, B.. and J. Wyman, Jr., "The Titration Curves of Oxygenated and Reduced Hemoglobin," _J. Biol. Chem._, Vol. 117, No. 2, February 193ˉ, pp. 533-550.

37. Davenport, H. W., _ABC of Acid-Base Chemistry_, 4th ed., University of Chicago Press, Chicago, 1958.

38. Bock, A. N., H. Field, Jr., and G. S. Adair, "The Oxygen and Carbon Dioxide Dissociation Curves of Human Blood," _J. Biol. Chem._ Vol. 59, No. 2, March 1924, pp. 353-378.

39. Drabkin, D. L., "Aspects of the Oxygenation and Oxidation Functions," No. 1 of "II. Reversible Reactions with Oxygen and Carbon Monoxide," in _Haemoglobin_, F.J.W. Roughton and J. C. Kendrew (eds.), Interscience Publishers, Inc., New York, 1949, pp. 35-52.

40. Anderson, Ole Siggaard, and K. Engel, "A New Acid-Base Nomogram," The Department of Clinical Chemistry, Rigshospitalet, Copenhagen, Denmark (manuscript accepted for publication by the _Scandinavian Journal of Clinical and Laboratory Investigation_).

DOCUMENT CONTROL DATA

1 ORIGINATING ACTIVITY	2a REPORT SECURITY CLASSIFICATION
THE RAND CORPORATION	UNCLASSIFIED
	2b. GROUP

3 REPORT TITLE

THE CLASSICAL STRUCTURE OF BLOOD BIOCHEMISTRY--A MATHEMATICAL MODEL

4. AUTHOR(S) (Last name, first name, initial)

DeLand, E. C.

5. REPORT DATE	6a TOTAL No OF PAGES	6b. No. OF REFS
July 1966	135	40

7 CONTRACT OR GRANT No.	8. ORIGINATOR'S REPORT No.
AF 49(638)-1700	RM-4962-PR

9a AVAILABILITY / LIMITATION NOTICES	9b. SPONSORING AGENCY
DDC 1	United States Air Force Project RAND

10. ABSTRACT	11 KEY WORDS

A mathematical simulation of human blood biochemistry that includes the results of a detailed chemical analysis of human blood under a variety of chemical stresses. Mathematical simulations of increasing degrees of complexity are developed. A rudimentary blood model assumes the conventional roles of the fixed proteins, the neutral electrostatic charge constraints, and the active cation pump as the major characteristics of hemostatic blood. The microscopic properties of the proteins, particularly their buffering behavior, are incorporated into the model by a mathematical procedure that assumes that the serum albumin and the various globulins represent all of the important buffering power of the plasma fraction. A model of the respiratory biochemistry of the blood, embodying the results of the previous biochemical structural detail, is tested under various conditions. Properties of the mathematical model, such as gas exchange, buffering, and response to chemical stress in the steady state, are practically indistinguishable from those properties of real blood within the limits of the present validation program. 135 pp. Illus. Biblog.

KEY WORDS:

Biochemistry
Medicine
Biology
Physiology
Models
Blood